SPE TRANSACTIONS

devoted to plastics science and engineering

VOL. 1, NO. 2 APRIL 1961

PUBLISHED BY THE SOCIETY OF PLASTICS ENGINEERS, INC.

SPE TRANSACTIONS

. . . is a new journal containing fundamental data in the field of plastics science and engineering. Each issue will contain a selection of polymer articles, both original and review type, including translations of significant articles from foreign publications. In addition to being readily available as a permanent reference source, SPE TRANSACTIONS will be regularly indexed in the permanent literature. Also, the table of contents of quarterly issues of TRANSACTIONS will be published in the preceding issue of the SPE Journal, also published by the Society.

Society of Plastics Engineers, Inc.

Executive and Business Offices
65 Prospect St.
Stamford, Conn.

1961 Officers of the Society —

President — FRANK W. REYNOLDS
Vice Pres., Eng. — JAMES R. LAMPMAN
Vice Pres., Adm. — JOHN DELMONTE
Secretary — MAURICE F. MALONE
Treasurer — JOHN N. BERUTICH
Exec. Secretary — THOMAS A. BISSELL

Neither the Society of Plastics Engineers, Inc., nor the SPE TRANSACTIONS is responsible for the views expressed by individual contributors either in articles published in SPE TRANSACTIONS or in technical papers presented at meetings of the Society.

Editor — MELVYN A. KOHUDIC
Layout, Production — LEE COOPER
Editorial Assistant — HELEN B. TIEDEMANN
Circulation Manager — LEWIS A. BERNHARD

SPE Publications Committee
MAURICE F. MALONE, *Adm.* — EUGENE C. QUEAR
DR. ALEX SACHER, *Chmn.* — DR. FRANK W. REINHART
DR. RAYMOND F. BOYER — IRVIN I. RUBIN
DR. JESSE H. DAY — DR. SIDNEY J. STEIN
DR. HERMAN F. MARK — PARKE WOODWORTH
FRANK A. MARTIN

Editorial Advisory Board
DR. FRANK W. REINHART, *Chmn.*

ROBERT W. BARBER — DR. HERMAN S. KAUFMAN
DR. EDWARD G. BOBALEK — JOHN P. LOMBARDI
DR. LUTHER BOLSTAD — DR. BRYCE MAXWELL
EDWARD F. BORRO, SR. — DR. FREDERICK J. McGARRY
BENJAMIN S. COLLINS — THOMAS F. McLAUGHLIN
WILLIAM CROLL — DR. ROBERT B. MESROBIAN
LAWRENCE M. DEBING — ROBERT E. MONICA
EDWARD J. FITZPATRICK — JULES PINSKY
RUSSELL M. HOUGHTON — ROBERT D. SACKETT
JOHN B. HOWARD — EDWARD W. VAILL

• SPE TRANSACTIONS is Published at 215 Canal St., Manchester, N. H. Address changes, undeliverable copies and orders for subscriptions should be sent to 65 Prospect St., Stamford, Conn.

• *Permit for second-class matter at the Post Office at Manchester, New Hampshire, at special postal rate provided in paragraph (d-2), Sec. 34.40 P.L. and R., of 1918, applied for.*

• *Copyright by the Society of Plastics Engineers, Inc., 1961. Reproduction in whole or part without written permission is strictly prohibited.*

— Subscription Rates —

SPE Members
1 Yr.—$10 2 Yrs.—$18 3 Yrs.—$25

Non-Members
(US and North America)
1 Yr.—$15 2 Yrs.—$28 3 Yrs.—$40

Non-Members *(Overseas)*
1 Yr.—$25 2 Yrs.—$47 3 Yrs.—$67

Table of Contents

VOLUME 1 • NO. 2

ABSTRACTS of Articles in this Issue 54

EDITORIAL Dr. E. V. Murphree, *President, Esso Research and Engineering Co.* 56

Some Functions of 2-Hydroxybenzophenones as Weathering Stabilizers for Polymers 57

J. H. Chaudet and **J. W. Tamblyn,** Tennessee Eastman Co., Division of Eastman Kodak Co., Kingsport, Tenn.

NMR spectroscopy provides means for evaluation of a 2-hydroxybenzophenone weathering stabilizer

Method for Determination of Maximum Heat Resistance of Plastics 63

I. F. Kanavetz and **L. G. Batalov,** Moscow, U.S.S.R.

Onset of thermal degradation determined with high accuracy with method which determines heat resistance by measuring changes in modulus of elasticity

Dielectric Flow Properties of Plasticized Melamine Resins 68

W. C. Schneider, American Cyanamid Co., Research Laboratory, Stamford, Conn.

Polymer structure related to changes in dielectric properties of melamine resins

Cryogenic Adhesive Properties of Bisphenol-A Epoxy Resins 73

M. J. Hiza and **P. L. Barrick,** National Bureau of Standards, Boulder Laboratories, Boulder, Colo.

Experimental studies provide a basis for formulation of a structural adhesive with optimum cryogenic properties

Electrical Resistivity of Polymers 80

R. W. Warfield and **M. C. Petree,** U. S. Naval Ordnance Laboratory, Silver Spring, Md.

Measurements of the temperature dependence of volume resistivity of a variety of polymers are used to elucidate polymer structure and mechanism of electrical conduction

Polyethylene Flow Data from Melt Viscometer and Extruder Measurements 86

H. P. Schreiber, Central Research Laboratory, Canadian Industries Ltd., McMasterville, Quebec, Canada

Flow data from a melt viscometer may be used to predict extruder performance, for instance screw power requirement

An Investigation of Some Variables Affecting Impact Resistant Thermoplastics 93

Edward G. Bobalek, Case Institute of Technology, Cleveland, Ohio, and **Robert M. Evans,** Master Mechanics Co., Cleveland, Ohio

Experiments and theory leading to the development of polymers which do not exhibit brittle fracture

abstracts of articles in this issue

SOME FUNCTIONS OF 2-HYDROXYBENZOPHENONES AS WEATHERING STABILIZERS FOR POLYMERS

J. H. Chaudet and J. W. Tamblyn

Tennessee Eastman Company, Division of Eastman Kodak Company, Kingsport, Tennessee

Derivatives of 2-hydroxybenzophenone are well-known stabilizers for such polymers as cellulose acetate butyrate and polyesters. Their stabilization effectiveness is commonly associated with their ability to screen a polymer from the harmful ultraviolet radiation found in sunlight. They also satisfy other requirements for effective stabilizers, namely, compatibility with many polymers and an inherent stability to ultraviolet light. Several other functions of 2 hydroxybenzophenones in stabilizing a polymer to ultraviolet light have been postulated, but little experimental data related to them are available. This paper deals with some of the additional functions of 2-hydroxybenzophenones in weathering stabilization as investigated by nuclear magnetic resonance spectroscopy (NMR) and electron paramagnetic resonance spectroscopy (EPR).

A METHOD FOR DETERMINATION OF MAXIMUM HEAT RESISTANCE OF PLASTICS

I. F. Kanavetz and L. G. Batalov

Translated from: Russian Plastics, March 1960

A new method for measuring heat stability and temperature of degradation of thermosetting plastics is described, as well as an improved method for the determination of transition temperature into glassy or viscous state for thermosetting resins. Magnitude of elastic deformation is tied in with length of polymer chain and lattice density.

DIELECTRIC PROPERTIES OF PLASTICIZED MELAMINE RESINS

W. C. Schneider

American Cyanamid Company, Stamford, Conn.

During the last thirty years, dielectric measurements have been employed extensively to provide a better understanding of the interactions between polymer and plasticizer in various thermoplastic formulations. Recently, a series of melamine resins, plasticized to the extent that shrinkage and internal stress were modified, became available. Since there is little information in the literature concerning the dielectric properties of such thermosetting resins, a study was made of the variation of dielectric constant and loss as a function of frequency and temperature.

CRYOGENIC ADHESIVE PROPERTIES OF BISPHENOL-A EPOXY RESINS

M. J. Hiza and P. L. Barrick

Cryogenic Engineering Laboratory, National Bureau of Standards

This article includes a comparison of the adhesive properties of bisphenol-A expoxides at 300°K and 76°K

clip these briefs for easy reference on 3" x 5" or other suitable filing cards

with respect to the molecular weight of the uncured resins. Joints of 2024 aluminum were tested at 300°K and 76°K in tensile-shear and in impact-shear, and total linear thermal contraction of the cured resins was measured between the two temperatures. Results are discussed with respect to residual joint stresses and adsorptive properties of the resins.

ELECTRICAL RESISTIVITY OF POLYMERS

R. W. Warfield and M. C. Petree

U.S. Naval Ordnance Laboratory, Silver Spring, Md.

The magnitude and temperature dependence of the electrical resistivities of a number of thermoplastic and thermosetting high polymers have been determined. Activation energies for the electrical conduction process E_c, have been calculated and found to vary from 12 to 60 Kcal/mole depending upon the structure of the polymer. Results are interpreted in terms of an ionic diffusion process and discussed in terms of the structure of the polymers.

POLYETHYLENE FLOW DATA FROM MELT VISCOMETER AND COMMERCIAL EXTRUDER MEASUREMENTS

H. P. Schreiber

Central Research Laboratory, Canadian Industries Ltd., McMasterville, Que., Canada

For broad ranges of operating conditions and a wide variety of high pressure polyethylenes, the flow data obtained from a high shear viscometer and a commercial extruder are identical. Discrepancies between flow data can result from non steady state viscosities in the high shear viscometer, or from cooled screw extruder operation. In the broad regions in which the flow data concur, the readily obtained viscometer data are suitable for predictions of extruder performance. The principle is illustrated by the good correlation of a viscometer flow curve parameter and the screw power consumption in the extruder. Principles outlined for flow data identity and extruder performance prediction are believed to be general, but the quantitative limits defined are specific to the extrusion devices involved.

AN INVESTIGATION OF SOME VARIABLES AFFECTING IMPACT RESISTANCE OF THERMOPLASTICS

E. G. Bobalek and R. M. Evans*

*Case Institute of Technology, *Master Mechanics Co., Cleveland, O.*

Recent technology has evolved a number of dissimilar thermoplastics which under conditions of ambient temperature and impact loading show both the high modulus, which is mainly a property of brittle polymers in the glassy state, and also the impact resistance, such as may be expected of polymers in the rubbery state. Several of these special plastics were examined by electronmicroscopy and also with respect to several aspects of their mechanical behavior to establish by direct observation and inference whether or not different types of plastics exhibit some common features of structure which promote impact resistance. These observations suggest the hypothesis that special circumstances of domain heterogeneity can override many other variables of composition or molecular structures in controlling the fracture mechanism.

Editorial

How Can Scientists Keep Up With Science?

The spectacular growth of scientific research and technology in recent years has led to vast changes in the lives of people all over the world. At the same time, the great outpouring of new technical information has posed a staggering question for the architect of this progress—the technical man. In an age of such rapid technical development, how does he keep from becoming technically obsolete?

The technical man has to take some preventive steps of his own.

He must realize that keeping himself aware of the pertinent happenings in the world of science is his personal responsibility. It has been said that science is not an activity that goes on in laboratories but rather is an activity that takes place in the mind. The man who doesn't keep up with his contemporaries betrays himself and his profession.

He must accept the fact that no man can master more than one general field. Science and technology have become too comprehensive to allow for the technical jack-of-all-trades.

He must recognize the absolute need for continuing to broaden his knowledge—in his own and in related fields—without letting his basic tools of knowledge, the fundamentals, grow dull. New developments may come with dizzying speed, but the fundamentals change scarcely at all.

In order to keep himself abreast of new developments, new concepts and new technical tools, the perceptive individual quickly learns the value of being an avid but selective reader. He learns the mechanics of getting information—that is, where to obtain facts, whom to ask for specialized knowledge, what facilities for advanced study are available, etc. Finally, he seeks to widen his acquaintance among other people doing technical work, particularly in different fields. The "lone wolf" who keeps aloof from his fellows doesn't allow himself much opportunity to grow.

There is much each man can and should do for himself to guard against obsolescence, but of course he cannot do all of it alone. In an industrial research organization, the top echelon of management bears a supplemental responsibility.

Management has to help the industrial research man grow by offering him challenging work—work that will stretch his brains and tempt his intellectual powers. A good system of handling technical information should be maintained, along with an efficiently operated and well-stocked technical library.

There are other things management can do. Technical people should be encouraged to participate in a reasonable number of scientific meetings. They should be urged to publish their work when it is worth while, *but dissuaded from flooding the literature.* They should not be encumbered by unessential administrative duties. And they should be adequately rewarded for technical achievement, both in money and recognition, since such rewards can be a strong stimulus for people to keep up to date in their professions. The technical man exists, in a sense, to carry out what an economist recently referred to as "creative destruction"—he works to make technology obsolete.

But he doesn't let the same thing happen to him.

EGER V. MURPHREE
President
Esso Research and Engineering Company

Some Functions of 2-Hydroxybenzophenones as Weathering Stabilizers for Polymers

Nuclear magnetic resonance spectroscopy shows that these compounds increase ultraviolet stabilization by increasing chelate hydrogen bond strength. Also 2-hydroxybenzophenones interferes with free radical reactions

J. H. Chaudet and J. W. Tamblyn

Tennessee Eastman Company
Division of Eastman Kodak Company
Kingsport, Tennessee

Derivatives of 2-hydroxybenzophenone are well-known stabilizers for such polymers as cellulose acetate butyrate and polyesters. Their stabilization effectiveness is commonly associated with their ability to screen a polymer from the harmful ultraviolet radiation found in sunlight. They also satisfy other requirements for effective stabilizers, namely, compatibility with many polymers and an inherent stability to ultraviolet light.

Several other functions of 2-hydroxybenzophenones in stabilizing a polymer to ultraviolet light have been postulated, but little experimental data related to them are available (1). This paper deals with some of the additional functions of 2-hydroxybenzophenones in weathering stabilization as investigated by nuclear magnetic resonance spectroscopy (NMR) and electron paramagnetic resonance spectroscopy (EPR).

Chelate Hydrogen Bonding and Polymer Stabilization

The NMR spectra of 2-hydroxybenzophenone derivatives usually show a hydroxy proton resonance near −300 cps relative to the proton resonance of water. The spectrum of 2-hydroxy-4-methoxybenzophenone in methylene chloride is given in *Figure 1*. The peak assignments are indicated. This spectrum is fairly typical for 2-hydroxybenzophenones. This spectrum, as well as other NMR data reported here, were obtained with a Varian high-resolution instrument at a frequency of 40 mc. Tetramethylsilane was used as an internal reference for determining peak positions.

The hydroxy proton resonance observed for the 2-hydroxybenzophenones did not shift in position when a given derivative was diluted with solvent. This insensitivity to concentration attested to the stability of the hydrogen bonding in the chelate structure. In structures in which there is only intermolecular hydrogen bonding, such as 4-hydroxybenzophenone, the hydroxy resonance shifted to higher field values with dilution. This shift corresponded to a reduction in hydrogen bond strength.

It was observed that the chemical shift position of the hydroxy proton resonance differed somewhat for the various 2-hydroxybenzophenones. This variation suggested that the hydrogen bond strength was not the same in the chelates of all the compounds. The chemical shift position for the hydroxy proton resonance has been shown to be a measure of the hydrogen bond strength in chelate structures. The more negative the chemical shift position for this proton, the stronger is the hydrogen bond strength in the chelate (2).

In *Table 1* are listed the hydroxy chemical shift positions for several 2-hydroxybenzophenone derivatives. Methylene chloride or acetone was used as the solvent. Also given are the ultraviolet stabilization values for these compounds in cellulose acetate butyrate. It appears from these data that, as the position of the hydroxy resonance goes to lower field values, the stabilization effectiveness increases.

More detailed data are given in *Figure 2*, where the stabilization ratings for several 2-hydroxybenzophenones in cellulose acetate butyrate at a concentration of 1% are plotted against the corresponding hydroxy chemical shift positions. The stabilization ratings were determined on 50-mil-thick, compression-molded sheets of polymer containing dibutyl sebacate as a plasticizer. Ultraviolet exposures were made in a modified Atlas Weather-Ometer (3). A condition of brittleness was defined to have been reached when the sample broke at a bend angle of less than 90° in the Tour-Marshall test for stiffness in flexure (4). The stabilization rating of the additive was the ratio of the embrittlement time for the polymer with additive to the embrittlement time in the absence of additive.

The highest point on this curve is that for 3-benzoyl-2,4-dihydroxybenzophenone and the lowest points, −150

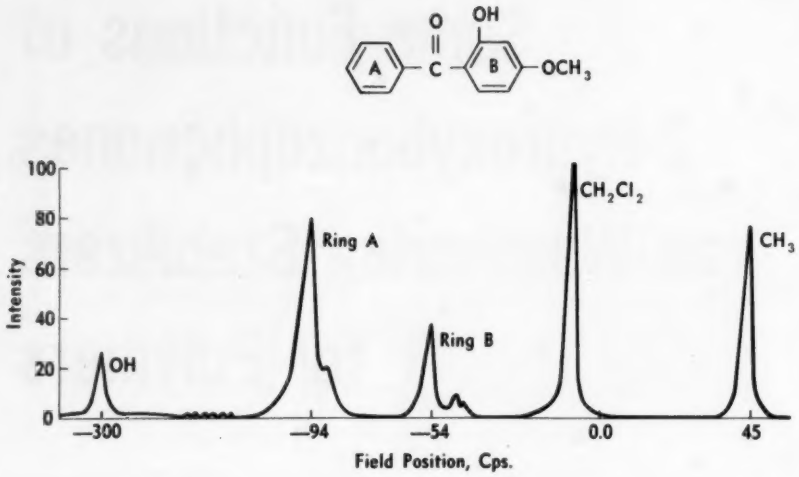

Figure 1. NMR spectrum of 2-hydroxy-4-methoxybenzophenone

and —162 cps, are for 4,4'-dihydroxybenzophenone (concentrated solution) and 2,6-dihydroxybenzophenone, respectively. The point corresponding to a chemical shift of —220 cps is that for 2,2'-dihydroxybenzophenone. The other points, which are centered near —300 cps, are for 2-hydroxybenzophenone derivatives which contain a single hydroxy group ortho to the carbonyl group.

The relation of *Figure 2* shows that the ultraviolet stabilization observed for the hydroxybenzophenones is related to the chemical shift position of the hydroxy proton. The more negative this position, that is, the stronger the hydrogen bonding in the chelate, the better the compound is as a light stabilizer.

In *Figure 3* is shown a similar relation between the stabilization rating and hydroxy peak position for 2-hydroxybenzophenones in 5% concentration in a sulfone polyester having the structure indicated. The dotted line is the relation observed for cellulose acetate butyrate from *Figure 2*. The sulfone polyester is inherently less stable to sunlight than cellulose acetate butyrate. Again this plot implies that the stronger the hydrogen bonding in the chelate the more effective the 2-hydroxybenzophenone is as a weathering stabilizer.

The role that the hydrogen bonding plays in the ultraviolet stabilization by 2-hydroxybenzophenones is not clearly known. Hydrogen bonding probably accounts to a certain extent for the screening action shown by these compounds in the ultraviolet region of 300 to 400 mμ; however, no direct correlation between ultraviolet absorption data and stabilization has been found. In addition, this bonding is believed to be involved in the degradation of absorbed ultraviolet quanta. One way in which such a degradation of energy may occur is as follows:

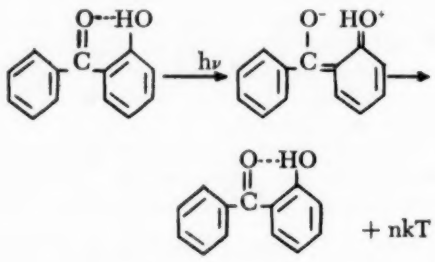

An ionic resonance structure resulting from electronic excitation may be formed with the absorption of an ultraviolet quantum. In this structure the hydrogen atom would be expected to be shared more equally between the two oxygen atoms. A stronger hydrogen bond in the chelate would be expected to promote the formation of the ionic structure. The resonance energy of this system could feasibly be redistributed among the various vibrational modes in the molecule in returning to the non-ionic state and eventually be transferred harmlessly to the polymer as heat.

Table 1. Relation of Hydroxy Chemical Shift in 2-Hydroxybenzophenones to Their Effectiveness in Stabilizing Cellulose Acetate Butyrate

Additive (1% concn.)	OH Chem. Shift, Cps	Stabilizing Effectiveness,[a] Hr. in Modified Weather-Ometer
None	—	200
2,6-Dihydroxybenzophenone	—160	600
2,2'-Dihydroxybenzophenone	—222	1000
2,4-Dihydroxybenzophenone	—282	2400
2-Hydroxy-4, 4'-dimethoxybenzophenone	—312	>2600
3-Benzoyl-2, 4-dihydroxybenzophenone	—358	>4000

[a] Exposure time required to cause 25% loss in flexural strength.

Factors Affecting the Chelate Hydrogen Bond Strength

From data collected on approximately forty 2-hydroxybenzophenone derivatives by NMR, certain trends which seem to have some bearing on the chemical shift position of the hydroxy proton and consequently on the

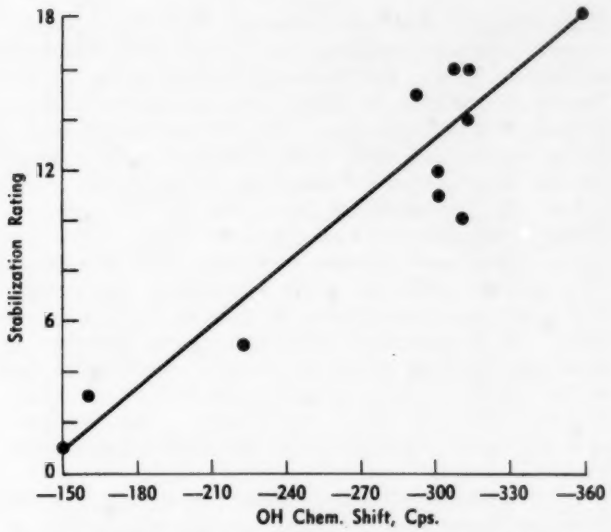

Figure 2. Relation of hydroxy chemical shift in 2-hydroxybenzophenones to their effectiveness in stabilizing cellulose acetate butyrate

hydrogen bond strength in the chelate were indicated. In *Table 2* are given the hydroxy chemical shift positions for 2-hydroxybenzophenone and several related compounds of interest. These data indicate that the unsubstituted phenyl group does not make an appreciable contribution to the hydrogen bonding. Where this group is replaced by a methyl group, as in 2'-hydroxyacetophenone, the hydroxy chemical shift value is slightly more negative, and the hydrogen bond strength is increased somewhat. A similar increase in bond strength was observed in going from 2-hydroxy-4-methylbenzophenone to the corresponding dichelate structure in which the chelates are separated by a polymethylene bridge.

Models for 2-hydroxybenzophenone indicate that, for maximum hydrogen bond strength in the chelate, the carbonyl group and the benzene ring to which the hydroxy group is attached must be approximately coplanar.

Table 2. Contribution of Phenyl Group to Hydroxy Chemical Shift

Structure	OH Chem. Shift, Cps
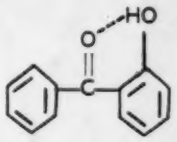	—270
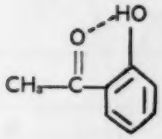	—280
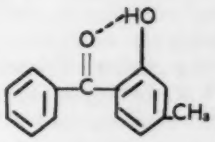	—286
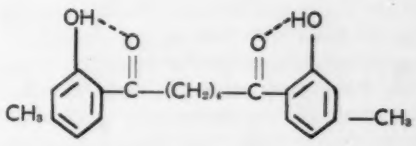	—299

The unsubstituted phenyl group in these compounds under these conditions is sterically hindered from being coplanar with the carbonyl group.

The hydroxy chemical shift of the 2-hydroxybenzophenones varied somewhat as different functional groups were substituted on the ring to which the hydroxy

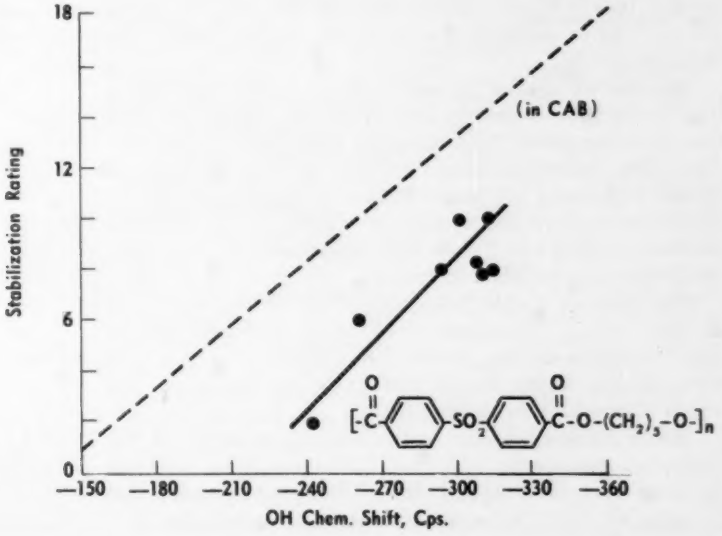

Figure 3. Relation of hydroxy chemical shift in 2-hydroxybenzophenones to their effectiveness in stabilizing a polyester

Table 3. Effect of Substituents on Hydrogen Bond Strength in 2-Hydroxybenzophenones

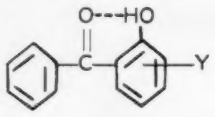

Y	OH Chem. Shift, Cps
None	—270
4-Methoxy-	—310
5-Methoxy-	—244
5-Nitro-	—307
4-Methoxy-5-nitro-	—323

group was attached. Substituents on the other benzene ring usually did not alter it appreciably. Substituents on the ring containing the hydroxy group may through resonance with the coplanar carbonyl group and the hydroxy group determine to some extent the hydrogen bond strength in the chelate. Substituents on the nonplanar ring cannot make appreciable resonance contributions to hydrogen bonding, and only inductive effects appear operative.

The strength of the hydrogen bonding in the chelate may be increased or decreased by making proper substitutions on the benzene ring to which the hydroxy group is attached. In *Table 3* are given chemical shift data for several 2-hydroxybenzophenone derivatives which illustrate this point. In going from 2-hydroxybenzophenone to 2-hydroxy-4-methoxybenzophenone the strength of the hydrogen bond increased. A similar effect was observed when the methoxy group was replaced by other alkoxy groups, such as dodecyloxy group. In 2-hydroxy-5-methoxybenzophenone the bonding was weaker.

Through resonance, the methoxy group in the 4-position may increase the electronic density within the carbonyl group which is para to it, but not in the hydroxy group. In the 5-position, the methoxy group is now para to the hydroxy group and meta to the carbonyl group. Its resonance contributions in this position would be such as to increase the electronic density within the hydroxy group.

An electronegative group, such as a nitro group, in the 5-position decreases the electronic density within the hydroxy group both through resonance and induction. The hydrogen bond strength in 2-hydroxy-5-nitrobenzophenone is greater than that in 2-hydroxybenzophenone. Note the combined effects of the methoxy and nitro groups in the 4- and 5-positions, respectively, in increasing the bond strength.

The data of *Table 3* indicate that, as the electronic density within the carbonyl group is increased and as the electronic density within the hydroxy group is decreased, the strength of the hydrogen bond in the chelate structure becomes greater.

When more than one hydroxy group is ortho to the carbonyl group, the resultant hydrogen bond strength is less than that found for 2-hydroxybenzophenone (*Table 4*). For 2,2′-dihydroxybenzophenone, the hydroxy chemical shift peak comes at —220 cps, a position some 50 cps more positive than that for 2-hydroxybenzophenone. Since the carbonyl oxygen atom in the double chelate must be shared between the two hydroxy protons, the hydrogen bond strength here might be expected to be less than that associated with a single chelate structure as in 2-hydroxybenzophenone.

For the asymmetrical structure 2,2′-dihydroxy-4-methoxybenzophenone, two hydroxy peaks were observed. These corresponded to distinct hydrogen bonds. The peak at —268 cps, which represented the stronger hydrogen bond, would from the data of *Table 3* be expected to be associated with the chelate structure to which the methoxy group can make a contribution, that is, the chelate structure involving the hydroxy group attached to the same ring as the methoxy group. The peak at —207 cps is associated with the other chelate structure.

In 2,6-dihydroxybenzophenone the strength of the hydrogen bond was the weakest observed for the 2-hydroxybenzophenone derivatives. The distances between the hydroxy protons and the carbonyl oxygen atom are relatively great compared with those for the other structures. If it is to be shared equally with the two hydroxy groups, the carbonyl group must be in an average position approximately at right angles to the disubstituted phenyl group.

Table 4. Hydrogen Bond Strength in Double Chelate Structures

Structure	OH Chem. Shift, Cps
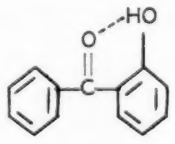	—270
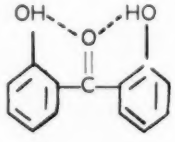	—220
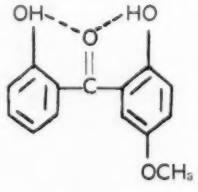	—268, —207
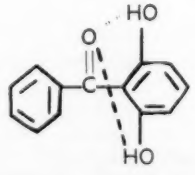	—160

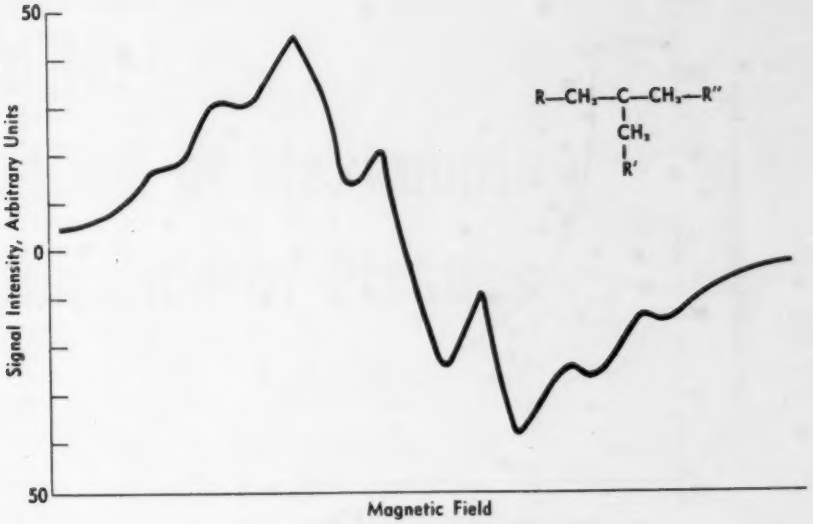

Figure 4. EPR spectrum of x-irradiated polyethylene

Radical Suppression in Polyethylene by 2-Hydroxybenzophenones

When polyethylene is x-irradiated in air, a fairly intense electron paramagnetic resonance free radical signal is observed, as shown in *Figure 4*. We were unable to detect free radicals by this means when the polymer was irradiated with ultraviolet light. The curve shown in *Figure 4* is the derivative of the absorption signal. A Varian V-4500 electron paramagnetic resonance spectrometer was used for this and other EPR recordings. Electron resonance conditions were 9500 mc and 3400 gauss.

The presence of seven peaks in this spectrum suggests that the unpaired electron is interacting equally with six protons. The tertiary radical indicated is a likely structure.

The concentration of radicals produced by x-irradiation of polyethylene may be markedly reduced by incorporating antioxidants into the polymer. In *Table 5* are given the relative free radical concentrations found in polyethylene containing three known antioxidants as well as several 2-hydroxybenzophenones. These samples were x-irradiated for 1 hour. The dosage was sufficient to produce about 10^{17} radicals per gram in the unstabilized polymer. Also included in this table are weathering stress life values for the different samples.

The antioxidants—the first three additives—were very effective in suppressing radical formation, but they were not particularly effective as weathering stabilizers. The 2-hydroxybenzophenones listed also reduced the radical concentration. Some of them approached the activity of the antioxidants as radical suppressors. The intensity of the free radical signal in polyethylene which contained the 2-hydroxybenzophenones was inversely related to the weathering life of the sample.

These data as well as additional data obtained for the 2-hydroxybenzophenones in polyethylene give the relation of *Figure 5*. Note in *Figure 5* that all 2-hydroxybenzophenones reduced the radical concentration found in the polymer, the extent of the reduction varying quite markedly in going from mediocre to good weathering stabilizers. It appears that no correlation between radical concentration and stress life values of two years or less exists. For stress life values greater than two years there is a pronounced reduction in free radical concentration. The most effective weathering stabilizers are able to suppress effectively the radical formation in polyethylene by x-rays.

It seems that the 2-hydroxybenzophenones might be showing some antioxidant activity in the weathering stabilization of the polymer. The 2-hydroxybenzophenones do not screen the polymer from x-rays since they show at most only a slight absorption for them.

Thermal stabilization tests were made at 110°C on polypropylene which contained various 2-hydroxyben-

Table 5. Relation of Radical Concentration to Weatherability of Polyethylene Containing Additives

Additive		EPR	Weathering
Name	Concn., %	Signal Intensity	Stress Life,[a] Yr.
Control	—	107	1.0
Zinc dibutyldithiocarbamate	0.5	22	1.0
2,2′-Methylenebis[6-(1-methylcyclohexyl)-p-cresol]	0.5	16	1.1
N,N′-Diphenyl-p-phenylenediamine	0.5	14	1.6
5-Chloro-2-hydroxybenzophenone	1	74	1.5
2-Hydroxy-5-methoxybenzophenone	1	63	1.5
2,2′-Dihydroxy-4,4′-dimethoxybenzophenone	1	40	3.5
4,4′-Bis(dodecyloxy)-2-hydroxybenzophenone	1	27	>4.0
4-Dodecyloxy-2-hydroxybenzophenone	1	29	>5.0

[a] Time for 5 of 10 stressed samples to crack.

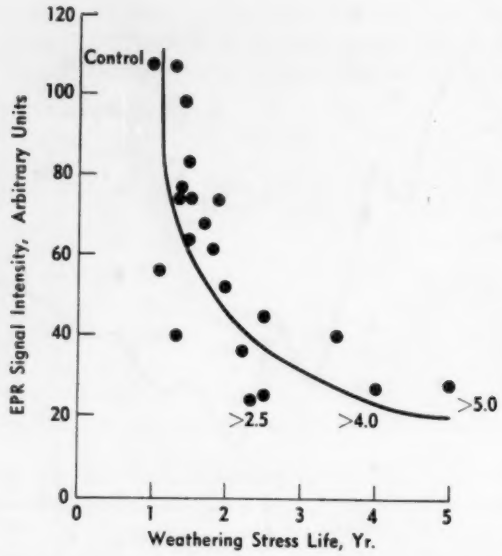

Figure 5. Relation of radical concentration to weatherability of polyethylene containing 2-hydroxybenzophenones

zophenone derivatives. The results of these tests are given in *Table 6*. Polypropylene was chosen because of its relative instability at this temperature. The EPR signal intensities resulting from the x-irradiation of polyethylene which contained each of the 2-hydroxybenzophenones are also given.

All of the 2-hydroxybenzophenones tested thermally stabilized polypropylene at 110°C. 4,4'-Bis(dodecyloxy)-2-hydroxybenzophenone gave a thermal stability in excess of 4100 hours. None of these 2-hydroxybenzophenone derivatives were effective at 160°C.

The data of *Table 6* also show a correlation between the radical concentration values and thermal stabilization values; that is, the lower the radical concentration, the more effective the compound is as a thermal stabilizer. These data show that the 2-hydroxybenzophenone derivatives are functioning as antioxidants. They probably act in much the same way as the more conventional phenolic-type antioxidants.

Table 6. Thermal Stabilization of Polypropylene by 2-Hydroxybenzophenones

Additive (1% concn.)	Time to Stress Crack at 110°C., Hr.	EPR Signal Intensity[a]
Control	15	107
2,2'-Dihydroxybenzophenone	22	76
2-Hydroxy-4,4'-dimethoxybenzophenone	22	82
2-Hydroxy-5-methoxybenzophenone	120	63
4-Dodecycloxy-2-hydroxybenzophenone	387	29
4,4'-Bis(dodecyloxy)-2-hydroxybenzophenone	>4100	27

[a] After 1 hr. x-irradiation of additive in polyethylene at 1% concn.

Conclusions

The NMR chemical shift data, along with the EPR free radical suppression data, should provide a good means for the preliminary evaluation of a 2-hydroxybenzophenone weathering stabilizer. The first measurement assesses the ability of the prospective stabilizer to dispose safely of the incoming ultraviolet energy. The second assesses its effectiveness in stopping the secondary, thermal reactions started by those few, ultraviolet quanta which escaped absorption and inactivation by the stabilizer.

The NMR data revealed that highly electronegative and electropositive groups in the proper positions on the coplanar benzene ring in the 2-hydroxybenzophenones should be effective in increasing the chelate hydrogen bond strength and, hence, ultraviolet stabilization. 3-Benzoyl-2,4-dihydroxybenzophenone, with a chemical shift value of around −350 cps, showed the strongest hydrogen bonding and is the best ultraviolet stabilizer of this class for cellulose acetate butyrate found to date.

The function of 2-hydroxybenzophenones as antioxidants may be a very important one in weathering stabilization. 2-Hydroxybenzophenones are not perfect ultraviolet screening agents and some ultraviolet quanta will be absorbed by the polymer. It might be expected that the extent of polymer degradation in the presence of a stabilizer would be related to the quanta actually taken up by the polymer. (Quanta absorbed by the 2-hydroxybenzophenones are probably converted into harmless packets of energy via the chelate hydrogen bond.) In the presence of a 2-hydroxybenzophenone, the free radical reactions normally involved in the degradation of the polymer may be partially terminated by proton transfer from the stabilizer. The 2-hydroxybenzophenones in functioning as antioxidants may be able to compensate to a certain extent for their inability to completely screen the polymer from ultraviolet light.

Literature References

1. Burgess, A. R., "Polymer Degradation Mechanisms," *Nat. Bur. Standards Circ.* No. 525, 157 (1953).
2. Porte, A. L., Gutowsky, H. S., and Hunsberger, I. M., *J. Am. Chem. Soc.*, 82, 5057 (1960).
3. Tamblyn, J. W., and Armstrong, G. M., *Anal. Chem.*, 25, 460 (1953).
4. ASTM D747-50, "ASTM Standards on Plastics," American Society for Testing Materials, Philadelphia 3, Pa., Sept., 1958, p. 309.

Acknowledgment

We would like to acknowledge the assistance of G. C. Newland in the collection of the ultraviolet and thermal stabilization data and of Evelyn M. Simons in the collection of the NMR and EPR data. We are indebted to W. D. Kennedy and H. W. Patton for many helpful discussions in connection with this problem.

Presented at the 138th National Meeting of the American Chemical Society, New York, N. Y., September 11-16, 1960.

A Method for Determination of Maximum Heat Resistance of Plastics

This article describes a method for measuring heat resistance of polymers based on measuring changes in modulus of elasticity. Novel specimen configurations are described. The method is reported to give more accurate determination for the onset of thermal degradation

I. F. Kanavetz and L. G. Batalov, U.S.S.R.

In the plastics industry, at present, the unsatisfactory methods of Martens and Vick are used to determine the heat resistance of polymers. These methods are based on the measurement of artificial constants. Derived from contemporary concepts of close relationship between the properties and molecular structure of polymers, to correctly determine the heat resistance it is necessary to employ methods based on the measurement of elastic and plastic properties of materials through a wide range of temperatures, moduli of elasticity, specific heats, linear thermal expansions, etc.

In the choice of the method of measurement, the complexity of the apparatus and the accuracy of measurements must be considered. It is worth mentioning in this connection, the thermo-mechanical method developed by V. A. Kargin and his co-workers (1, 3).

The New Method

S. N. Jurkov, I. S. Maygeldinov, A. I. Marey (10, 13) and others studied the heat resistance of polymers by measuring the changes in the moduli of elasticity of polymers caused by increase in temperature. The calculation of the modulus of elasticity in kg per cm^2 can be made using Hertz's formula based on the depth of of penetration of the ball.

$$E = .795 \frac{P}{D\,3/2 \cdot d\,1/2}$$

where

P — load on the ball-kg.
D — depth of penetration in cm.
d — diameter of the ball in cm.

V. U. Tarasov studied structural changes in silicates and polymeric materials by measuring changes in specific heats (14, 16).

Increase of temperature in polymers increases the mobility of molecular components and molecules themselves. Heating beyond the point of thermoplasticity radically changes the modulus of elasticity of polymers. Therefore, the use of changes in the modulus of elasticity to determine heat resistance is more significant than the deformation of the material under linear compression. Monomeric material exhibit a large drop in viscosity at temperatures above the melting point temperature (heat stability).

The unique characteristic of this method lies in the use of three types of novel specimen configurations, small in size and simple in design:

Specimen A—(Composite) measuring 15 x 10 x 3 mm (*Figure 2*)—Only 2 grs. are required for its preparation. This specimen can be used for testing thermoplastic and thermosetting plastics in a wide range of temperatures to measure deformation in pure shear. The material to be tested is molded between two outer and an inner corrugated plate.

Specimen B—The working part measures 15 x 10 x 3 mm—Used for thermoplastics and thermosets to measure tensile deformation.

Specimen C—Used for testing laminated and sheet materials measures 40 x 10 x 3 mm (*Figure 4*).

Translated especially for SPE TRANSACTIONS from Russian "Plastics" Magazine No. 3, p. 58, March 1960

by George Lubin
Grumman Aircraft Engineering Corp.

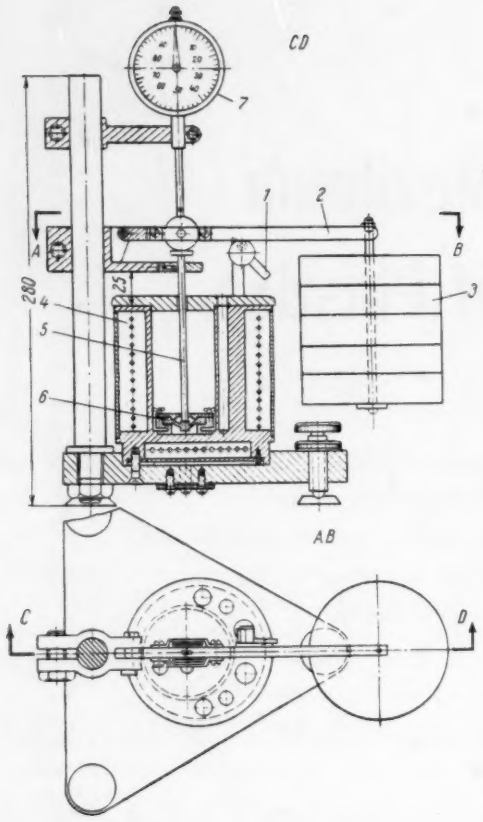

Figure 1. Schematic diagram of the instrument for the measurement of thermal stability of polymers:
1. eccentric cam; 2. lever arm; 3. load; 4. heating system; 5. rod; 6. test specimen; 7. indicator

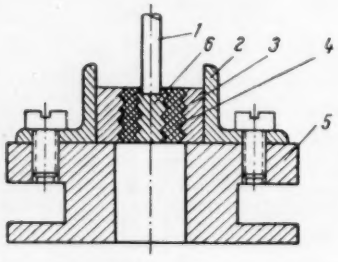

Figure 2

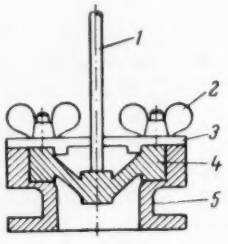

Figure 3

Figure 2. Fixture for the determination of heat resistance of plastics by measurement of deformation under shear
(Specimen A)
1. loading rod; 2. sample holder; 3. outer plate; 4. material being tested; 5. holder to locate specimen in test unit; 6. center core

Figure 3. Fixture for the determination of the temperature of transition of plastics
(Specimen B, offset)
1. loading rod; 2. wing nut; 3. specimen holder plate; 4. test specimen; 5. holder to locate specimen in test unit

All specimens are simply clamped in the jigs. They all exclude the possibility of obtaining distorted test results due to slippage. This is important for the measurements of heat stability by the use of the modulus of elasticity in shear and tension. Specimens A and B are made by compression molding or casting on simple laboratory equipment.

Residual stresses remaining in the material due to non-optimum cure cycles for Specimen A do not materially change the magnitude of measurements.

Before starting the test it is necessary to preload the specimen, remove the load and set the indicator to zero.

The technique for testing thermoplastics is analogous to that used in the thermo-mechanical method namely, raising of the temperature uniformly at the rate of 50 to 60°C per hour. Periodically, every 5 to 10° the load on the specimen is increased by from 0.1 to 0.3 kg/cm² depending on the rigidity of the material.

The interval of application of the load is 10 seconds. The deformation of the specimen is measured under load and under no load to 0.01 mm by the use of an indicator gage. In the range of temperatures slightly above the melting point temperature resilient and elastic deformations occur primarily under short time loading. The increase in deformation with increase in temperature indicates plastic flow in the material (viscous state). Under long time load condition at temperatures lower than the thermal stability temperature, beside the resilient deformation, there appears elastic deformation, and above the temperature of thermal stability there is in addition irreversible flow; therefore, on the thermo-mechanical curve the transition temperature of the polymer from elastic to plastic flow is less distinct.

During the tests of thermosetting materials, Specimens A and B, a constant load of 10 kg/cm² is imposed because of long periods of relaxation for these materials. What is measured is the change of total deformation for the specimen during the test with the temperature being raised at the rate of 50-60°C per hour. The rate of temperature rise is regulated by a program controller and thermal capacity of the heating unit.

The graphs of test results with deformation plotted against temperature, enable one (by the radical change in slope) to determine the heat resistance, range of temperatures of structural changes in the material and the temperature indicating the beginning of degradation of thermosetting plastic materials.

For thermoplastics, in addition, the change occurring in elastic deformation after 2-3 seconds after the removal of the load can be measured. Tests on thermoplastics can also be performed on a round specimen 20 mm in diameter and 3 mm thick (*Figure* 5). Linear compression is used in this case under loads of .25 to 4 kg/cm². This type of test is less characteristic of materials than the deformation under pure shear. In addition the test results often include the results of deformation from residual internal stresses.

In tests performed on specimen A (*Figure* 2) the applied force or stress, is shown as follows:

$$F = \frac{P}{2S}$$

where P is the applied tangential load on the center core of the specimen in kg.
S is working area of the molded plastic material.
Shear deformation ϵ (relative strain) is shown as:

$$\epsilon = \frac{\Delta X}{d}$$

where ΔX is total motion of the core with respect to side plates.
d is width of space between inner and outer plates (at high points of the raised nibs.)
Elastic Modulus (Shear modulus) in kg/cm² can be determined from the formula:

$$E = \frac{F}{\epsilon} = \frac{Pd}{2S\Delta X}$$

Elastic Deformation of Various Resins

Thermo-mechanical graphs obtained on Specimen A samples for some thermoplastic materials under a load of 0.25 kg/cm² are shown on *Figure 6*. The results of other tests on thermosetting materials obtained on the same specimen A, are shown in *Figure 7*. The effects of heat on deformation as can be seen in *Figures 6-11*, allow the tracing of the growth of resilient and elastic deformation and plastic flow of the material. At sharp changes in curvature can be determined the transition of thermoplastics into viscous state.

The temperature of thermal stability or heat resistance of thermosetting materials is determined at the point of sharp rise in the curves 7-9. Further upward slope of the curves and the transition into parallelism with the abscissa shows the growths of the plastic flow. Second change in the slope corresponds with the temperature of the beginning of thermal degradation of the polymer chains. Epoxy resins (*Figure 7*) show a high level of elastic deformation which indicates a loose structural lattice of molecular chains. Compositions of furfuraldehyde-based resins (curve 3, *figure 7*) are characterized by only a single bend in the curve in the range of thermal degradation at about 340°F. The absence of elastic deformation on this curve can be explained by a tight molecular lattice. Other materials (*Figures 7-9*) are characterized by values of elastic deformation failing between the limits mentioned above. Particularly noteworthy is the decrease in deformation of silicone base resin (*Figure 7*) at temperatures of over 100°C. This can be tentatively explained by structural changes in the plastic leading to the densification of this material. The changes in the curvatures of the polymer represented by the solid line 3 in *Figure 8* in the region of 350°C also show structural changes in the material.

Characteristically, it was determined that the post cure of material CFFC (Phenolformaldehyde) at about 300°C curve 1 on *Figure 8* also raises impact strength from 4-6 kg. cm/cm² proving the theory of densification of polymer structure at 300°C.

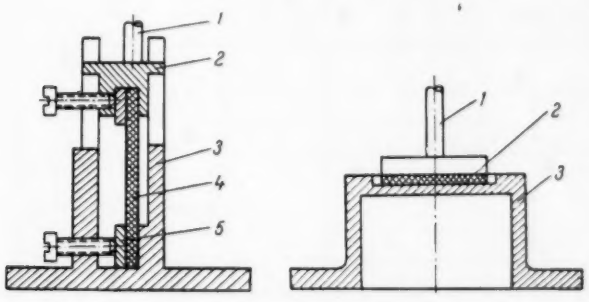

Figure 4. Fixture for the measurement of heat resistance of sheet and laminated materials (left)
(Specimen C for laminated plastics)
1. loading rod; 2. upper holder; 3. specimen holder; 4. test specimen; 5. lower clamping plate

Figure 5. Fixture for the measurement of temperature of transition by the measurement of deformation between layers
(Specimen-a flat disk)
1. loading rod; 2. test specimen; 3. specimen holder

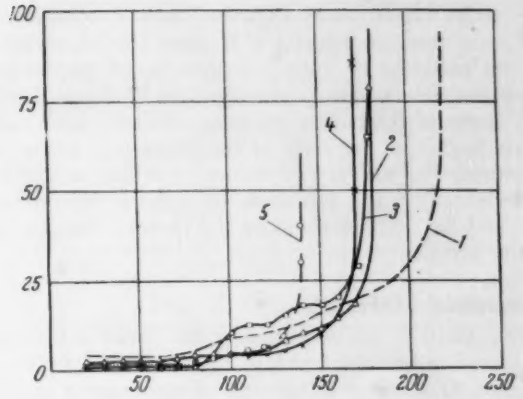

Figure 6. Relationships between deformation of thermoplastics and temperature under constant load
(Specimen A)
1. Teflon; 2. Moplen (——); 3. Vinyl chloride; 4. Polypropylene (experimental); 5. Hostalen (——); Measurements made under load of .25 kg/cm², and for Teflon 1 kg/cm²

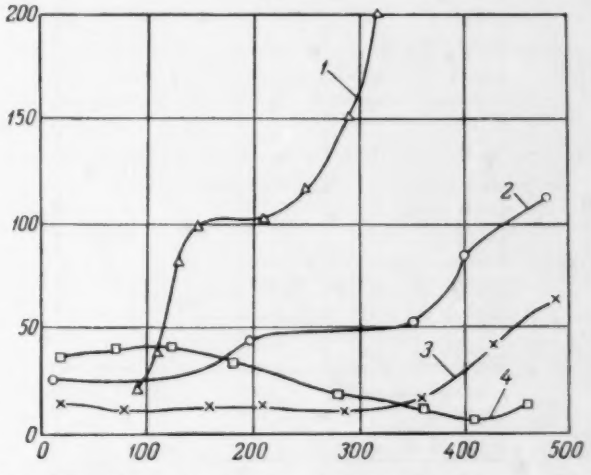

Figure 7. Relationship between deformation of thermosetting plastics and temperature under a constant load of 10 kg/cm²
(Specimen B)
1. epoxides; 2. polyester type K-15-6 (ref. 2); 3. furfural-acetone resin with asbestos filler; 4. silicone resin type KMK-9

A series of curves of *Figures 7 and 9*, obtained from results of tests on Specimen B show the effects of heat on the behavior of various materials. Of particular interest are the various magnitudes of the elastic deformation. Some of the curves are generally horizontal and the curve begins to rise only in the regions of higher temperatures. The absence of deformation can be accounted by, apparently, the formation of a dense structural lattice, and its rapid increase by the thermal decomposition of the polymer.

Laminated Materials

The method of determining the heat resistance of laminated materials by loss of rigidity, Specimen C, (*Figure 4*) has the advantage of minimizing the effect of the reinforcement on the index of thermal stability.

Results of tests on disk-shaped samples of polycarbonate, using the unidirectional compression method are shown on *Figure 11*. Here it shows that a lower molecular weight resin is characterized by a curve displaced in the direction of lower temperatures. Optimum condition for tests: Where a maximum deformation results from a minimum load.

Discussion of Results

The results obtained from the tests show that the proposed method can be used to investigate the progress of elastic deformation and plastic flow of various polymers. This guarantees a more accurate determination of criteria for heat resistance and the temperatures of transition into viscous flow of thermoplastics, and for built up polymers, (thermosets) the beginning of thermal degradation.

The basic aim of this method is to assist in the development of technological processes to obtain polymers of better quality and to better insure their evaluation. Methods of Martens, Vick and the determination of heat distortion by bending a specimen supported on two knife edges, do not satisfy the above requirements since they depend on the measurement of relative artificial constants.

When testing a specimen supported on two knife edges it is expected to obtain a defection of small magnitude which occurs in the region of elastic deformation. Further increasing the deflection will invariably make the specimen slide on the knife edges thus distorting the readings. At small deflections the range of transition into upper elastic limit state is not reached.

The various types of polymers possess a great range of values for plastic and elastic flow. Besides, in the cases of molecular structure changes caused by heat, the deformation of the material is decreased despite the fact that it remains under constant load. Therefore, test methods are required covering all types of deformation: Resilient, plastic and elastic. The magnitude of elastic deformation is tied in with the length of polymer chains and lattice density. (i.e. phenolic plastics). Sharp changes in the slope of temperature deformation curves attest the existence of structural changes or the beginning of thermal degradation of the space lattice.

Such information is important to correctly assess the properties of polymers and to select the ranges of their application. Similar data cannot be obtained from techniques based on the measurements of heat distortion for a predetermined deflection (i.e. deflection of 6mm for the Martens' method, 1mm for Vick's and 0.3mm for ASTM). Inasmuch as the same magnitude of deformation for different materials may be related to different phases of deformation (resilient, elastic and plastic), the criterion of heat resistance obtained by these measurements will not indicate the true changes in the materials under the action of heat. Products made from materials characterized by curves 1, 2 and 3 on *Figure 7* will have dissimilar properties at higher temperatures.

It appears practical to use the above method for heat resistance measurements in laboratory work of appraising production of plastics, development of better materials, etc. For further improvement of this technique the

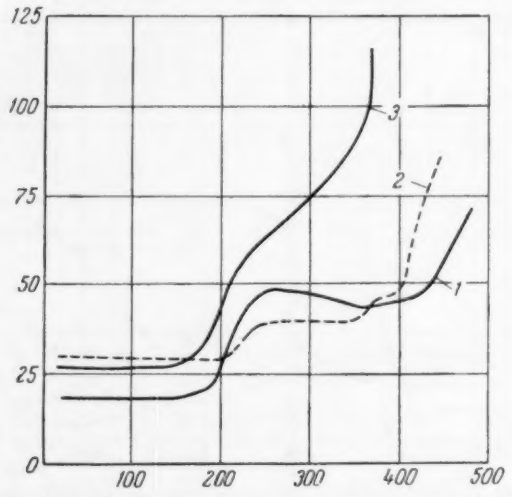

Figure 8. Relationship between deformation of thermosetting plastics and temperature under a constant load of 10 kg/cm² (Specimen A)
1. CFFC (Phenol formaldehyde); 2. FKPN-15T (Phenol-Cresol formaldehyde); 3. NFFC (unidentified)

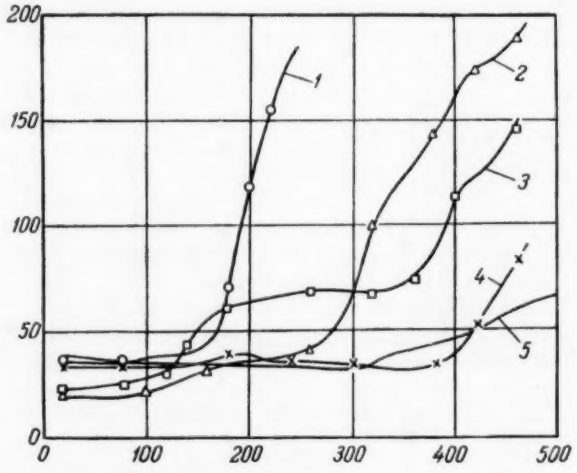

Figure 9. Relationship between deformation of thermosetting plastics and temperature under a constant load of 10 kg/cm² (Specimen B)
1. polyester type K-18-2; 2. epoxy-furfural plastic; 3. phenol furfural plastic; 4. furfural acetate plastic with graphite; 5. furfural acetone plastic

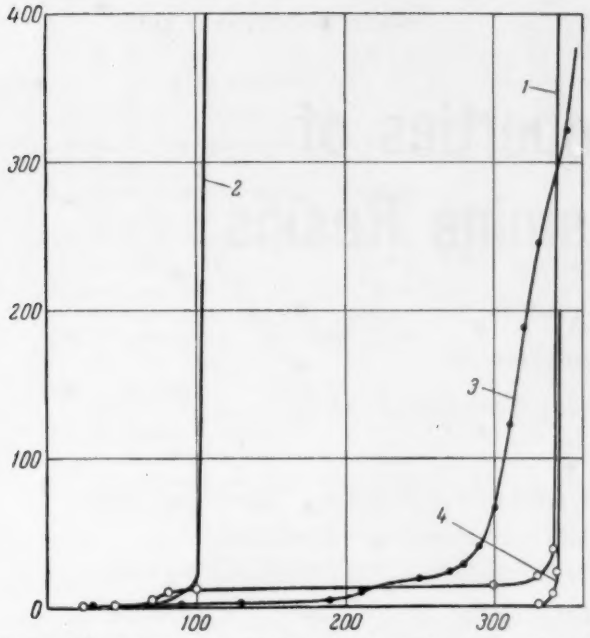

Figure 10. Relationship between deformation of laminated sheet materials and temperature under a constant load of 10 kg/cm²
(Specimen C)
1. fiberglas mat-polyester resin; 2. fiberglas-polystyrene resin; 3. melamine formaldehyde, laminated; 4. fiberglas fabric-polyester resin

use of automatic recording devices for plotting deflection-temperature curves is indicated.

Conclusions

1. Proposed are 3 types of original specimen configurations of small size which insure accurate measurement of deformation in shear and elongation at different temperatures and consequently accurate determination of the modulus of elasticity. The use of these specimens eliminates the distortion of results from slippage of specimens in specimen holder.

2. Method allows the investigation of changes in thermosetting materials, connected with structural changes in the polymer structure leading to variations in density and shrinkage.

3. During measurements of heat resistance of laminated materials (including reinforced fiberglas) the effect of reinforcement is minimized, important in development of better heat resisting resins.

Literature References

1. Kargin, V. A., Sokolova, T. I., The Question of Three Physical States of Amorpho-Liquid Linear Polymers, *Jour. Phys. Chem.* 23 iss. 5, 530 (1949).
2. Kargin, V. A., Malinski, U. M., Effect of Molecular Weight on the Transition Temperature of Polystyrene, *DAN U.S.S.R.* iss. 5, 915 (1950).
3. Kargin, V. A., Shteding, M. H., Thermomechanical Method of Study for High Polymers, J. P. C. 2 (1955).
4. Kargin, V. A., Slonimski, G. L., Determination of Molecular Weight of Linear Polymers from their Mechanical Properties, J. P. C. 23, 363 (1949).

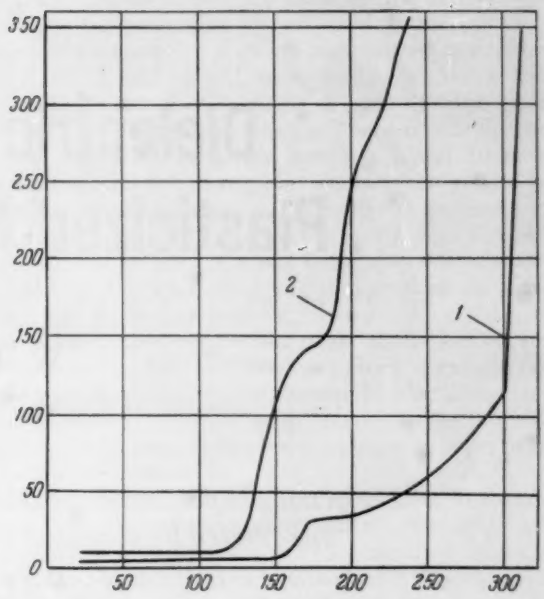

Figure 11. Relationship of deformation of polycarbonates with temperature under unilateral pressure
(Specimen-fig. 5)
1. resin with molecular weight of 63,000; 2. resin with molecular weight of 10,000

5. Slonimski, G. L. Kargin, V. A. Golubenkova, L. I., *DAN U.S.S.R.*, 93, 2 (1953).
6. Igonin, L. A., Krassulina, N. A, Kargin, V A., *Colloid Journ.* 17, 4 (1955).
7. Same as above-18, 1 (1956).
8. Slonimski, G. L., Kovarska, B. M., Klas, C. I., *Colloid Journ.* 16, 5, 390 (1954).
9. Regirer, E. N., Kalantarova, M. C., Methods of Obtaining and Interpreting Thermomechanical Curves, *Colloid Journ.* 17, 6 (1955).
10. Jurkov, C. N., Molecular Mechanism of Hardening of Polymers, *DAN U.S.S.R.*, 47, 7, 493 (1946), 49, 201 (1945).
11. Jurkov, C. N., Investigation of the Mechanism of Hardening of Polymers, Proceedings I and II of the Conference on High Polymer Bonds, Ed. AN U.S.S.R., 1945.
12. Maygeldinov, I. A., Report to the 7th Conference on High Polymer Bonds, Ed AN U.S.S.R. 1952.
13. Marey, A. I., Report to the 7th Conference on High Polymer Bonds, Ed. AN U.S.S.R. 1952.
14 Tarasov, V. V., Theory of Thermal Capacity of High Polymers, DAN U.S.S.R. 46, 3, 117 (1945).
15. Tarasov, V. V., Hydrogen Bonds in Crystals and Glasses and the Quantum Theory of Thermal Capacity of Chain and Laminated Structures, J. P. C. 26, 9 (1952).
16. Tarasov, V. V., Theory of Thermal Capacity of Chain & Laminated Structures, J. P. C. 24, 1. 111 (1950).
17. Zetlin, B. L., Gavrilov, V. A., Velicanova, K. A., Setup for the Investigation of Thermomechanical Characteristics of Polymers, Lab. Rep. No. 3 (1956).

Dielectric Properties of Plasticized Melamine Resins

W. C. Schneider

American Cyanamid Company, Stamford, Conn.

Dielectric properties of melamine resins may be affected by "dangling chains" surrounded by unreactive sites in a three-dimensional network polymer chain. It is further theorized that the number of dangling chains may be a function only of polymerization conditions (time, temperature, pressure) rather than the total amount of resin

There is little information in the literature concerning the dielectric properties of plasticized melamine resins. Therefore, a study was made of the variation of dielectric constant and loss as a function of frequency and temperature. Data are summarized below together with an indication of the major differences between these systems and thermoplastic systems.

Experimental

The materials investigated are listed in *Table 1*. They were formed into circular disc ⅛" thick and 4" in diameter by conventional compression molding techniques. Two-inch sample discs were cut from these larger discs and coated with "aqua-dag" to provide electrodes.

The electrical properties were determined with a Schering bridge constructed in these Laboratories. A sample cell similar to that described by Yager (1) was employed. Temperature control was provided by circulating cooled or heated toluene through the double walled jacket of a thermostat surrounding the sample cell. A current of dry nitrogen was passed through the space about the cell to prevent condensation of water

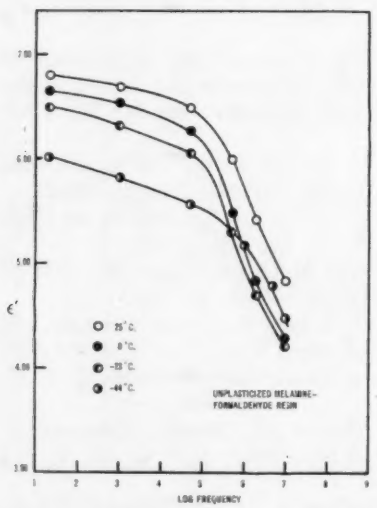

Figure 1. Frequency Variation of Dielectric Constant for Unplasticized Melamine Formaldehyde Resin At Various Temperatures.

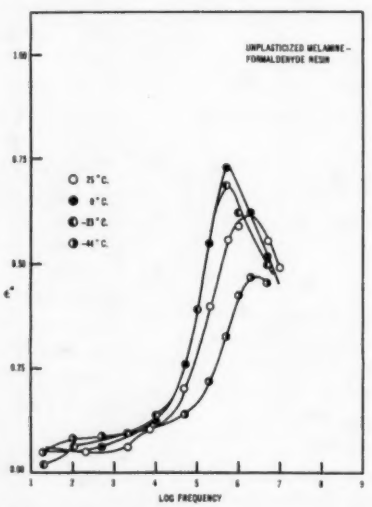

Figure 2. Frequency Variation of Dielectric Loss for Unplasticized Melamine Formaldehyde Resin At Various Temperatures.

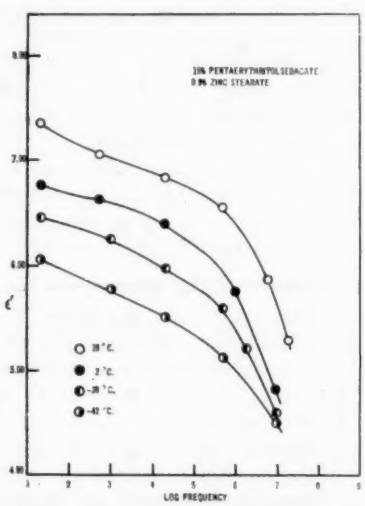

Figure 3. Frequency Variation of Dielectric Constant for the System Melamine Resin—15% Pentaerythritolsebacate at Various Temperatures.

Table 1. Materials Studied

Samples	Composition[a]	Cure
I	100% Melamine—Formaldehyde Resin F/M = 2.0)	
II	15% Pentaerythritolsebacate + 0.5% Zinc Stearate	10′ at 155°C
III	35% Pentaerythritolsebacate + 1.0% Zinc Stearate	10′ at 155°C
IV[b]	25% Polyvinylbutyral + 10% Benzamide + 1.0% Zinc Stearate	10′ at 155°C
V[c]	10% Polyesteramide + 1% Zinc Stearate	10′ at 155°C
VI[d]	10% Nylon FM-101 + 5% Mono O-Cresylglycerylether + 1.0% Zinc Stearate	15′ at 155°C
VII[d]	20% Nylon FM-101 + 10% O-Cresylglycerylether + 1.0% Zinc Stearate	20′ at 155°C

[a] In those cases not totaling 100% the difference is melamine-formaldehyde resin.
[b] U.S.: 2, 546,841
[c] U.S.: 2, 801,226
[d] U.S.: 2,739,081

vapor on the cell leads at low temperatures. Measurements were made over the frequency range 20 to 10^7 cps., and at the nominal temperatures −40°, −20°, 0°, and +25°C.

Melamines vs Thermoplastics—Marked Contrast

The plasticizers listed in *Table 1* represent a range of types: Pentaerythritolsebacate, a relatively low-molecular weight, compound; polyvinylbutyral, a high-molecular weight, polymer; and an experimental polyesteramide, and a polyamide, Nylon FM-101 both being polycondensation polymers. All of these materials contained polar groups to provide some degree of compatability with the melamine-formaldehyde resin.

Dielectric constant (ϵ') data are summarized in *Figures 1, 3, 5, 7, 9, 11, and 13* and corresponding dielectric loss (ϵ'') data in *Figures 2, 4, 6, 8, 10, 12, and 14*. The gross features of these curves are similar. There is a high frequency ϵ'' maximum occurring between 1 and 10 mcs. The frequency at this maximum seems to be relatively independent of temperature and of both the amount and type of plasticizer. This is in marked contrast to the behavior observed in most thermoplastic systems, wherein the loss-factor maximum is strongly dependent on temperature and plasticizer content.

In addition to the primary loss peak, all the loss curves are skewed toward low frequencies. Indeed, some display an indisputable secondary maximum. Similar secondary maxima have been observed with thermoplastics and are thought to reflect interactions between polar groups, pendant to the main chain.

The observations noted above are qualitative in nature. However, over the years a more quantitative approach has developed. Initially, Debye (2) postulated that the dispersion in dielectric properties (rapid decrease of ϵ' and associated peak in ϵ'') was a relaxation process, wherein dipoles could not stay in phase with an applied, alternating, electric field. A characteristic relaxation time time could be associated with this process. Experiments soon showed that many real systems (associated liquids, polymers, etc.) could not be described by a single relaxation time, but required a distribution of relaxation times. Several semi-empirical distribution functions have been derived (3, 4, 5). That proposed by Cole and Cole (4) has been employed to analyze the data presented here.

Briefly, Cole and Cole found that a plot of ϵ'' versus ϵ' would yield a semi-circle for systems described by a single relaxation time, but only a circular arc for those requiring a distribution of relaxation times. A parameter characterizing the distribution could be calculated from

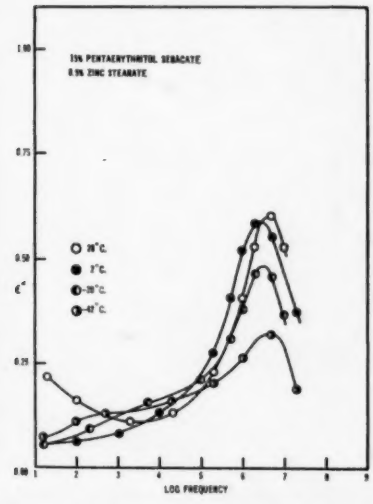

Figure 4. Frequency Variation of Dielectric Loss for the System Melamine Resin—15% Penaerythritolsebacate at Various Temperatures.

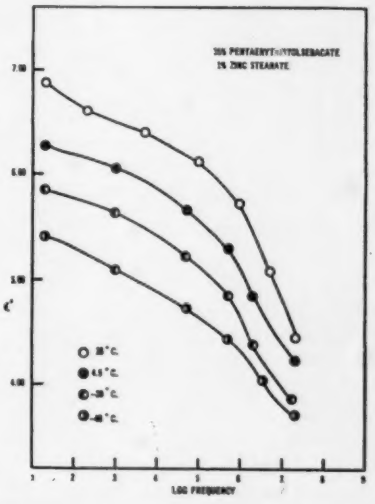

Figure 5. Frequency of Dielectric Constant for the System Melamine Resin —35% Pentaerythritolsebacate at Various Temperatures.

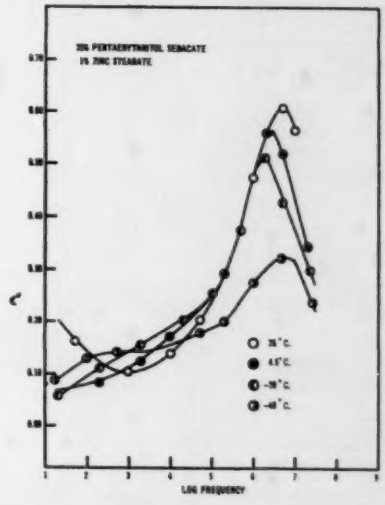

Figure 6. Frequency Variation of Dielectric Loss for the System Melamine Resin—35% Pentaerythritolsebacate at Various Temperatures.

Table 2. Critical Frequencies and Cole and Cole Distribution Parameter

Sample		High Frequency (ν_c in megacycles)				Low Frequency (ν_c in kilocycles)			
		—40°C	—20°C	0°C	25°C	—40°C	—20°C	0°C	25°C
I	ν_c[a]	3.1	0.83	—	2.2	—	—	—	—
	β[b]	0.29	0.42	—	0.47	—	—	—	—
II	ν_c	5	3.5	2.5	8.0	—	—	—	—
	β	0.55	0.40	0.34	0.38	—	—	—	—
III	ν_c	3.2	1.8	2.2	3.5	1.8	5	28.2	—
	β	0.39	0.32	0.19	0.32	0.68	0.56	0.42	—
IV	ν_c	12	12	~12.5	~10	0.4	3.5	70.5	159
	β	0	0.23	0.41	0.28	0.64	0.62	0.70	0.50
V	ν_c	3.2	2.5	2.7	2.2	—	0.2	5.6	50
	β	0.36	0.19	0.35	0.26	—	—	0.35	0.26
VI	ν_c	—	5.0	4.0	5.0	—	—	0.1	11
	β	—	0.26	0.28	0.12	—	—	—	0.54
VII	ν_c	2.0	1.6	1.6	1.6	—	—	0.22	20
	β	0.46	0.32	0.12	0.58	—	—	0.71	0.31

[a] Critical frequency calculated from Cole and Cole plot.
[b] Cole and Cole distribution parameter.

the angle of depression of the diameter of the semi-circle below the ϵ'' axis required to fit any given experimental system. The Cole and Cole distribution function was selected because it (1) yields a parameter characterizing the distribution of relaxation times, (2) allows a separation of dispersion regions when more than one is present, (3) provides values of the limiting dielectric constants for each dispersion region, and (4) enables a more precise determination of critical frequency (frequency of maximum ϵ'') than is afforded by simple inspection of dielectric loss curves. A typical example (from the present work) of a Cole and Cole plot is given in Figure 15.

Table 2 lists critical frequencies and distribution parameters determined from Cole and Cole plots. Again, the apparent insensitivity of the high-frequency losses to temperature is noted. One possible cause of this behavior is that the units giving rise to this loss are "dangling chains", surrounded by unreactive sites in a three-dimensional network. Since the structure is quite rigid, due to cross-linking, the local environment of these "dangling chains" is altered only slightly by temperature. It is believed that this loss is associated with the melamine-formaldehyde resin in the system, since this is the only loss peak observed in the non-plasticized sample. It is not clear why the height of this loss peak is essentially independent of the amount of melamine-formaldehyde resin present. This independence suggests that the number of "dangling chains" may be a function only of polymerization conditions (time, temperature, pressure, etc.) rather than total amount of resin.

In contrast to the high-frequency losses, the secondary losses observed at lower frequencies exhibit the same general behavior as found with thermoplastic systems. This is not too surprising since it is believed that the secondary losses result almost entirely from the plasticizers. There is some evidence in the literature to support this view. Sample IV, *Figure 9*, (plasticized with polyvinylbutyral) possesses a loss maximum at 158 kc at 28°C. Funt (6) has measured the electrical properties of polyvinylbutyral over a range of frequencies and temperatures. Although he was primarily concerned with the high-temperature, primary losses, his data strongly suggest that the losses at 30°C are approaching a maximum near 100 kc. Also, samples VI and VIII, *Figures 12 and 14* (plasticized with nylon) exhibit loss maxima in the region 10 to 20 kc at 25°C. Recently, Ishida (7) has reported a similar maximum in nylon 6, occurring at 40 kc at 25°C.

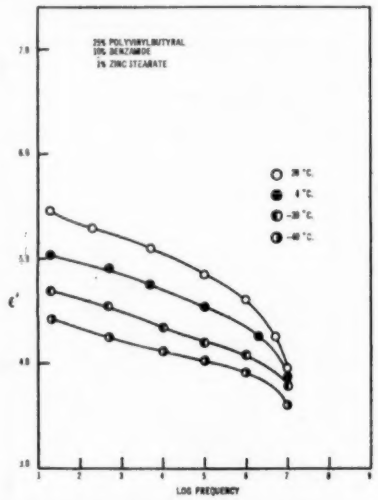

Figure 7. Frequency Variation of Dielectric Constant for the System Melamine Resin—25% Polyvinylbutyral—10% Benzamide at Various Temperatures.

The low-frequency loss maxima shift toward lower frequency with decreasing temperature and become

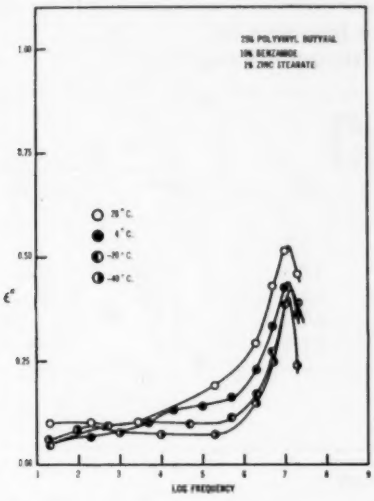

Figure 8. Frequency Variation of Dielectric Loss for the System Melamine Resin—25% Polyvinylbutyral—10% Benzamide at Various Temperatures.

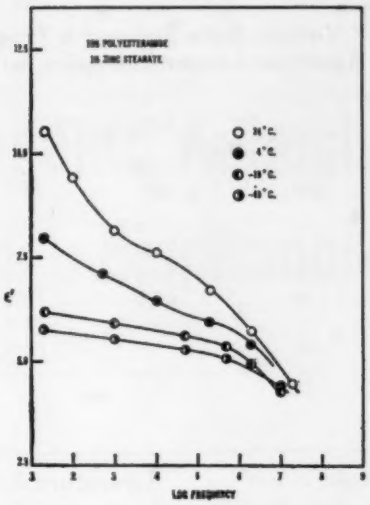

Figure 9. Frequency Variation of Dielectric Constant for the System Melamine Resin—10% Polyesteramide at Various Temperatures.

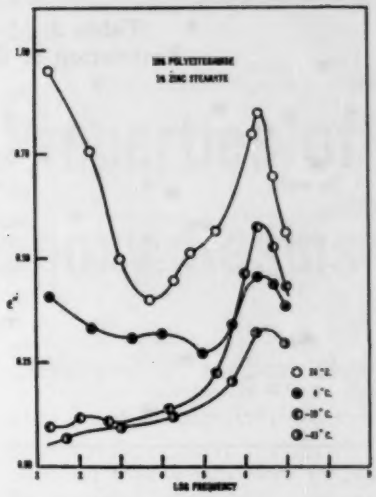

Figure 10. Frequency Variation of Dielectric Loss for the System Melamine Resin—10% Polyesteramide at Various Temperatures.

somewhat broader and flatter. The Cole and Cole parameter β listed in *Table 2* gives a more quantitative indication of the wider distribution of relaxation times at low temperatures. This frequency shift with temperature provides a means for obtaining a qualitative measure of the size of the relaxing units and the energies involved in the relaxation process. Following Eyring (8), free energy, ΔF°, enthalpy, ΔH°, and entropy, ΔS°, of activation may be determined from the critical frequencies, f_c, by using the expressions:

$$\Delta F^\circ = 4.6\ T\ \log\left[3.34 \times \frac{T}{f_c} \times 10^9\right]$$

$$\log\ (fc/T) = \frac{\Delta S^\circ}{2.3R} + \log\frac{10^{-9}}{3.34} - \frac{\Delta H^\circ}{2.3RT}$$

The enthalpy of activation is most easily determined graphically. Typical plots are given Figure 16. Values found are as follows, listed in the sequence, sample: ΔH° (kcal./mol.): III: 8.5, IV: 13.4, V: 22.2, VI: 25.5, VII: 38.3. Values of ΔF° determined by the relation given above and values of ΔS° obtained by subtraction are recorded in *Table 3*. All of these data suggest a progressive increase in restriction of dipole rotation, larger entropies and enthalpies of activation, as the plasticizer changes from a low molecular weight plasticizer to a

* ΔF in kcal/mol
ΔS in kcal/mol/°K

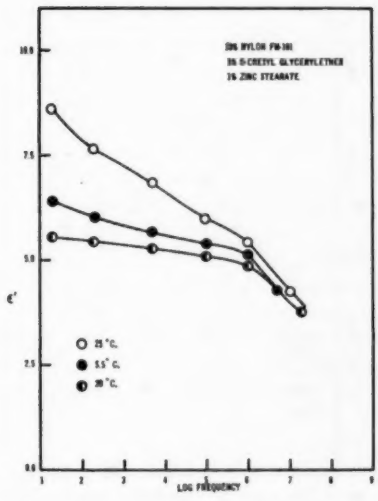

Figure 11. Frequency Variation of Dielectric Constant for the System Melamine Resin—10% Nylon FM-101-5% O-Cresylglycerylether at Various Temperatures.

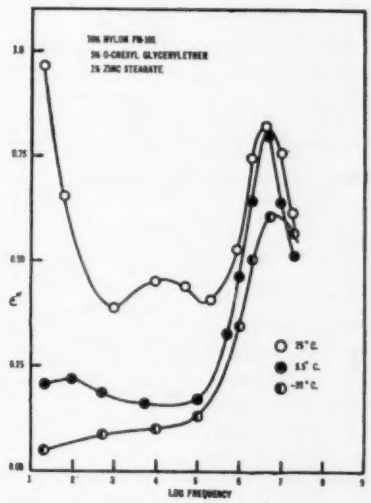

Figure 12. Frequency Variation of Dielectric Loss for the System Melamine Resin—10% Nylon FM-101-5% O-Cresylglycerylether at Various Temperatures.

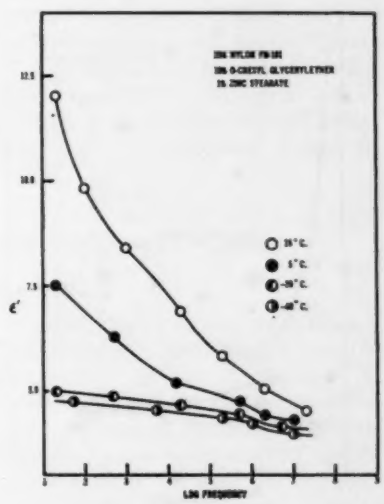

Figure 13. Frequency Variation of Dielectric Constant for the System Melamine Resin—20% Nylon FM-101-10% O-Cresylglycerylether at Various Temperatures.

Table 3. ΔS and ΔF Values. Data Suggest a Progressive Increase in Restriction of Dipole Rotation, Larger Entropies, with Plasticizer Changes

	Temperature °C							
	−40		−20		0		25	
Sample	ΔF#	ΔS#	ΔF#	ΔS#	ΔF#	ΔS#	ΔF#	ΔS#
III[a]	9.25	(−3.2)	9.60	(−4.4)	9.50	(−3.6)	—	—
IV	9.95	14.4	9.75	14.4	9.06	15.6	9.42	13.2
V	—	—	11.3	43.0	10.5	42.5	9.95	41.5
VI	—	—	—	—	12.8	45.5	10.9	49.0
VII	—	—	—	—	12.4	93.0	10.3	94.0

[a] ΔF# in kcal/mol
ΔS# in kcal/mol/°K

higher molecular weight polymer. This could reflect increasing interaction between plasticizer and thermosetting resin. It is of interest to note that ranking, according to efficiency of plasticization, as defined by reduction of shrinkage and internal stress, yields essentially the same sequence as *Table 3*.

However, the degree of interaction between plasticizer and resin at the molecular level appears to be only slight. The high frequency loss peak is essentially unaffected by plasticization. Also, the dielectric behavior of the plasticizing compounds (at least from −40° to +25°C) seems to be little influenced by the resin. The data are not inconsistent with the hypothesis that the compounds discussed here, containing enough polar groups similar to those of the resin to allow sufficient compatability, can affect the macro-mechanical properties to provide some degree of toughness. Unpublished work of the author has disclosed that the dynamic mechanical Young's modulus of these systems is lowered, and that Samples VI and VII exhibit a maximum in the mechanical loss factor at approximately the same frequency as the maximum in ϵ'' reported here.

Literature References

1. Yager, W. A., Trans. Electrochem. Soc., *74* 117 (1938).
2. Debye, P., Polar Molecules, 77 Chem Catalog Co., New York (1929).
3. Yager, W. A. *Physics* 7 434 (1936).
4. Cole, K. S. and Cole, R. H., *J Chem. Phys.*, 9 341 (1941).
5. Kirkwood, J. G. and Fuoss, R. M., *J. Amer. Chem. Soc. 63* 395 (1941).
6. Funt, B. L., Can. *J. Chem. 30* 84 (1952).
7. Ishida, Y., Kolloid—Z., *168* 29 (1960).
8. Powell, R. E. and Eyring, H., *Advances in Colloid Science*. Vol. I Interscience, New York (1942).

Acknowledgments

The author wishes to thank Mr. H. Wohnsiedler for providing the experimental resins and Mr. R. MacFarlane, Jr. for assistance in carrying out the electrical measurements.

This article was adapted from a paper presented to the American Chemical Society, 138th National Meeting, New York, N. Y.

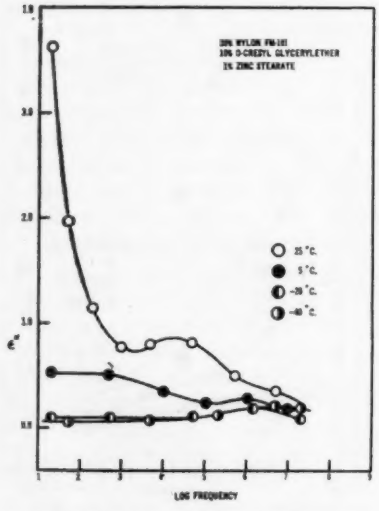

Figure 14. Frequency Variation of Dielectric Loss for the System Melamine Resin—20% Nylon FM-101-10% O-Cresylglycerylether at Various Temperatures.

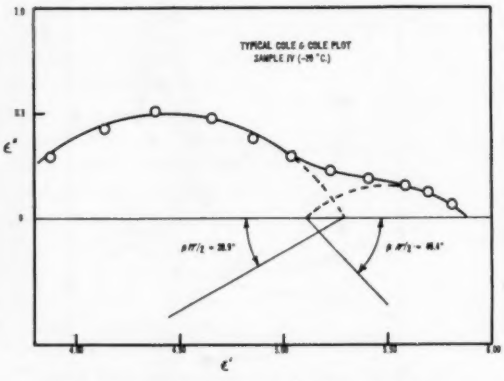

Figure 15. A Typical Cole and Cole Plot Using Data Obtained with the System Melamine Resin—25% Polyvinylbutyral—10% Benzamide.

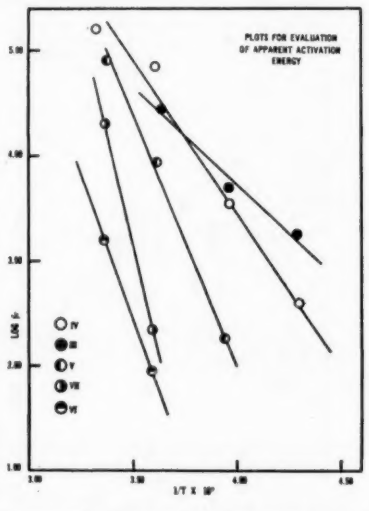

Figure 16. Plots of the Logarithm of the Critical Frequency as a Function of the Reciprocal of the Absolute Temperature.

Cryogenic Adhesive Properties of Bisphenol-A Epoxy Resins

M. J. Hiza and P. L. Barrick*

Cryogenic Engineering Laboratory
National Bureau of Standards

This article describes studies designed to extend the performance characteristics of adhesive systems of a selected resin type to temperatures below 100°K and, specifically, to provide in part a basis for the formulation of a structural adhesive with optimum cryogenic properties

The present study includes a comparison of the adhesive properties of bisphenol-A epoxides at 300°K and 76°K with respect to the molecular weight of the uncured resins. Joints of 2024 aluminum were tested at 300°K and 76°K in tensile-shear and in impact-shear, and total linear thermal contraction of the cured resins was measured between the two temperatures. Results are discussed with respect to residual joint stresses and adsorptive properties of the resins. In the past, work with adhesives in the extremely low temperature region has been restricted to testing of commercial adhesives which were not specifically formulated for low temperature applications (1, 2, 3, 4).

A basic study to achieve the optimum cryogenic adhesive might well include: 1. the selection of a promising resin type; 2. the determination of effect of chemical structure of this type on adhesive properties at the low temperatures in comparison with ambient temperature properties; 3. optimization of low temperature properties by chemical means; 4. optimization of low temperature properties by physical means; and 5. an extension of such a program to other promising resin types, and finally to resin mixtures. It is recognized that all of these considerations are not independent nor necessarily applicable in all cases, and that other variables might be significant. Since it is not practical to investigate all combinations of factors, the present study has been limited to parts 1 and 2 with some consideration of part 3.

The epoxy resins selected as the subject of this investigation produce bonds of varying strength dependent on the chain length of the resin and the crosslinking agent used in curing. N. A. de Bruyne (5) has shown this dependence of strength on chemical structure of the resin with aluminum lap joints at normal temperatures using phthalic anhydride as a curing agent. Such a relation may also exist at cryogenic temperatures provided thermal stresses developed in cooling do not act to reduce the native strength of the stronger bonds.

It was decided that experiments with unmodified epoxy resins of the same chemical derivation to determine the effect of molecular weight variation of the uncured resins would provide the best criteria for further development of the desired systems. These experiments consist of (a) the quantitative determination of epoxide equivalents, (b) measurements of total linear thermal contraction of the bulk cured resins from 300°K (27°C) to 76°K, and (c) the determination of tensile-shear strengths of aluminum lap joints at 300°K and at 76°K, and (d) the impact-shear strengths of aluminum block joints at 300°K and at 76°K as a function of molecular weight of the uncured resins. The molecular weight is calculated from item (a).

MATERIALS AND METHODS

Resins and Curing Agent

Epoxy resins, derived from the polycondensation of epichlorohydrin and bisphenol-A, have the following general formula: (next page)
where "n" varies between 0 and 10 for the commercial resins (6). The epoxide equivalent, representing the grams of resin containing one gram equivalent of epoxide, was determined experimentally for each resin tested by reaction of the epoxide groups with known amounts of HCl and titrating with a base to determine the quantity of unreacted Cl (7). The average molecular weight of the resin fraction is twice the epoxide equivalent. These and calculated values of "n" are shown in *Table 1*.

* Professor of Chemical Engineering, University of Colorado.

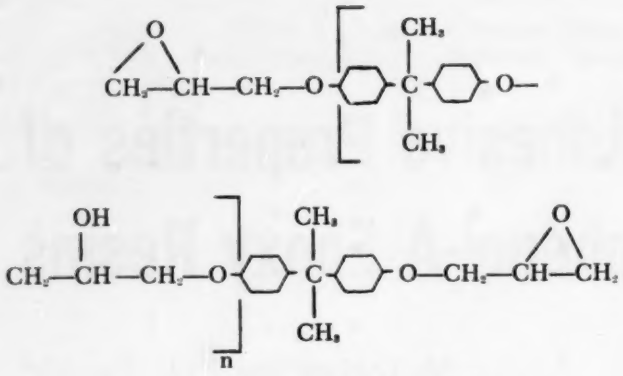

structure continues

Meta-phenylenediamine (MPD) was used in this investigation, primarily to eliminate the need of determining optimum amounts of curing agent for each of the resins. This aromatic compound can be assumed to have four reactive hydrogens, each capable of reacting with an epoxide group without the formation of by-products. The stoichiometry of the resin-curing agent system is readily calculated from the experimentally determined epoxide equivalents (8). It was assumed that when complete reaction occurs, one-fourth of a gram molecular weight of meta-phenylenediamine reacts with one epoxide equivalent of the resin. These values are also listed in *Table 1*.

In addition to low shrinkage typical of amine cures, adhesives hardened with MPD display much better shear strengths at elevated temperatures than those cured with aliphatic amines (9). Assuming that either adhesive system is susceptible to chemical damage at the higher temperature, a difference in strength retention would be due partially to a difference in thermal expansivity of the two adhesive systems. Low cure shrinkage and low thermal expansivity are both desirable for applications at cryogenic temperatures.

Specimen Preparation

Specimens for tensile-shear and impact-shear are shown in *Figure 1*. The lap shear specimens of 0.125 inch thick 2024 aluminum were fabricated to provide a bond width and an overlap length of ½ inch with a bonding area of ¼ square inch. Impact specimens of 2024 aluminum were fabricated to conform to ASTM (D950-52T) (10). All surfaces were prepared for bonding by 1. mechanical cleaning to remove foreign particles and heavy oxide coatings, 2. solvent degreasing by immersion in carbon tetrachloride, and 3. chromic acid etching. Mechanical cleaning of the impact specimens was unnecessary since these pieces were machined to size. The specimens were then given a final water rinse and dabbed dry with tissue.

Adhesive bonding was completed as soon after surface preparation as possible using a hot melt technique. Specimens were cured one hour at 110°C with bonding pressure sufficient only to ensure good contact (maximum ¼ psi). Adhesive thickness for all specimens varied from a minimum of 5 to a maximum of 20 mils. Thin adhesive layers were generally representative of the low molecular weight, and the thicker ones of the high molecular weight. Within these limits, variations in the thickness of the adhesive layer would produce no noticeable variation in bond strength (3).

Table 1. Resin Descriptions and Curing Agent Proportions

Resin	Melting Point °C	Epoxide Equivalent	Molecular Weight	n	phr MPD[a]
R-1	liquid	192	384	0.15	14.1
R-2	40-45	317	634	1.03	8.5
R-3	65-75	519	1038	2.46	5.2
R-4	95-105	904	1808	5.16	3.0

[a] Parts of meta-phenylenediamine per hundred parts of resin, by weight

Test Procedures

The lap shear specimens were loaded in tension in a hydraulic tensile testing machine at load rates not exceeding 150 pounds per minute. In addition to the axle type supports used for these specimens, a chain section of several links was added at each end of the test specimen to minimize bending loads. The specimens tested at 76°K were immersed in a bath of liquid nitrogen during the test, and for a sufficient time prior to testing to ensure complete cooling. No precaution was taken to control the cooling rate of any of the specimens, including those tested in impact.

Block shear specimens were subjected to impact loads in a standard plastics impact testing machine at a pendulum heat velocity of 17 feet per second. Due to the nature of this test, specimens to be broken at 76°K had to be retained in a liquid nitrogen bath remote from the test position and transferred to the machine supports for testing. As a result, the temperature of the joint at the time of failure was higher than 76°K. Measurements were made to determine the magnitude of this temperature change from the time the specimen was removed

Figure 1. Adhesive specimens for (top to bottom) impact-shear and tensile-shear tests and thermal contraction measurements

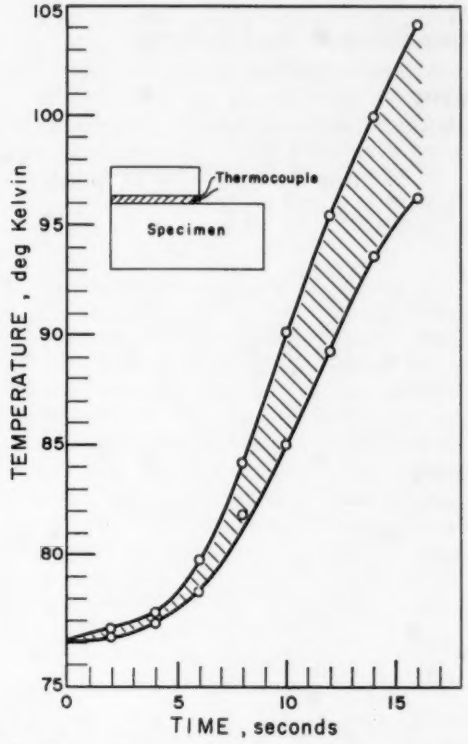

Figure 2. Temperature change of adhesive vs time after removal of an impact-shear specimen from liquid nitrogen

from the bath up to 10 seconds after it was in the test position. The measuring thermocouple was positioned in the leading edge of the adhesive layer since this would be the most critical temperature. The results shown in *Figure 2* are the highest and lowest temperatures attained at the indicated times in five determinations. The average time to transfer the specimen to the support was 3.5 seconds; the test was completed in 5 seconds or less, with a maximum temperature increase in the adhesive layer of 2°K.

A bulk specimen of each resin system was cast in an aluminum foil mold using the same technique and cure schedule as for the bonded specimens. The ends and one side were finished flat with a final specimen length of approximately 10 cm. (*Figure 1*). The thermal contraction was determined by measuring the specimen length with a horizontal cathetometer at room temperature and submerged in liquid nitrogen. At least five length measurements were made at each temperature with a reproducibility of ±0.01 mm. For an average total specimen contraction of 0.84 mm., the error involved is not more than 5 percent, neglecting a relatively small change in room temperature from 300°K.

RESULTS

Mechanical Strength

The tensile-shear strengths obtained in these tests are shown in *Figures 3 and 4*. The point and the line at each point represent an average strength for five specimens at each test condition, unless otherwise noted in *Table 2* (Tensile-Shear Strengths), and the spread in the data respectively. These values do not represent absolute shear stress but rather a combination of stresses due to the offset loading and the specimen deformation that occurs in a lap joint. However, this joint can be used to describe relative adhesive strengths of the different resins investigated. No permanent deformation of adherend was observed for any of the lap joints tested.

To compare the tensile-shear values of this investigation with those obtained by other experimenters, allowance must be made for the difference in adherend thickness and the effect of eccentric loading, assuming overlap length and adherend material are the same. Other factors being equal, stronger joints will be produced with the thicker adherends than the thinner ones, dependent on the cohesive strength of the adhesive (11).

A comparison is made in *Figure 3* between the room temperature strengths of the resins tested and those of resins with the same chemical derivation reported by N. A. de Bruyne (5). The specimens in the latter case were lap joints made with 0.064 inch thick 24S (2024) aluminum, 1 inch wide, with ½ inch overlap. The two sets of experiments show a similar increase in tensile-

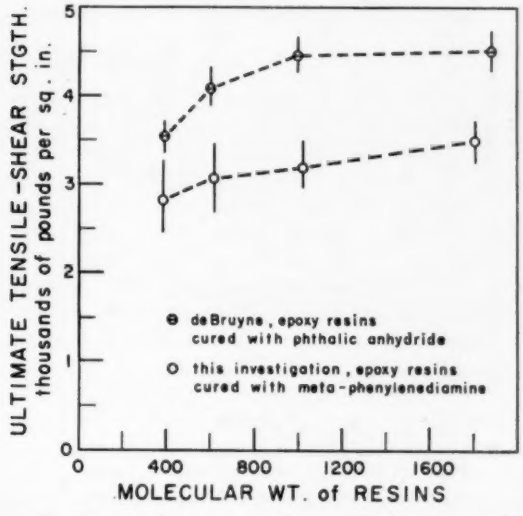

Figure 3. Tensile-shear strengths at 300°K vs molecular weight

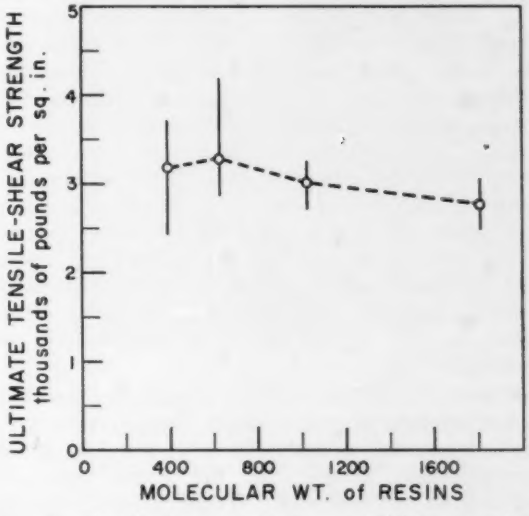

Figure 4. Tensile-shear strengths at 76°K vs molecular weight

Table 2. Analysis of Significance of Temperature Effect at the 5% Level

TENSILE-SHEAR STRENGTHS

Resin	R-1		R-2		R-3		R-4	
T °K	300(1)	76(2)	300	76	300	76	300	76
n (OBS)	4	4	5	5	5	5	5	5
$\bar{X}$ (psi)	2829	3185	3074	3272	3187	3027	3501	2778
$s_{\bar{x}}$	189	280	166	242	88	87	78	91
$s_{(\bar{x}_1 - \bar{x}_2)}$	338		293		124		120	
t (calc.)	1.053 N.S.		0.676 N.S.		1.29 N.S.		6.03 S.	
$t_{\frac{\alpha}{2}, n_1 + n_2 - 2}$	2.447		2.306		2.306		2.306	

IMPACT-SHEAR STRENGTHS

Resin	R-1		R-2		R-3	
T °K	300(1)	76(2)	300	76	300	76
n (OBS)	4	4	5	5	3	3
$\bar{X}$ (Ft-lb)	14.08	3.07	12.09	1.75	9.39	3.49
$s_{\bar{x}}$	0.61	0.41	0.81	0.74	1.15	1.70
$s_{(\bar{x}_1 - \bar{x}_2)}$	0.74		1.05		2.06	
t (calc.)	14.88 S.		9.85 S.		2.86 S.	
$t_{\frac{\alpha}{2}, n_1 + n_2 - 2}$	2.447		2.306		2.776	

shear strength with molecular weight and indicate a strength superiority of the phthalic anhydride cured resins over those cured with meta-phenylenediamine. The difference in strength between the two cures would be more pronounced had identical adherend thicknesses been used.

The 76°K tensile-shear strengths (*Figure 4*) do not vary in the same manner as the room temperature values. Apparently, the strength increases with an increase in molecular weight to approximately 700; thereafter, the strength decreases. The average 76°K strengths of joints made with the 384 and 634 molecular weight resins are higher than for the respective room temperature joints.

The impact-shear strengths shown in *Figure 5* are the energies required to cause failure in the joints. As in the tensile-shear strength plots, the point is the average value of strength for the specimens tested and the line represents the spread in data. These values do not include the energy required to accelerate the top adherend piece out of the test support. Five specimens were prepared for each impact test condition; however, several specimens were rejected due to imperfections in geometry (*Table 2*, Impact-Shear Strength). Impact strengths for the highest molecular weight resin were not determined.

For the resins tested, resistance to impact loading at room temperature decreases almost linearly with an increase in molecular weight. The impact values at 76°K are considerably lower than the room temperature values due to embrittlement of the polymer structure. Because of the large spread in values and the small number of specimens tested, the variation in impact strength at 76°K with molecular weight is not indicative of any real trend.

Modes of Failure

A change in mode of failure occurred between the 300°K and the 76°K tests, and the distribution of adhesive between adherend pieces in most cases was dependent on molecular weight.

All tensile-shear failures at 300°K occurred at or very near the adhesive-adherend interface involving both adherend surfaces; the total amount of adhesive was

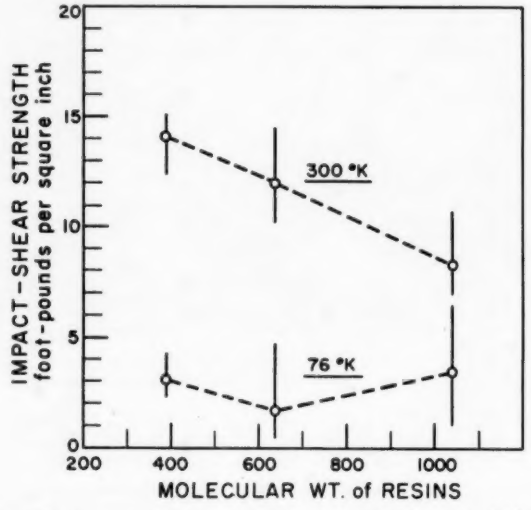

Figure 5. Impact-shear strengths at 300°K and 76°K vs molecular weight

distributed between the two surfaces in a varying manner. The transition of failure between surfaces for specimens of the two lower molecular weight resins was random. However, the transition in specimens of the higher molecular weight material occurred near the center of overlap with nearly the entire amount of adhesive remaining on one adherend piece on either side of the transition. This latter effect was more pronounced in specimens of R-4 (M.W. = 1808) than in those of R-3 (M.W. = 1038).

The tensile-shear failures at 76°K occurred in a plane at or near one adherend surface leaving the bulk of the adhesive on the other adherend piece. These failures varied with molecular weight in such a manner that no visible adhesive film was left on one adherend surface for specimens of the lowest molecular weight resin whereas a thin adhesive layer, increasing in thickness with molecular weight, was left on one of the adherend surfaces for specimens of the three higher molecular weight resins. This thin adhesive layer was almost nondetectable in specimens of R-2 (M.W. = 634). This suggests that even specimens of R-1 (M.W. = 384) might have failed in the same manner as the higher molecular weight resins leaving an adhesive film which was not detectable by visual means.

Typical failures of joints made with R-2 (*Figure 6*) illustrate the random distribution of adhesive between adherend surfaces at 300°K and the change in mode of failure of 76°K from that at 300°K.

Failures in impact-shear at 300°K resembled the corresponding tensile-shear failures in that all appear to have failed at or very near the adhesive-adherend interface and the size of the adhesive pieces clinging to adherend surfaces increased with molecular weight. However, the distribution of adhesive between mating surfaces was random in all impact specimens tested at this temperature. The lower temperature tests produced the same change in mode of failure from the room temperature tests except that failures of specimens resulted in a thin adhesive layer remaining on one adherend surface with no noticeable variation in the thickness of this layer. Specimens of R-2 (*Figure 7*) illustrate typical impact-shear failures obtained at both temperatures.

Thermal Contraction

The magnitudes of shrinkage involved in cooling the bulk adhesives, cured with MPD, to the temperature of liquid nitrogen are compared in *Figure 8* with the graphically integrated thermal expansivity of aluminum between 76°K and 300°K and the thermal contraction of an epoxy resin (approximate M.W. = 400), filled and unfilled, which was cured with an aliphatic amine. The filled resin contained approximately 50 percent by weight of alumina, and the curing agent used in both cases was diethylaminopropylamine (DEAPA).

The values given for the adhesives represent the negative change in total length between 300°K and 76°K divided by the 300°K length. As a result, they are not equivalent to integrated linear thermal expansivity. However, since change in length per unit length between the two temperatures is much less than unity, values for a given material derived from the two methods would differ only by about 1 percent.

Figure 6. Tensile-shear failures (top to bottom) at 300°K and 76°K

DISCUSSION OF RESULTS

Mechanical Strength

A statistical analysis of the significance of temperature effect on both tensile-shear and impact-shear strengths for each resin tested is summarized in *Table 2*. Assuming normal distribution, the student "t" was used to test the hypothesis that the true mean of the population at 76°K is equal to the true mean of the population at 300°K for an equal tails test at the 5% level (12). The notations N.S., S. and Q.S. after the calculated "t" indicate not significant, significant and questionable significance respectively.

It should be noted that measurements of the mechanical strength of adhesive joints provide numbers indicative of strength available to endure service loads for the type of joint used and are not generally applicable for the evaluation of one specific property (13).

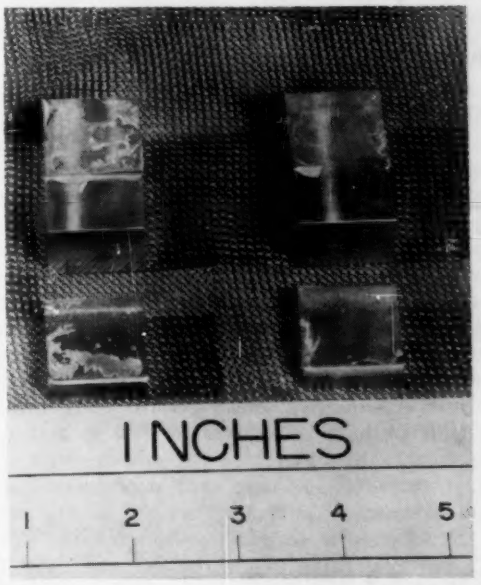

Figure 7. Impact-shear failures (left to right) at 300°K and 76°K

Figure 8. Total thermal contraction of cured epoxy resins and aluminum between 300°K and 76°K

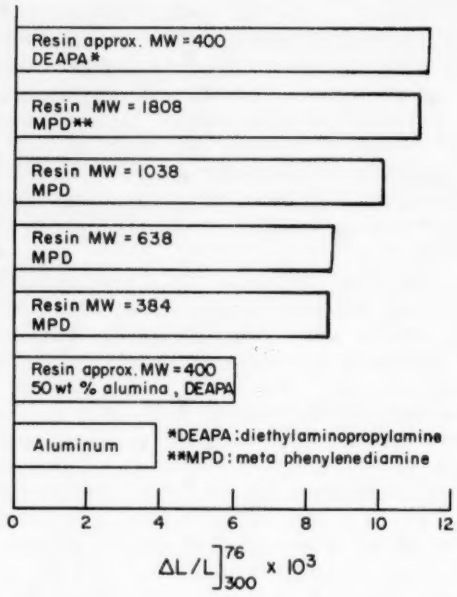

Other than variations in geometry, the three factors which contribute most to the ultimate joint strength and mode of failure are adhesive properties at the adhesive-adherend interface, cohesive properties of the adhesive, and residual stresses resulting from differential dimensional changes between the adhesive and adherend after a bond has been established at the interface. To interpret the results of this investigation, then, each of these factors and its contribution to the properties of the joint must be considered.

Adhesive and Cohesive Properties

Adhesive properties are developed in the early stages of bond preparation. It can be postulated that the uncured resin (in this case at the cure temperature) is adsorbed by the adherend and that the adhesive strength is relative to the magnitude of the adsorptive forces; the strength of adsorption of epoxy resins increases with molecular weight (5). Interesting similarities between adsorption and adhesion and the relation between adsorption and physical characteristics of macromolecules have been discussed by other investigators (14, 15). As the chemical curing reaction progresses, the mobility of the resin molecules is reduced, thus limiting any further possible adsorption. The cohesive strength is developed as a result of this chemical reaction changing the thermoplastic resin into a tough thermosetting polymer structure.

Assuming that forces of adsorption increase as the temperature is decreased suggests that bonds at 76°K should be stronger in adhesion than those at 300°K. If one considers that most polymeric materials also tend to increase in cohesive strength at low temperatures, accompanied by embrittlement, it would be reasonable to expect tensile-shear bonds at 76°K to be stronger than those at 300°K provided that residual thermal stresses are not limiting. Though not statistically significant, average tensile-shear strengths of R-1 and R-2 specimens seem to support this hypothesis.

Residual Stresses

Since the resin molecules are essentially anchored to the adherend, any differential dimensional change between adhesive and adherend during or after cure results in stresses in the bond which are greatest at the interface. Residual stresses at the service temperature then would impose a larger decrease in adhesive rather than in cohesive strength. The total difference in dimensions is actually from two separate causes. The first of these is chemical shrinkage of the adhesive during cure; the second is the differential thermal contraction between adherend and adhesive in cooling to the service temperature.

The total contraction exhibited by epoxy resins in curing with phthalic anhydride at 120°C and cooling to room temperature increases with the amount of curing agent required for cure and decreases, therefore, with an increase in molecular weight of the uncured resins (5). A similar shrinkage, though not necessarily of the same magnitude, would be expected with epoxy resin-metaphenylenediamine systems. Since the thermal contraction of the bulk adhesives varies directly with molecular weight of the resins as shown by the measurements between 300°K and 76°K, chemical shrinkage must be the contributor causing the inverse effect at normal temperatures.

The net effect of residual stresses is dependent on the service temperature and the magnitude of thermal contraction of the adherend material. At 300°K the thermal effect is small compared to that of the chemical reaction, and the residual stresses are due predominantly to cure shrinkage. As a result, bonds of the low molecular weight resins suffer the greatest reduction in room temperature strength. At 76°K the differential thermal contraction between adhesive and adherend adds stresses to those already present at 300°K. Then, from room temperature to liquid nitrogen temperature, bonds of the high molecular weight resins suffer the greatest loss in strength. *Figure* 9 illustrates the relation between change in the arithmetic means of the tensile-shear strengths and thermal contraction from 300°K to 76°K.

Aliphatic Versus Aromatic Cures

At the outset of this investigation three preliminary lap shear specimens were prepared from R-1 cured with diethylaminopropylamine for two hours at 165°F. One of these specimens, tested at 300°K, failed at 2170 psi; the other two, tested at 76°K, failed at 2170 and 1180 psi. Modes of failure were the same as those observed with the MPD cure. However, the specimen producing the low value at 76°K showed signs of adherend discoloration, and the strength obtained is not thought to be representative of the aliphatic amine cure. Assuming that the two remaining values are representative, a limited comparison can be made between aliphatic and aromatic amine type cures.

If adhesive properties are truly developed by an adsorption mechanism, then the curing agent must also play a significant role in this step. Considering only specimens of R-1 tested at 300°K, the average strength of those cured with MPD was 30 percent higher than

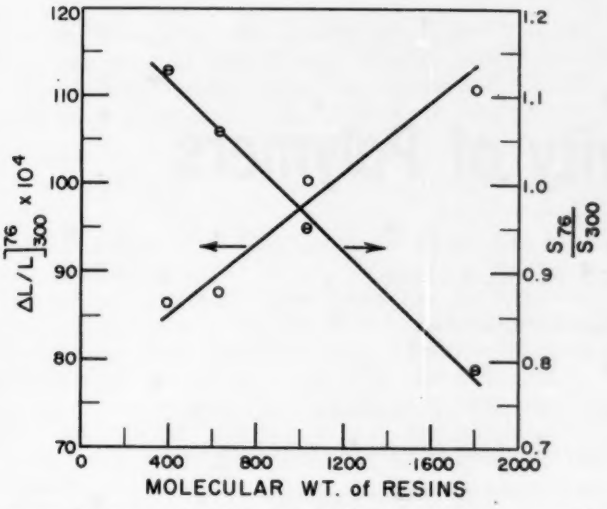

Figure 9. Ratio of 76°K and 300°K tensile-shear strengths compared to thermal contraction of the adhesives

the strength of the specimen cured with DEAPA. Aliphatic amines might offer a greater interference to the resin adsorption responsible for adhesive strength. As mentioned previously, if the apparent adhesive failures observed actually occurred in a plane very close to the adherend surface leaving a film not visibly discernible, the difference in ultimate stress could be attributed to a difference in cohesive strength of the adhesives.

The low temperature strength obtained with the DEAPA cure is approximately 60 percent lower than the average of those cured with MPD. The fact that the thermal contraction between 300°K and 76°K with the DEAPA cure is greater than with that of MPD (*Figure 8*) could account for this increase in strength difference.

Conclusions

- Failures at 300°K occur at or very near the adhesive-adherend interface.
- Joints become stronger but less resistant to impact loading with increase in MW of resins.
- Residual stresses at room temperature act to increase the tensile-shear strength and to minimize the decrease in impact resistance with an increase in MW.
- At 76°K joint failures occur in a plane near the interface where residual stresses are probably at a maximum within the adhesive.
- Measurements of total linear thermal contraction between 300°K and 76°K provide useful indices of the residual stresses which are added to those at normal temperatures in cooling adhesive joints to the temperature of liquid nitrogen. Since most of the thermal contraction occurs between normal temperatures and liquid nitrogen temperature, residual stresses involved in cooling down to the temperature of liquid helium (4.2°K), for example, will not be much greater.
- These added stresses increase with molecular weight of the resins in such magnitudes to affect a significant decrease from 300°K to 76°K in the strength of tensile-shear joints of high molecular weight resins, probably above 1000.
- There is no significant trend in impact strength with molecular weight at the low temperature.
- The implication from (6 and 7) is that if the magnitude of the 76°K residual stress was independent of molecular weight of the resins, bond strengths might well increase with molecular weight for both tensile and impact loading.
- An aromatic amine cure would probably produce better bond strengths at both 300°K and 76°K with less residual stresses at the low temperature than an aliphatic amine cure.
- In general, of those tested, the bisphenol-A epoxy resin with a molecular weight of 634 would produce the best adhesive. This is a compromise of tensile-shear and impact-shear strengths at both temperatures and ease of handling.

Literature References

1. Epstein, G., Adhesive Bonding of Metals, p. 103-104, Reinhold Publ. Corp., New York, N. Y. (1954).
2. Dietz, A. G. H., "Non-destructive Testing of Adhesives by Ultra-Sonic Waves", Adhesion and Adhesive Fundamentals and Practice (a symposium), p. 218, John Wiley and Sons, Inc., New York, N. Y. (1954).
3. McClintock, R. M. and Hiza, M. J., *Modern Plastics*, 35, No. 10, 172 (1958).
4. Frost, W. M., Paper presented at the Cryogenic Engineering Conference at the University of California, Berkeley, Calif. (1959).
5. Bruyne, N. A. de, *J. Appl. Chem. 6*, 303 (1956).
6. Polymer Progress, Shell Chemical Corporation Technical Bulletin 55-5, March (1955).
7. Determination of a-Epoxy Group: Hydrochloric Acid-dioxane Method, Shell Development Company Analytical Department, EMS 3E10/56.
8. Hopper, F. C., of the Shell Development Company, Private Communication dated Nov. 26, 1956.
9. Bandaruk, Wm., *Plastics World 15*, No. 11, 6 (1957).
10. A.S.T.M. Standards, Part 7, P1024-9, American Society for Testing Materials, Philadelphia, Pennsylvania (1952).
11. Muchnick, S. N., *Mechanical Engineering 78*, 19 (1956).
12. Crow, E. L., Davis, F. A. and Maxfield, M. W., Statistics Manual, U. S. Naval Ordnance Test Station, China Lake, California (1955).
13. Reinhart, F. W., "Survey of Adhesion and Types of Bonds Involved," Adhesion and Adhesives Fundamentals and Practice (a symposium) p. 9-15, John Wiley and Sons, Inc., New York, N. Y. (1954).
14. Alter, H. and Soller, W., "Molecular Structure of Epoxy Polymers as a Basis for Adhesions," AFOSR TN 57-279, ASTIA Doc. AD 126580, March 27, 1957.
15. Simha, R., Frisch, H. and Eirich, F., *J. Phys. Chem.* 57, 584 (1953).

Acknowledgment

The authors wish to acknowledge the aid of F. C. Hopper of the Shell Development Company for his generous contribution in furnishing personal and company technical information pertinent to this investigation, and in arranging for the supply of epoxy resins through the Shell Chemical Corporation.

Electrical Resistivity of Polymers

R. W. Warfield and M. C. Petree

U.S. Naval Ordnance Laboratory
White Oak, Silver Spring, Maryland

Measurements of the temperature dependence of volume resistivity of a variety of polymers are used to elucidate polymer structure and the mechanism of electrical conduction

One of the more important measurements made by those investigating high polymers is that of the magnitude and temperature dependence of the electrical volume resistivity. Such data can be used to calculate the activation energy, E_c, for the electrical conduction process in the polymer and to estimate the extent of polymerization. The magnitude and temperature dependence of the electrical resistivity (or conductivity) of a polymer is a function of the molecular structure of the polymer, the nature and number of the current carriers, and the temperature. Resistivity determinations have been used for many years by physicists in studying the structure of both elements and inorganic compounds (1), and more recently they have been applied to solid organic compounds (2). However, the use of this measurement on high polymers has not been widespread. A number of years ago studies by Fuoss (3) and by Baker and Yager (4) utilized the temperature dependence of the resistivity as an aid in studying the molecular structure of polymers. Following their work, use of the technique has slowly become more widespread. However, the literature still does not contain any significant amount of accurate data on the magnitude and temperature dependence of the electrical resistivities of thermoplastic and thermosetting polymers.

Such information is of great importance not only in technological applications of these materials but also in theoretical investigations. The values reported here and the experimental technique are of interest to those considering the possibility of employing modified polymers (5) as organic semiconductors. These data could also serve as an index for the characterization of polymers. In addition to the experimental work and data reported here, the available literature values for the temperature dependence of the resistivity of various polymers are also included.

Theoretical

The theoretical basis for calculating the activation energy, E_c, of the electrical conduction process has been developed by Glasstone, Laidler, and Eyring (6) who have shown that the concepts used in chemical kinetic studies can be successfully applied to physical processes. The change in the electrical resistivity of a polymer with temperature can be considered to be a rate process similar to those encountered in chemical kinetic studies and the same equations can be applied to both chemical and physical rate processes.

Equation (1) is used to calculate the activation energy for the conduction process.

$$\rho = A_o \exp (+ E_c/RT) \qquad (1)$$

where ρ is the resistivity, A_o is a temperature independent constant, R is the molar gas constant 1.987 cal/deg-mole, T is the absolute temperature, and E_c is the activation energy for the conduction process.

Many investigators have studied the electrical conduction process in high polymers, (3, 7) and the evidence is that conduction is an ionic process. Ions stem from three sources. The first and largest source of ions consists of impurities which are not part of the structure of the polymer and will migrate under the influence of an externally applied electric field. Secondly, thermal agitation causes some ionic dissociation. The number of ions from this source increases exponentially with temperature as shown in equation (2)

$$N = C_1 \exp (- E_1/kT) \qquad (2)$$

where N is the number of ions formed, C_1 is a constant, E_1 is the activation energy for the formation of an ion, k is the Boltzmann constant, and T the absolute temperature. Thirdly, some ions are formed by background radiation (7). In addition, McCall and Anderson (8) have recently suggested that electrical conduction in polyamides is due to proton migration in the amorphous region of the polymer.

Conduction in polymers depends not only on the number of ions present but also upon the mobility of the ions. This mobility, which is proportional to the reciprocal of the viscosity of the system, increases exponentially with temperature as shown in equation (3).

$$M = C_2 \exp (- E_2/kT) \qquad (3)$$

Where M is the mobility, C_2 is a constant, E_2 is the

activation energy for the mobility of an ion, k is the Boltzmann constant, and T is the absolute temperature.

The electrical conductivity of a polymer is the product of the number and the mobility of the ions present, or

$$\sigma = C_1 C_2 \exp \frac{-(E_1 + E_2)}{kT} = C \exp (-E_c/kT) \quad (4)$$

where σ is the conductivity and the other symbols have their usual meaning.

Stearn and Eyring (9) have shown that the migration of ions in solids in an electric field can be represented by the absolute reaction rate theory (6). The observed ionic currents are the resultant of the movement of the ions in the direction of the applied field and the backward diffusion of ions because of the concentration gradient thus established. The rate can be represented by equation (5)

$$\text{Rate} = (NDc\,\epsilon\, ze/kT) - ND\frac{dc}{dx} \quad (5)$$

where N is Avogadro's number, D is the diffusion constant of the ion, c is the ionic concentration, ϵ is the potential gradient, z is the valence of the ion, e is the electronic charge, dc/dx is the concentration gradient, k is the Boltzmann constant, and T is the absolute temperature.

It has been shown by Speigler and Coryell (10) that conduction and diffusion in polymers follow the same mechanism and that a general treatment of ionic mobilities should apply to both phenomena. Diffusion is a rate process governed by an activation energy as shown in equation (6)

$$D = D_o \exp (-E_d/RT) \quad (6)$$

where D is the diffusivity, D_o is a temperature independent constant, R is the molar gas constant, T is the absolute temperature, and E_d is the activation energy for the diffusion process. Since diffusion and conduction in polymers are in effect identical processes, it follows, for a given polymer and identical diffusing species, that E_c and E_d should have similar values. Unfortunately, available literature values for both E_c and E_d on the same polymers are very limited.

Experimental

The temperature dependence of the electrical resistivity is obtained by monitoring the resistivity and the temperature of a polymer while being heated in an oven at the rate of about 15°C per hour. The polymer is previously polymerized directly (in the cases of polyethylene and polystyrene melted) to parallel strip electrodes which are completely embedded in the polymer. A thermocouple is taped to one of the electrodes and allows measurement of the temperature of the polymer at the electrode. These electrodes are connected to a Continuous Current Monitoring Device (CCMD) (11).

The CCMD, which is a simple application of Ohm's Law, is used to determine the temperature dependence of the electrical resistivity of various polymers. This device consists of a Keithley Model 210 Electrometer, a Keithley Model 2008 decade shunt, and the parallel strip electrodes. This instrumentation can monitor the large change in resistivity (10^6 to 10^{16} ohm-cm) which

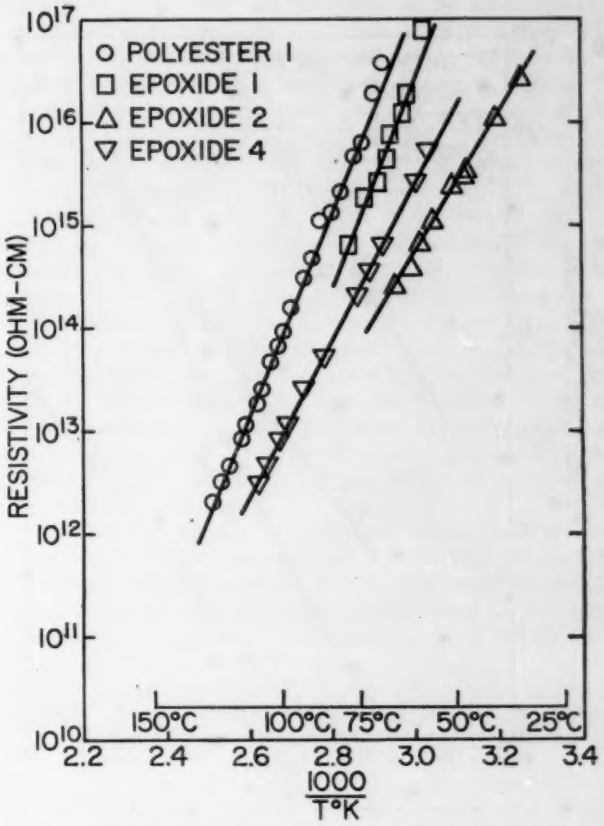

Figure 1. Temperature dependence of the electrical resistivity of various polymers

may occur in a polymer upon heating. A complete description of the CCMD, the parallel strip electrodes, and the experimental arrangement have been previously presented (11). The measurements reported here were made at a field strength of 225 volts/cm. To insure complete polymerization, each sample was post polymerized for at least 16 hours at a temperature higher than the maximum to be attained during the subsequent resistivity determination.

Materials

The polymers used in this study consisted of commercially available materials. With the exception of the polyethylene and polystyrene, the polymers consisted of viscous liquids to which it was necessary to add a suitable hardener in order to induce polymerization. The polyethylene and polystyrene samples were supplied in the form of small pellets. These were melted around the electrodes at 150°C.

The polymers studied can be defined in terms of starting materials, basic unit structure, and reactive functional groups. Epon 828 (Shell Chemical Corp.) is reported to be prepared from two moles of epichlorohydrin and one mole of bis(4-hydroxyphenyl)dimethylmethane (12) and has an epoxide value of 0.54 per 100 grams and a hydroxyl value of 0.08 per 100 grams. Details of the preparation of this epoxide and the basic unit structure have been previously given (12). Epon 828 was polymerized with the stoichiometric amount of each

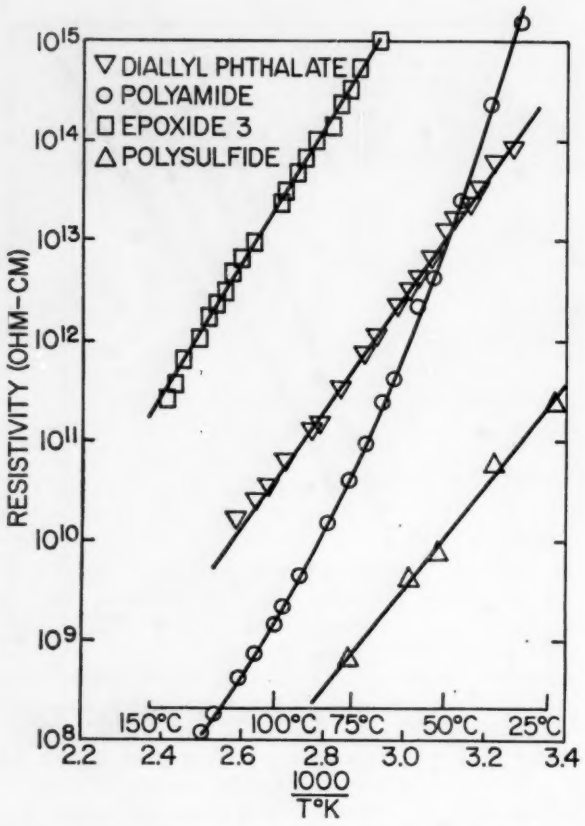

Figure 2. Temperature dependence of the electrical resistivity of various polymers

of the following hardeners, 13% of tris(dimethylaminomethyl)phenol tri(2-ethyl hexoate) [DMP], 12.6% of m-phenylene diamine (MPDA), 5.7% of diethylaminopropylamine (DEAPA), 59.5% of dodecenyl succinic anhydride (DDSA), and 37% of maleic anhydride (MA).

Both of the styrene base polyesters, Paraplex P-43 (Rohm and Haas Corp.) and Laminac 4116 (American Cyanamid Co.) are reported to consist of 70% of an unsaturated linear polyester dissolved in 30% of styrene monomer. The polyester component consists of a linear reaction product of the condensation of phthalic and maleic acids with propylene glycol. Crosslinking by the styrene was initiated by 1% of methyl ethyl ketone peroxide. The basic unit structure of these polymers has been given by Anderson and Freeman (13).

The polyamide-epoxide copolymer consisted of 60% of an epoxide, ERL-2795 (Bakelite Corp.). This epoxide is very similar in structure to Epon 828 and is mixed with 10% of a reactive diluent, butyl glycidyl ether (14). This mixture of epoxides has an epoxide value of 0.54 per 100 grams. Polymerization was effected by 40% of an amine terminated aliphatic polyamide, Versamid 125 (General Mills Corp.). This polyamide is a condensation polymer of a dimerized linoleic unsaturated fatty acid and an excess of an alkyl polyamine and has an amine value of 290-320 (15).

Dow 2633 (Dow Chemical Co.) is an epoxide similar in structure to Epon 828 with an epoxide value of 0.53 per 100 grams. This was polymerized with 10% of DMP. Hysol 6600 (Hysol Corp.) is an epoxide containing polyester groups and 50% of SiO_2 filler and was polymerized with 14% of phthalic anhydride.

The polysulfide-epoxide copolymer was a 50:50 mixture of Epon 828 and a mercaptan terminated saturated elastomer having the structure (16) $HS(CH_2CH_2OCH_2OCH_2CH_2SS)_8CH_2CH_2OCH_2OCH_2CH_2SH$. This was polymerized with 3% of diethylaminopropylamine (DEAPA). The polyurethane was a reaction product of a polyester glycol and 2, 4-tolylene diisocyanate which was crosslinked with 40% castor oil.

The polyethylene was Marlex 50 (Phillips Petroleum Corp.) and the polystyrene was Styron 666 (Dow Chemical Corp.). Both of these polymers were used as received. The diallyl phthalate (Shell Chemical Corp.) was polymerized with 1.96% of benzoyl peroxide.

Results and Discussion

The results of this investigation are shown in *Figures 1 to 4* which are Arrhenius plots of the resistivity vs the reciprocal of the absolute temperature. *Table 1* lists the polymers studied, the temperature range considered, and the calculated values of E_c. *Table 2* lists the litera-

Table 1. Activation Energy, E_c, For Electrical Conduction in Polymers

Polymer	Designation in Figures	Temperature Range	E_c, Kcal/mole
Paraplex P-43	Polyester 1	65-125°C	46
Dow 2633 + D	Epoxide 1	50-75°C	47
Epon 828 + D	Epoxide 2	35-65°C	30
Epon 828 + MPDA	Epoxide 3	60-145°C	30
Epon 828 + DEAPA	Epoxide 4	50-110°C	38
Polyamide-Epoxide	Polyamide	30-150°C	—
Diallyl phthalate	Diallyl phthalate	35-120°C	26
Polysulfide-Epoxide	Polysulfide	20-85°C	24
Polyethylene	Polyethylene	40-125°C	13
Polystyrene	Polystyrene	40-80°C	30
Hysol 6600	Epoxide 5	60-135°C	54
Epon 828 + MA	Epoxide 6	85-150°C	38
Polyurethane	Polyurethane	35-75°C	—
Epon 828 + DDSA	Epoxide 7	40-95°C	46
Laminac 4116	Polyester 2	55-125°C	46

Table 2. Literature Values of the Activation Energy for Electrical Conduction in Polymers

Polymer	Temperature Range	E_c, Kcal/mole	Reference
Polyhexamethylene sebacamide	60-140°C	29.7	4
Polytrifluoro-chloroethylene	20-100°C	24	7
Polyvinyl chloride	60-100°C	64	3 and 22
Polyethylene terephthalate	100-200°C	38	28
Polymethyl methacrylate	21-60°C	33	29
Various Styrene-Acrylonitrile copolymers	25-150°C	—	30
Nylon 66	40-160°C	40	8

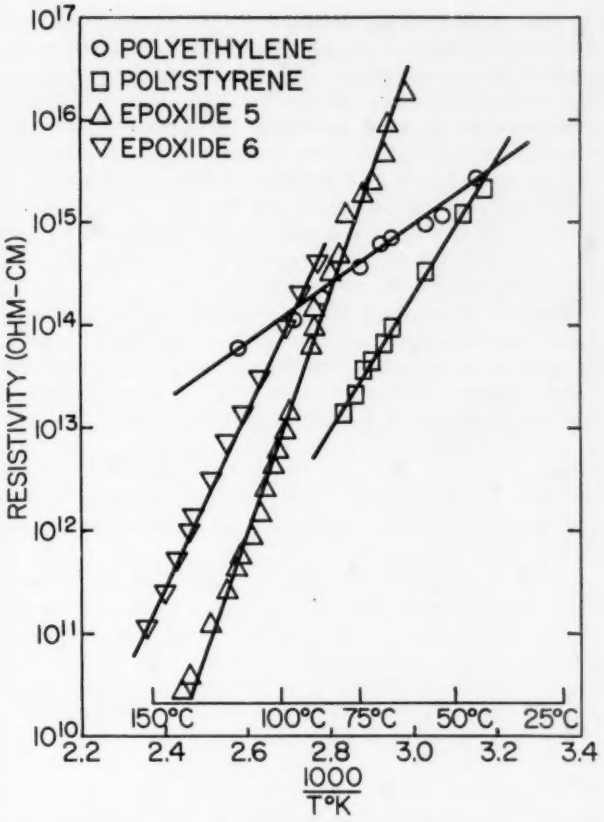

Figure 3. Temperature dependence of the electrical resistivity of various polymers

ture values for E_c for various polymers. The polymers considered here were completely polymerized and the E_c values are the maximum that have been obtained for these polymers. These results were reproducible within about 3%.

The activation energies for conduction in the polymers considered fall into three groups which appear to be dependent upon the structure of the polymer. In the first group are those polymers in which E_c is less than 25 Kcal/mole. These polymers are usually either thermoplastic or not highly crosslinked and only slightly polar. Many are flexible and the ions can diffuse through the relatively open structures with a minimum of difficulty. A second group of polymers are those in which E_c is between 25 and 40 Kcal/mole. Almost all of these polymers are crosslinked but the crosslinking density is not necessarily high. For example, diallyl phthalate when completely polymerized is about 70% converted. Although the crosslinking density is not high, these polymers are not flexible. Finally, there is a third group of polymers for which E_c is above 40 Kcal/mole. The last group is characterized by high crosslinking densities and there is very little unconverted monomer or low molecular weight polymer present.

There are exceptions to the above generalizations. A high E_c value does not always indicate that the polymer is highly crosslinked. Highly polar polymers have E_c values higher than would normally be expected. For example, polyvinylchloride is a highly polar thermoplastic polymer with an E_c value of 64 Kcal/mole.(3) The electrical conduction process in polyvinyl chloride has been attributed by Fuoss (3) to traces of hydrogen chloride released as a result of pyrolysis during the preparation of the polymer. It thus appears that this combination of a highly polar polymer and bulky current carriers accounts for the high E_c value. In contrast, low pressure polyethylene (Marlex 50), which is nonpolar, has a low E_c value of 13 Kcal/mole. The high E_c value for polystyrene of 30 Kcal/mole is rather surprising, as this polymer is only slightly polar. However, this value is in good agreement with the value of 28 Kcal/mole found by Fowler and Farmer. (17) The amorphous thermosetting polymers such as the epoxides and polyesters are very complex in structure, and only a very limited amount of data are available as to the polar properties of these polymers. However, the high crosslinking density results in a rigid molecular structure, which minimizes the possibility of any dipole orientation occurring.

In the case of the polyethylene noted above, diffusion studies have been carried out on this polymer by Auerbach and co-workers.(18) E_d was found to be 12.2 Kcal/mole for the diffusion of octadecane in polyethylene. The value of 13 Kcal/mole for E_c is therefore in good agreement.

The extent to which E_c depends upon the molecular weight of the diffusing current carriers cannot be determined at present. However, it appears that for the

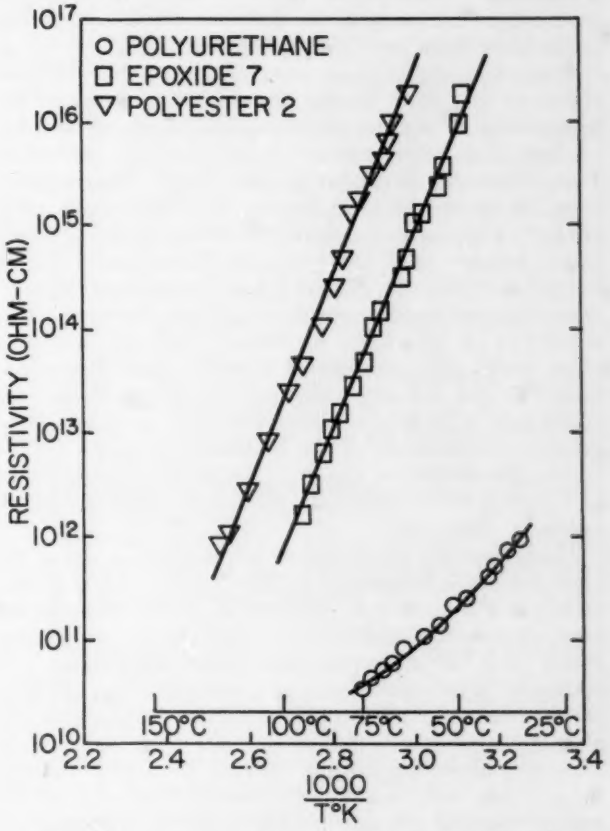

Figure 4. Temperature dependence of the electrical resistivity of various polymers

most part the current carriers are of relatively low molecular weight. The sizes and types of current carriers are very important. It would be expected that small compact ions would diffuse through the polymer structure more easily than large bulky ions. This has been observed by Meares (19) who studied diffusion in swollen polymer networks. Determination of the exact nature of the current carriers would be very difficult because of the small number and size of the ions.

Warner (20) determined the temperature dependence of the resistivity of two vinyl polymers, identical in structure except that one polymer was carefully purified to remove ionic impurities. Upon determining the temperature dependence of the resistivity it was found that, while both polymers exhibited the same dependence, i.e., the same E_c value, the resistivity of the purified polymer was greater in magnitude by one decade.

With the single exception of the polysulfide-epoxide copolymer, the polymers considered here were studied at temperatures below the glass or second order transition temperature. At temperatures below the transition point (or range) the polymers were hard and brittle, while above the transition temperature they were rubbery and soft. It has been previously shown (21) that the glass or second order transition temperature can be determined by noting the temperature at which a change of slope occurs in a plot of resistivity vs temperature. Most of the polymers considered here will exhibit a glass transition at temperatures above those considered in this paper. Data on the glass transition temperature for many of the polymers considered in this paper have been previously published. (21)

Dielectrics differ from metals in that the electrical resistivity decreases as an exponential function of the temperature. It will be noted that the slopes of the plots of logarithm of resistivity vs temperature shown in *Figures 1 and 3* all exhibit a linear temperature dependence. However, in addition to the previously cited change of slope at the glass transition range, a plasticized polymer will exhibit a nonlinear resistivity vs temperature plot. In *Figure 2* the temperature dependence of a polyamide-epoxide copolymer is shown. This copolymer is internally plasticized (15) by the long chain polyamide component. Specific heat determinations (22) on this material have also indicated that the copolymer is internally plasticized. The nonlinear temperature dependence of the resistivity prevents an accurate calculation of the E_c. The polyurethane shown in *Figure 4* is also internally plasticized, probably by an excess of castor oil.

Plasticizers are often added to polymers to lower the glass transition temperature. The addition of a plasticizer has a considerable effect on E_c as has been shown by Caillon and Groubert (23) and Davies, Miller and Busse (24). Plasticization takes place through the formation of a gel which can be considered as a solution of the plasticizer in the polymer. The structure of the plasticized polymer is thus made more open and flexible. This will allow the current carriers to diffuse through the polymer more easily with a resultant lowering of the energy required for the process. Thus E_c will progressively decline as the amount of plasticizer is increased. Caillon and Groubert (23) have shown that as the amount of dioctyl phthalate is increased in polyvinylchloride, E_c drops from a value of 64 Kcal/mole in the unplasticized polymer to 16.5 Kcal/mole for the polymer containing 20% of dioctyl phthalate. Polyvinylchloride exhibits some tendency to crystallize, and the effect of crystallization is to increase E_c. It is expected that a crystal will act somewhat like crosslinking in preventing the diffusion of the current carriers. Conduction will occur more easily in the amorphous phase (8) and the presence of crystals raised both E_c, and the magnitude of the resistivity.

Recently Erath and Spurr (25) have presented evidence for the existence of highly crosslinked globular formations, or micelles embedded in a lower molecular weight matrix polymer. Since the micelles possess a greater density than the less crosslinked matrix polymer, it would appear probable that electrical conduction would preferably occur in the matrix rather than in the micelles. It thus appears probable that polymers with a high micelle to matrix ratio would be expected to exhibit higher E_c values.

It has been previously shown (26) that the magnitude and temperature dependence of the resistivity (hence E_c) increases as a function of the extent of polymerization. Thus, E_c is an index of the extent of polymerization in terms of a fundamental property of the polymer. Furthermore, Nakajima, Saito and Goto (27) have concluded that the larger the value of E_c the greater are the number of crosslinkages. In the case of a series of unsaturated polyesters crosslinked with styrene, the maximum magnitude of the resistivity will be attained by the copolymer crosslinked with an amount of styrene equivalent to the extent of unsaturation of the polyester. They further suggest that this indicates that if more than one molecule of styrene is used to crosslink two polyester chains, the resultant "styrene bridge" will hinder the intermolecular bonding between ester groups. This work is an example of a case where the magnitude of the resistivity and E_c data are used to yield specific information on polymer structure. Additional work in this field seems warranted.

While the magnitude and temperature dependence of the resistivity increase as a function of the extent of polymerization, both these parameters will decrease as a function of the extent of degradation. Recent work at this Laboratory has shown that as a polymer is progressively pyrolyzed both the magnitude and the temperature dependence of the resistivity decrease. These decreases can be attributed to an increase in the amount of polymer carbon present. When the noncarbon components have been volatilized the remaining polymer carbon will exhibit the flat or slightly negative temperature dependence of the resistivity which is characteristic of carbon. The results of this degradation study will be published later.

Munick (29) has found that the electrical conductivity of polymethyl methacrylate (PMMA) is ohmic at low and moderately high field strengths. At higher field strengths (10 Kilovolts per cm. and above) the conductivity exhibited a deviation from an ohmic dependence. At present only a limited amount of data is available on the dependence of the conductivity of polymers upon the electric field strength. However, in general, poly-

meric materials exhibit appreciable voltage coefficients of the electrical conductivity. Because of this, the field strength at which the measurements are made should be noted. Studies are in progress to further define the dependence of the electrical conductivity of polymers upon field strength.

Another aspect of resistivity measurements which should be stressed is their usefulness in long term studies of polymer stability. The parallel strip electrodes can be embedded in a polymer and the system measured periodically at constant temperature. Changes in the magnitude of the resistivity could be indicative of possible degradation, crystallization, polymerization or moisture absorption. Reversion in elastomers has been detected by this procedure.

The importance of resistivity measurements in the study of organic semi-conductors cannot be over emphasized. Not only are these measurements of technological importance but the data can be used to determine structural parameters and the nature of the conduction process in these new compounds (2). The experimental techniques and methods of analysis presented in this paper are immediately applicable to semi-conducting compounds.

It should also be noted that, while the resistivity measurements reported in this and in previous papers has been extensive, it is believed that additional parameters can be obtained by these measurements. It is expected that the additional data will be of a more fundamental type than has been previously obtained.

Conclusion

Electrical volume resistivity measurements made as a function of temperature on solid polymers can be used to yield data useful in elucidating polymer structure. The postulate that electrical conduction in polymers is an ionic diffusion process controlled by an activation energy appears to be valid. Magnitude and temperature dependence of the resistivity, as well as information on the extent of polymerization, the glass transition temperature, plasticization effects, the activation energy for the conduction process, and thermal degradation of a polymer can be obtained by resistivity measurements. This technique is not completely self-sufficient, but rather the emphasis for future work must be placed upon combining resistivity data with those obtained by other methods.

Acknowledgment

The authors would like to express their appreciation to Mr. Thomas J. Wade for making many of the resistivity measurements reported here and for valuable assistance throughout the course of this investigation.

Literature References

1. Seitz, F., *Modern Theory of Solids*, McGraw Hill, N. Y., N. Y., 1940
2. Akamutu, A., and Inokuchi, H., *J. Chem. Phy., 18*, 810 (1950). Eley, D., Parfitt, G., Perry, M. J. and Taysum, D. H., *Trans. Faraday Soc., 49*, 79 (1953)
3. Fuoss, R. M., *J. Am. Chem. Soc., 63*, 375, 382 (1941)
4. Baker, W. O., and Yager, W. A., *J. Am. Chem. Soc., 64*, 2171 (1942)
5. Topchiev, A. V., Geiderikh, M. A., Davydov, B. E., Kargin, V. A., Krenzel, B. A., Kustanovich, I. M., and Polak, L. S., Doklady Akad. Nauk., USSR., *128*, #2,312 (1959)
6. Glasstone, S., Laidler, K., and Eyring, H., *The Theory of Rate Processes*, McGraw Hill, N. Y., N. Y., 1941
7. Kallweit, J. H., *Kunststoffe, 47*, 651 (1957)
8. McCall, D. W., and Anderson, E. W., *J. Chem. Phys., 32*, 237 (1960)
9. Stearn, A. E., and Eyring, H. J., *J. Phy. Chem., 44*, 955 (1940)
10. Speigler, K. S., and Coryell, C. D., *J. Phys. Chem., 57*, 687 (1953)
11. a. Warfield, R. W., *SPE Journal, 14*, No. 11, 39 (1958)
    b. Aukward, J. A., and Warfield, R. W., Rev. Sci. Inst., *27*, 413 (1956)
12. Lee, H., and Neville, K,, *EPOXY RESINS*, McGraw-Hill, New York, N. Y., 1957
13. Anderson, D. A., and Freeman, E. S., *J. Applied Polymer Sci., 1*, 192 (1959)
14. Lee, H., and Neville, K., *SPE Journal, 16*, 315 (1960)
15. Floyd, D. E., Peerman, D. E., and Wittcoff, H., *J. Applied Chem., 7*, 250 (1957)
16. Cranker, K. R., and Breslau, A. J., *Ind. Eng. Chem., 48*, 98 (1956)
17. Fowler, J. F., and Farmer, F. T., *Nature, 174*, 800 (1954)
18. Auerbach, I., Miller, W. R., Kuryla, W. C., and Gehman, S. P., *J. Polymer Sci., 28*, 1929 (1958)
19. Meares, P., *J. Polymer Sci., 20*, 507 (1956)
20. Warner, A. J., *ASTM Bulletin, 153*, 60 (1948)
21. a. Warfield, R. W., *SPE Journal, 15*, 625 (1959)
    b. Warfield, R. W., NAVORD Report 6285 (1959)
22. Warfield, R. W., Petree, M. C., and Donovan, P., NAVORD Report 6255 (1959)
23. Caillon, P., and Groubert, E., Compt. Rend., *242*, 1313 (1956)
24. Davies, J. M., Miller, R. F., and Busse, W. F., *J. Am. Chem. Soc., 63*, 361 (1941)
25. Erath, E. H., and Spurr, R. A., *J. Polymer Sci., 35*, 391 (1959)
26. a. Warfield, R. W., and Petree, M. C., *J. Polymer Sci., 37*, 305 (1959)
    b. Warfield, R. W., and Petree, M. C., Paper presented at the 136th National Meeting of the American Chemical Society, Atlantic City, N. J., 15 Sept. 1959
27. a. Nakajima, T., and Saito, S., *J. Polymer Sci., 31*, 423 (1958)
    b. Nakajima, T., and Goto, K., *Chem. High Polymers* (Japan), *13*, 185 (1956)
28. Reddish, W., *Trans. Faraday Soc., 46*, 459 (1950)
29. Munick, R. J., *J. Applied Phys., 28*, 1301 (1957)
30. Ehrlich, P., and Delollis, N. J., *J. Res. Natl. Bu. Stand., 51*, No. 3, 145 (1953)

Polyethylene Flow Data From Melt Viscometer and Commercial Extruder Measurements

H. P. Schreiber

Central Research Laboratory, Canadian Industries Limited, McMasterville, Quebec, Canada.

For certain operating conditions, flow data obtained from a viscometer are suitable for predicting extruder performance

Recently, a high shear melt viscometer has been developed in this laboratory, by which it is possible to determine accurate shear rate-shear stress (flow) data of polymer melts like polyethylene with considerable speed. Such data can be of very real value in establishing the detailed structural properties of a polyethylene melt. An example of this value has been given by Mills and co-workers (1), who correlated shear rate-shear stress data with the molecular weight distribution in polyethylenes.

High shear viscometer (H.S.V.) flow data are also interesting from the viewpoint of their potential use in correlations with similar data obtained from a commercial extruder. Such an extruder, fitted with a monofilament extrusion die, may be considered as a capillary viscometer which is continuously fed by a melt conveying screw. A comparative study of H.S.V. and extruder flow data could therefore yield valuable information on the effects of melt compression and screw working. Furthermore, if a correlation between H.S.V. and extruder flow data can be established, then the H.S.V. data may be of definite value in predictions of the extrusion performance of polyethylene melts. Methods for predicting extrusion performance have already been developed (2, 3). These, however, involve rather lengthy calculations and tend to compromise accuracy for a generality of application by assuming the existence of general melt viscosity-shear rate, and melt viscosity-temperature relationships in polyethylene. The use of H.S.V. data would have the advantage of speed and by avoiding the use of general viscosity relationships would lead to predictions which are specific to the polymer melt under consideration.

This work was therefore undertaken to study the relationship between polyethylene flow data obtained from the H.S.V. and a commercial extruder, and to indicate some possible uses of the H.S.V. data in predicting the performance of the polymer in a commercial extruder.

Equipment and Procedure

Apparatus: The high shear viscometer used in this work has been previously described (1, 4). It consists of a barrel maintained at constant temperature, from

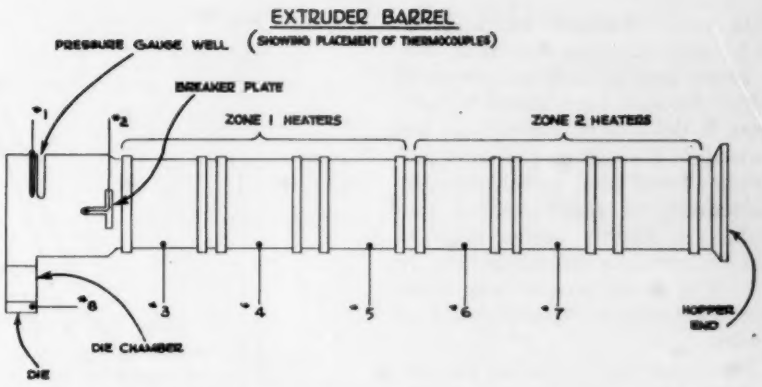

Figure 1. Diagram showing special instrumentation of extruder

which molten polyethylene is forced under precisely measured nitrogen pressures through a capillary orifice of closely specified dimensions. The capacity of the barrel was about 30 gm. of polyethylene.

A commercial, 2½ in. Hartig single screw extruder was used as representative of commercial extrusion devices. The unit was powered by a 7½ H.P. D.C. motor driving through a variable speed box and reduction gear. The extruder barrel and extruder die assembly were instrumented with additional thermocouples, as indicated in *Figure 1*. Thermocouple readings were recorded continuously on a Daystrom eight-point strip chart recorder, and the extruder was operated so as to maintain the temperature of the screw metering section and die chamber assembly (thermocouples 1, 2, 3 and 8) uniform and constant at any selected extrusion temperature. Pressure developed by the melt against the restricting die orifice was measured by means of a Bourdon gage of a similar type to that described by Carley (5). The gage was placed in the die chamber assembly near the extruder breaker plate (*see Figure 1*). No screen pack was used in any of the extruder experiments.

Throughout this work, a 2½ in. diameter metering type screw was used. The screw was 43 in. long, having a channel depth of 0.430 in. tapering to 0.115 in. in the foot long metering section. The screw root was drilled to allow the use of water cooling.

In all extruder experiments, the screw power requirement was estimated. To do this, the power consumption of the D.C. motor was evaluated from the sum of the power requirements, per unit time of operation, of its field and armature. The field power was obtained from simultaneous voltage and current readings of D.C. instruments. The more variable armature power was registered on an integrating wattmeter, which had been calibrated for various load applications by means of precision voltmeters and ammeters. The motor power requirement was converted to screw power by taking into account the gear box efficiency, which had been calibrated at various applied loads by means of a prony brake system.

Extrusion Dies: A total of four dies was used in these experiments. Two of the dies fitted the H.S.V. and a similar pair was constructed for use in the extruder. All dies had a length to radius ratio of 18.3, but one pair of dies had a flat entry, while the second pair had a conical tapered entry, with a taper angle of 60° (120° included angle). For practical reasons, the extruder dies were of larger bore, having radii of 1.40 mm. compared with 0.244 mm. radii of the H.S.V. dies. All dies were constructed of tool steel.

Materials: More than 50 samples of high pressure polyethylene were used in this study. The samples were obtained from different sources and covered the melt index (6) range from 0.1-10.0. Prior to extrusion either from the H.S.V. or the commercial extruder, all polyethylenes were compounded with 0.1% by weight of 4, 4'-thiobis-(3-methyl-6-tertbutylphenol) (Santanox) antioxidant to guard against the effects of oxidative changes.

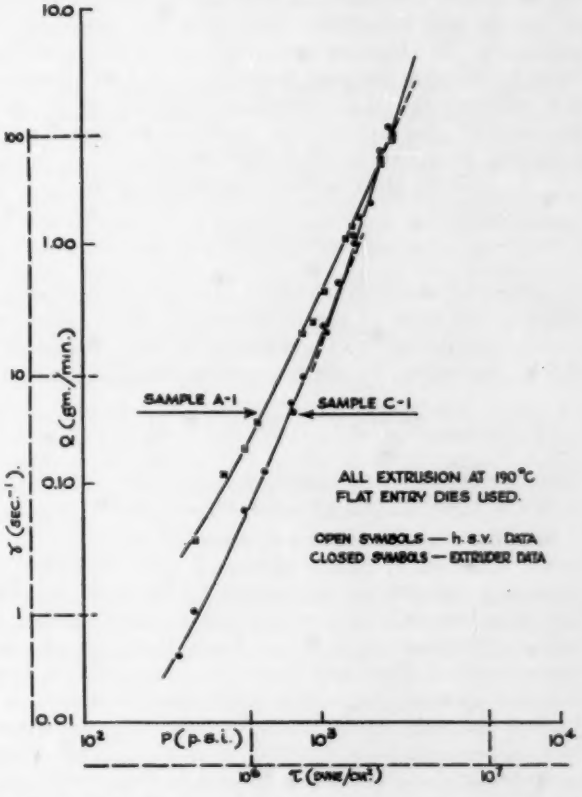

Figure 2. Concurrence of h.s.v. and extruder flow data. Neutral screw extrusion of polyethylene A-1 (m.i. = 6.9) and C-1 (m.i. = 2.0)

Procedure: Flow data were obtained for a given polyethylene from H.S.V. and extruder extrusion over broad ranges of shear stress, and at melt temperatures ranging from 160°-220°C. Stresses were varied by setting the nitrogen pressure in the case of the H.S.V., and by varying the screw speed in the extruder. Timed and weighed cutoffs of extrudate were used to calculate the shear rate. The reproducibility of H.S.V. output rate measurements was ± 3%; a slightly higher error of ± 5% was tolerated in the extruder measurements. In some cases re-extrusion of a given sample was made possible by continuously pelletizing the monofilament as it issued from the extruder.

The comparisons of flow data were made for the use of similar dies (either flat entry, or 60° taper) in the two extrusion devices. The comparison was made by superimposing the shear rate-shear stress graphs from extruder operation upon plots of the corresponding H.S.V. data. In these comparisons, the shear stresses were assumed to be directly superimposable. Maximum stresses, τ, at the die wall were computed from

$$\tau = \frac{P.R}{2.L} \qquad 1$$

where P is the extrusion pressure and R and L are the radius and length of the capillaries. The value of P in the extruder operation was that registered by the Bourdon gage in the die chamber assembly (*Figure 1*). This assumed that pressure was built up predominantly due to the orifice restriction, and that the pressure loss within the die chamber assembly was of minor importance. It was also assumed that values of the end correction entering the shear stress formula (4) were independent of die radius. This term could therefore be neglected in the shear stress calculations.

Shear rates, γ, were calculated from

$$\gamma = 4Q/\pi R^3 \qquad 2$$

Q being the volumetric output rate. Because of differences in the radii of the extruder and H.S.V. dies, extruder outputs had to be reduced to the corresponding H.S.V. die radius, by the correction formula

$$Q' \text{ H.S.V.} = 5.3 \times 10^{-3}\, Q_e \qquad 3$$

where Q' H.S.V. is the reduced H.S.V. output rate, and Q_e is the experimental extruder output rate.

Results: The experimental data fall into two categories. One set of results defines a field of resins and processing operations for which H.S.V. and extruder flow data concur within experimental error. Another set indicates limits beyond which there is a general nonconcurrence of flow data from the two sources. Apart from any general conclusions which may be drawn, it is stressed that the specific limits for flow data concurrence must necessarily be a function of the geometry of the extrusion devices. The limits quoted in this work should therefore be regarded as specific to the extrusion apparatus employed, and should not be assigned any general significance.

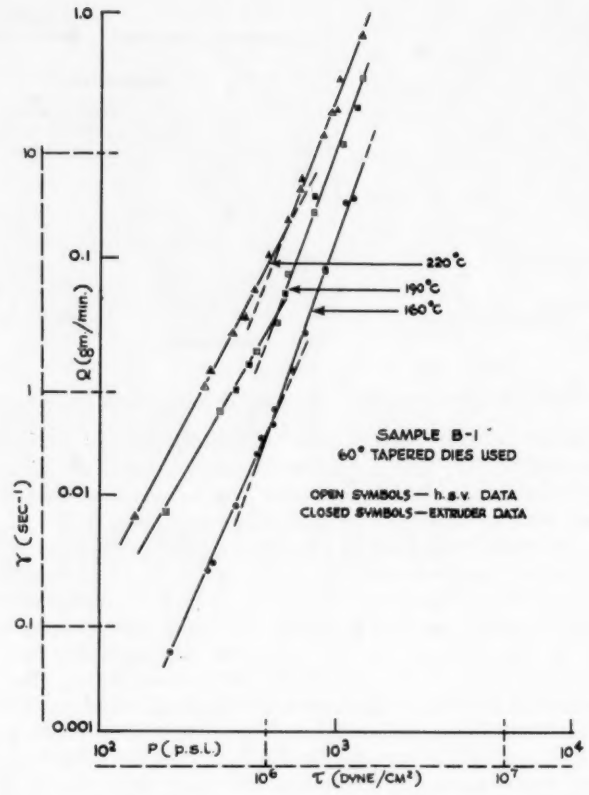

Figure 3. Concurrence of h.s.v. and neutral screw extruder flow data at varying stock temperatures. Resin B-1 (m.i. = 1.8)

Concurrence of Flow Data

A large body of experimental results showed that for resins with melt index equal to or greater than about 0.7, the flow data from the H.S.V. and the Hartig extruder concurred within the limits of experimental error, provided the extruder was operated with no cooling on the screw. Typical data are shown in *Figure 2*. The two polyethylenes are from different commercial sources (the capital symbols are used to code the source of the polymers), and both have melt indices exceeding 2.0. For convenience, both shear rate-shear stress and output-pressure values are given along the coordinates of the plot. The extruder data coincide with the H.S.V. results over the entire stress range covered by the viscometer, and do so well within the limits expected from the uncertainty of the extruder output and pressure measurements.

The concurrence of flow data from the H.S.V. and extruder instruments in question was not affected by the melt temperature in the investigated range 160-220C. This is illustrated by the data given in *Figure 3*. Polyethylene B-1 is a melt index 1.8 sample. The data in *Figure 3* also indicate the further general finding of concurrence between flow data regardless of whether flat entry or tapered entry extrusion dies were used.

In a number of cases, the extruder monofilament was pelletized and subsequently re-extruded. Within the

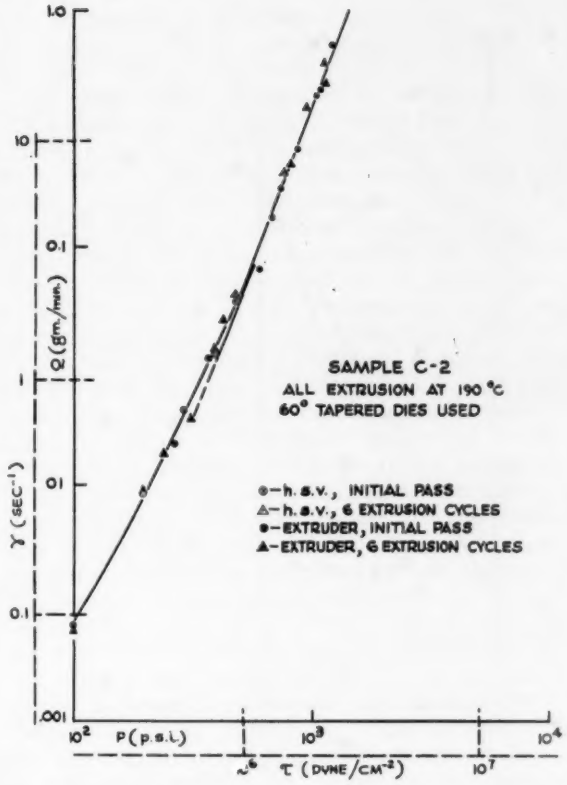

Figure 4. Effect of repeated re-extrusion of polyethylene on h.s.v. and extruder flow curve of resin C-2 (m.i. = 1.8)

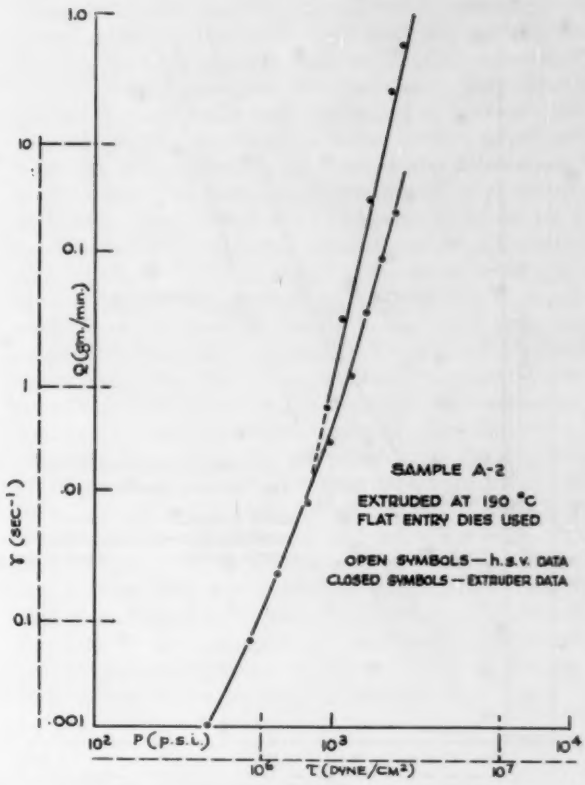

Figure 5. Non-concurrence of h.s.v. and extruder flow data. Neutral screw extrusion of polyethylene A-2 (m.i. = 0.23)

limits stated below, re-extrusion invariably was found to have no detectable effect on the flow behaviour of the polymer. An example is given in *Figure 4*. The initial H.S.V. and extruder flow data for resin C-2 (melt index 1.8) show the expected concurrence. The extruder and H.S.V. data for the sixth extrusion pass are also indicated, and evidently do not deviate significantly from the original flow results. In fact, this polyethylene sample only showed a significant deviation from the original flow data in its 12th extrusion cycle. At this stage, the extrudate was discoloured, suggesting oxidative degradation in the polymer. Similar findings apply to the other re-extrusion experiments, although the number of extrusion cycles before deviation from the original flow curve was noted varied from 9 to 12.

Non-concurrence of Flow Data

There are two distinct sets of experimental results in which a significant deviation between H.S.V. and extruder flow data was noted.

a) In most experiments involving polyethylenes with a melt index less than about 0.7, a non-concurrence of flow data was found. The extruder shear rates in these cases exceeded the H.S.V. shear rates at comparable stresses, and the deviation between flow data tended to become more pronounced as the melt index of the polymer decreased. Typical results are shown in *Figure 5* for a melt index 0.23 material. The shear stresses attainable in the extruder were somewhat limited in the low stress end for this polyethylene.

b) Water cooling of the extruder screw invariably led to extruder flow data which deviated appreciably from the H.S.V. results over broad portions of the investigated stress range. This was true regardless of the melt index of the polyethylene. Typical data are illustrated in *Figure 6*. Polyethylene B-1 had concurrent H.S.V. and neutral screw extruder flow data at 190°C (see also *Figure 3*), but imposition of screw cooling markedly altered the extruder flow curve. At low and intermediate stresses the extruder shear rates are now lower than corresponding H.S.V. values. The slope of the cooled-screw extruder flow curve is, however, greater than that of the reference curve, and there is therefore a tendency for the curves to intersect. The intersection is again noted in the case of polyethylene A-3 (m.i. = 0.22), and is a characteristic of all cooled screw-extruder and H.S.V. flow curves.

Discussion

The given results can be qualitatively interpreted in terms of the viscosity states of the melts being presented to the pertinent extrusion dies. In order for the flow data obtained from the H.S.V. and the extruder to concur for any given resin and operating conditions, it is necessary for the apparent viscosities of the melts presented to the comparison extrusion dies to be identical. That is to say, the response time of the melts to an imposition of stress must be short in comparison with the dwell time of any volume element of melt in the extrusion devices.

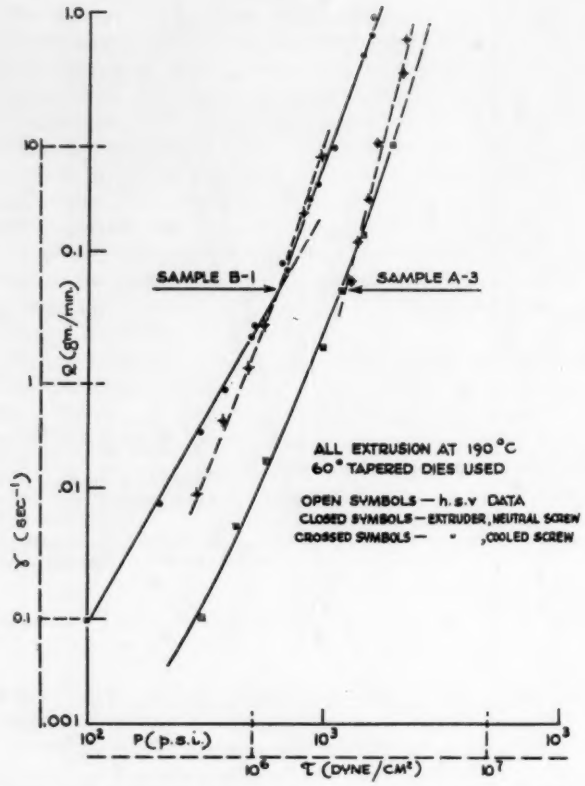

Figure 6. Non-concurrence of h.s.v. and extruder flow data. Water-cooled screw extrusion of polyethylenes B-1 (m.i. = 1.8) and A-3 (m.i. = 0.22)

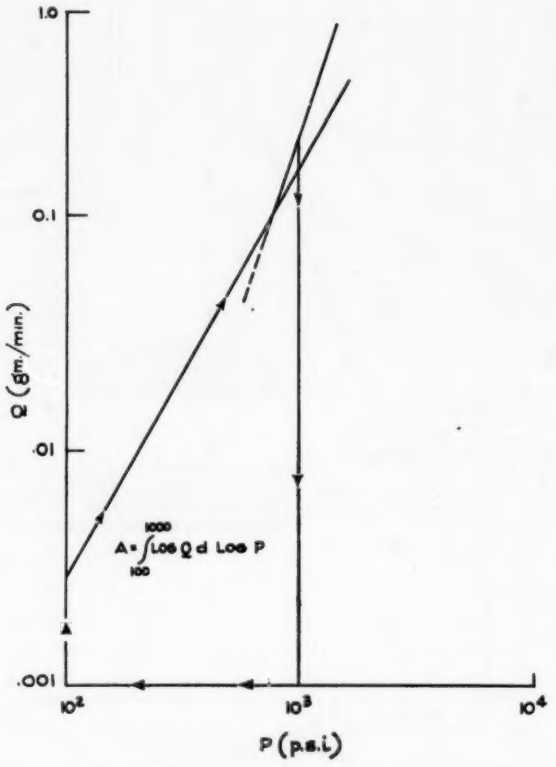

Figure 7. Definition of H.S.V. Area parameter. Arrows indicate integration path

This prerequisite for concurrence of flow data will in all probability depend on such properties of the polyethylene as molecular size, size distribution and degree of non-linearity, and on the specific operating conditions (extrusion temperature, pressure, etc.). In addition, however, the geometry of the extrusion apparatus must also be involved. The principle of flow data concurrence is then probably general to any capillary extrusion apparatus, but the stated limits of concurrence are applicable only to the described extrusion apparatus. For these, it can be concluded that for resins with melt index equal to a greater than 0.7 and neutral screw extruder operation, the apparent melt viscosities at the two dies are indeed identical in the investigated shear stress range of 10^5-7×10^6 dynes/cm^2. This was illustrated in *Figures 2 and 3*. The latter figure also indicated that this situation persists for the polyethylenes used over the studied temperature range of 160-220°C.

Cumulative effects of repeated extruder screw working are evidently also negligible under the investigated experimental conditions (see *Figure 4*). This finding is in general agreement with the results of Schott and Kaghan (7), who reported no significant change in the apparent viscosities of some high pressure polyethylenes after repeated extrusion from an extruder. This invariance of the flow curve on repeated extrusion does not, of course, preclude a change in the physical properties of the solid extrudate. The implication is simply that repeated exposure to high temperatures, and repeated application of shear energies by screw working was insufficient, in this case, to cause significant changes in those structural properties of the polymer which influence its flow behaviour. Similarly, such blending as the reasonably homogeneous polyethylene samples received in the present neutral screw extruder operation could have no appreciable effect on the melt viscosity-shear stress characteristics of the resins.

In terms of the above arguments, non-concurrence of H.S.V. and extruder flow data is viewed as an indication of differences in the apparent melt viscosities of the polyethylenes presented to the two extrusion dies. The non-concurrence in the flow data of polyethylenes having a melt index less than about 0.7 is consistent with recent evidence from this Laboratory (8, 9) concerning the time dependence of melt viscosities measured by capillary viscometers such as the present H.S.V. The application of any stress to a polyethylene melt does not result in an instantaneous establishment of a constant shear rate value. Rather, the shear rate increases with time toward a steady-state value. The magnitude of the shear rate increment and the time involved to reach the steady-state value in the H.S.V., depends on the polymer type and on the extrusion condition (8), but both the magnitude of the effect and the time required to attain a steady-state shear rate increase as the melt index of polyethylene decreases. The time effect was associated with a slow change in the orientational state of the polymer melt, following stress application.

The time lag in attaining a steady-state output may be responsible for the non-concurrence in flow data of low melt index polyethylenes.

Two contributing effects may be recognized: First, in the extruder the polyethylene chains have been in the molten state for relatively longer times prior to extrusion. There is therefore greater opportunity to attain a steady state at any given stress. Second, in a polymer melt the chains are probably in a highly entangled state (10). Because of prior screw working, the melts entering the extruder die chamber may be less severely entangled than their H.S.V. counterparts, and therefore more readily and effectively able to respond to the orientational forces acting in the die chamber. Extruder melts would therefore be presented to the extrusion die in a relatively less viscous state than in the corresponding H.S.V. experiment. Extruder shear rates would consequently be higher, with the resulting observed flow curve deviations. The extruder experiments could therefore be considered to give a shear rate value which is closer to the steady state value for the given polymer at any stated shear stress. Differences in the degree of non-concurrence between samples are probably to be associated with differences in the structural properties of the polyethylenes, but the limiting melt index value of 0.7 is more likely a characteristic of the employed extrusion apparatus.

The non-concurrence of flow data brought about by the application of screw cooling appears to be caused by two competing effects, which will be discussed in more detail in a forthcoming publication. Water cooling of the extruder screw can be shown to reduce markedly the channel depth in the metering section of the screw (11). As a result, the pumping rate of the extruder is reduced by an amount which is independent of the shear stress. The decreased channel depth, however, is tantamount to the creation of a new extrusion system, in which the shear history of the melts entering the extruder die chamber has been significantly modified. At any extrusion pressure, the effective amount of shear energy to which the melts have been exposed by screw working is now greater than under the corresponding neutral screw operation. Furthermore, the effect increases in magnitude with increasing apparent stress.

Thus, on the one hand in water cooled screw operation, the reduced pumping rate of the instrument will tend to result in lower extruder output rates compared with those from the H.S.V. This effect should be most pronounced at low shear stresses where differences in shear history are relatively unimportant. The experimental results substantiate this expectation; a typical example of the situation is seen in the lower stress region of polyethylene B-1, *Figure 6*. On the other hand as stress rises, the difference in shear histories results in increasing differences in the apparent melt viscosities of the H.S.V. and extruder melts in the respective die chamber assemblies, the extruder melts becoming progressively less viscous. A particular stress value should then exist for each melt, at which the H.S.V. and extruder flow curves intersect, and beyond which extruder outputs exceed their corresponding H.S.V. values. This intersection was also generally suggested by the data, and is indicated by both polyethylenes of *Figure 6*. In the case of the sample A-3, (melt index 0.22) the observed non-concurrence is probably due in part to the time effects characterizing attainment of a steady state in the H.S.V.

Prediction of Extruder Performance

Within the defined, broad range of operating conditions, the flow data obtained for a large number of low density polyethylenes from the H.S.V. and the 2½ in. Hartig extruder are identical within the experimental error. This indicates an identity of the apparent melt viscosities in the dies of the two instruments. Since for a given extrusion system, such performance characteristics as output rate, screw power requirement, etc. are

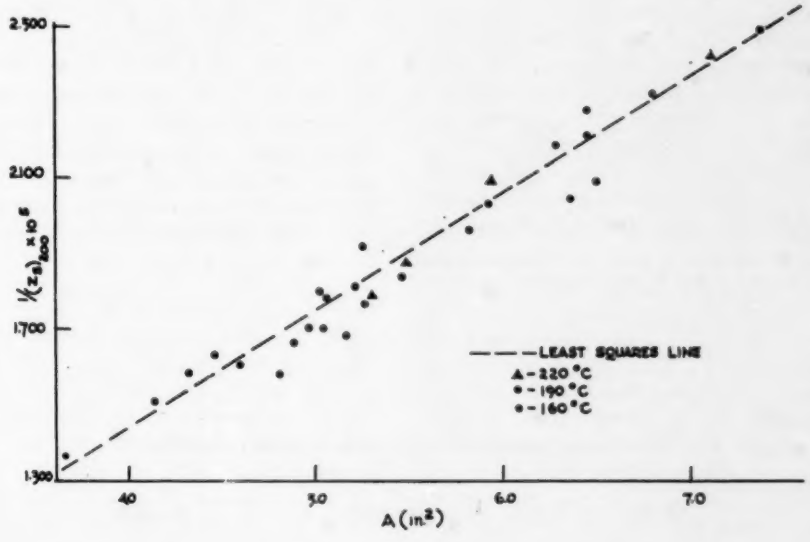

Figure 8. Correlation between h.s.v. flow curve parameter and extruder screw power consumption

principally dependent on the melt viscosity (12), the possibility arises of using H.S.V. flow data for predictions of extruder performance.

The principal problem in such a prediction is the definition of a suitable parameter of the H.S.V. flow curve. It was felt that a single parameter summarizing a major portion of the flow curve, would be most suitable for the purpose. One such parameter was arbitrarily defined as the area parameter, A, and is given by

$$\begin{aligned} P &= 1{,}000 \text{ p.s.i.} \\ A &= \int \log Q \, d \log P \\ P &= 100 \text{ p.s.i.} \\ Q &= .001 \text{ gm./min.} \end{aligned} \qquad 4$$

Referring now to *Figure* 7, A is the area under the H.S.V. flow curve taken in the applied pressure decade from 100-1000 p.s.i., using as a base line the 0.001 gm./min. output ordinate in the log Q-log P plot.

To test the possibility of using the A parameter in a prediction of extruder performance, its correlation with screw power requirement was investigated. The A values of arbitrarily selected low density polyethylenes were determined from their H.S.V. flow curves by means of a planimeter. The A values were then compared with various functions of the screw power requirement, $Z_{\bar{a}}^{-200}$, at the arbitrarily chosen output rate of 200 gm./min. The optimum correlation is shown in *Figure* 8*, where the reciprocal of the absolute power requirement is plotted versus A. The least squares line represents the relation

$$\left(Z_{\bar{a}}^{-200}\right)^{-1} = (0.310 \times 10^{-5})A + 0.203 \times 10^{-5} \qquad 5$$

which has a correlation coefficient of nearly 0.96. The data cover the entire investigated temperature range of 160-220°C; the A function was always taken from H.S.V. data determined at the same temperature as the extruder experiments.

The above example indicates that a rapid and quite accurate prediction of extruder performance, from H.S.V. data is feasible. The H.S.V. data required for the computation of an adequately defined A value can generally be determined in considerably less than one hour operating time, and the ensuing calculation of extruder performance parameters (for example screw power requirement) is specific to the polymer sample in question. Although the correlation equation 5 is clearly characteristic of the extrusion apparatus involved in this study, the present results may again be taken to indicate general patterns of extruder versus melt viscometer flow behaviour. Thus, the form of the correlations is thought to be general, but the proportionality constants must be determined for any set of extrusion devices.

* The area-screw power relationship is based on 52 experimental points. For simplicity only about one half of these are indicated in the plot.

Summary

For broad ranges of operating conditions and a wide variety of high pressure polyethylenes, the flow data obtained from a high shear viscometer and a commercial extruder are identical. Discrepancies between flow data can result from non steady-state viscosities in the high shear viscometer, or from cooled screw extruder operation. In the broad regions in which the flow data concur, the readily obtained viscometer data are suitable for predictions of extruder performance. The principle is illustrated by the good correlation of a viscometer flow curve parameter and the screw power consumption in the extruder. The principles outlined for flow data identity and extruder performance prediction are believed to be general, but the quantitative limits defined in this work are specific to the extrusion devices involved.

Literature References

1. Mills, D. R., Moore, G. E., and Pugh, D. W., 16 ANTEC—S.P.E. Chicago, 1960; *Technical Papers, Vol. VI*, paper 4.
2. Maddock, B. H., *Plastics Technology 3;* 385 (1957)
3. Maddock, B. H., Paper presented to Society of Plastics Engineers, Rochester, April 1956; also Kabelitems No. 92; June 1956.
4. Bagley, E. B., *J. Appl. Phys. 28;* 624 (1957)
5. Carley, J. F., *Ind. Eng. Chem. 45;* 858 (1953)
6. American Society for Testing Materials Standards on Plastics D 1238-57T.
7. Schott, H., and Kaghan, W. S., 16 ANTEC—S.P.E. Chicago, 1960, *Technical Papers Vol. VI*, paper 2.
8. Schreiber, H. P., *J. Appl. Polymer Sci. 4;* 38 (1960)
9. Schreiber, H. P. and Rudin, A., *J. Appl. Polymer Sci. 3;* 122 (1960)
10. Bueche, F., *J. Chem. Phys. 20;* 1959 (1952)
11. Maddock, B. H., Paper presented at 15 ANTEC, S.P.E. New York City, January 1959.
12. Gaspar, E., Fundamental Problems of Single Screw Thermoplastic Extruders; In Plastics Progress, Papers and Discussions at the British Plastics Convention; 1955. Iliffe and Sons Ltd., London.

Our authors would appreciate your comments.

Why not write your impressions . . . today?

An Investigation Of Some Variables Affecting Impact Resistant Thermoplastics

Edward G. Bobalek — *Professor of Chemical Engineering*
Case Institute of Technology, Cleveland 6, Ohio

Robert M. Evans — *Research Associate**

Experiments and theory which point the way to the development of plastics which do not exhibit brittle fracture

Theories which relate mechanical behavior to structural models of polymer networks (9, 10, 11) are most successful when applied under limiting conditions to systems which unambiguously show the characteristics of either the rubbery or of the glassy state. Neither of these classifications seems to fit precisely many of those more complex polymeric compositions of commercial importance commonly identified by the common name "high impact" thermoplastics**—whether amorphous polyblends, crystalline or block polymers.

Despite other irregularities in mechanical behavior, these special polymers show a characteristic type complex stress-strain curve (2). At low strains the elastic behavior is nearly linear and modulus is comparatively high as for glassy polymers. At some critical stress, the plastic yields, often showing rapid stress decay, ductile flow, and, in most instances, ultimately a strain-hardening. The shapes of the tensile curves and ultimate properties vary considerably depending upon chemical composition of the plastic and upon the speed of the test. However, when all are compared at straining speeds exceeding about 450 per cent per minute, many of the impact resistant types, irrespective of compositional differences, showed a linear correlation between area under the stress-strain curve and energy to cause failure in special falling weight tests (2). The tendency to show a higher tensile strength and modulus with increasing speeds is expected for glassy polymers (14). The fact that elongation is preserved with increasing speed seems not to fit simple theory. Possibly some structural features exist which dominate the fracture mechanism. These structural features may be larger than the molecular dimensions involved in the ordinary network models and perhaps are common characteristics of most species of the "impact resistant" group of polymers described in an earlier publication (2).

This study was directed mainly to a search for such common structural features by: (I) Thermal analysis involving determination of the dynamic modulus as a function of temperature, (II) Determination of stress relaxation behavior at room temperature, (III) Examinations of replicas of fracture sections with the electron microscope.

Although the empirical facts collected are not enough to lead to a satisfactory rheological model of structure, the experiments reviewed here point to some coincidences which will need to be considered in developing a better theory and which are immediately useful in guiding experimentation in development of tougher plastics; that is plastics which do not show brittle fracture and which exhibit a cold-flow region in high speed, stress-strain curves.

The group of polymers investigated contains species which at the start of this study in 1956 seemed to be

** For a discussion of a feasible way to classify plastics according to their impact resistance properties, see reference (2).

* Present Address: Technical Director, The Master Mechanics Co., Cleveland 28, Ohio.

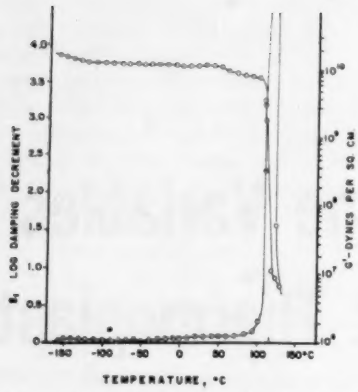

Figure 1. Shear Modulus (G') and Damping Decrement (δ) as a Function of Temperature for Poly(styrene)—PS (2)

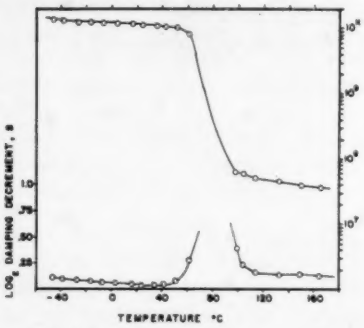

Figure 2. Shear Modulus (G') and Damping Decrement (δ) as a Function of Temperature for Rigid Poly(vinyl-chloride)—RVC (2)

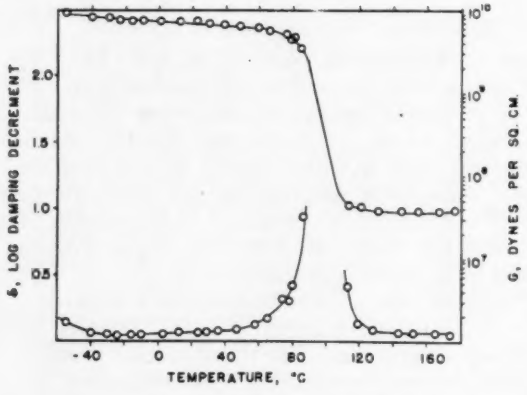

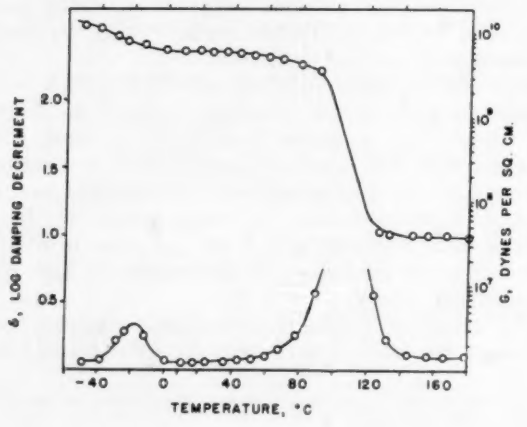

typical representatives of several classes of impact resistant polymers of commercial importance.

The sequence of code letters after the name of the polymer in the figures; for example, rigid poly(vinyl-chloride), "*(RVC)*", are included to refer the data here back to tensile data for the same polymers in an earlier publication (2).

Dynamic Modulus as a Function of Temperature

One of the convenient tools used to study the dynamic properties of plastics as a function of temperature is the torsion pendulum. Nielsen (3), Buchdahl and Nielsen (4), Jaenckel (5), Schmieder and Wolf (6), and Kuhn, Kunzle, and Preissman (7) are among those who have described its use and application. For example, Buchdahl and Nielsen (4) show that for a homopolymer or for two monomers which have been copolymerized to yield a homogeneous amorphous polymer, only a single transition can be observed in the plots of either the modulus or damping decrement versus temperature. However, when a rubber and another amorphous polymer were blended to produce a heterogeneous plastic, then two modulus transitions and two peaks in the damping curve were recognized, each one occurring in a transition temperature range near that which is characteristic for each polymeric phase in the blend. In these polyblends, the height of the peak of the damping curve and the extent to which the modulus declined near the glassy transition of the rubber phase depended upon the amount of rubber present.

To supplement the data already in the literature, some of which are cited here, a similar sort of thermal analysis with the torsion pendulum was performed for a number of the plastics described earlier (2). The equipment was as described by Buchdahl & Nielsen (4).

The curve shown in *Figure 1* for the brittle plastic, polystyrene, was drawn from data by Schmieder and Wolf (6) because their data extends to lower temperatures than ours. (In the common temperature range, down to −50°C, our data agree). Only one small drop in modulus occurs between the glass transition and −100°C. Low damping capacity is exhibited at all temperatures below the glass transition.

Figure 2 for another brittle plastic, partially crystalline poly(vinylchloride), shows only a slight drop in modulus between its amorphous transition and −50°C and damping capacity is low.

The amorphous polyblends of elastomers with glassy polymers show transitions characteristic of each component. For example, the medium impact, polyblend of poly(styrene) with an SBR-elastomer of *Figure 3*, has a peak beginning at −40°C. The blend of nitrile rubber with a styrene-acrylonitrile copolymer of *Figure 4* shows a very distinct low temperature peak at a temperature of −20°C.

Figure 3. Shear Modulus (G') and Damping Decrement (δ) as a Function of Temperature for Medium Impact Polyblend of Poly(styrene) and Styrene-Butadiene Copolymer Rubber—RSB (2)

Figure 4. Shear Modulus (G') and Damping Decrement (δ) as a Function of Temperature for High Impact Polyblend of Styrene-Acrylonitrile Copolymer with Acrylonitrile-Butadiene Copolymer Rubber—CRS (2)

A so-called "block copolymer", derived from copolymerization of styrene-butadiene-acrylonitrile has a curve (*Figure* 5) in which the rate of drop-off of modulus at lower temperature and the corresponding damping curve show a more gradual transition with temperature than do mechanically mixed polyblends (e.g. *Figure 4*); however, the general pattern is similar.

The curves for partially crystalline homopolymers show similarities to so-called "alloys" or "polyblends" or "block-copolymers". For example, a nylon 6 (data from reference 6) shows a series of low temperature damping peaks, (*Figure 6*) none as sharp as that shown in the foregoing illustration for some special copolymers (*Figure* 5) and the elastomer-poly(styrene) blends. Other nylon curves of similar type but not extending to as low a temperature are cited in reference 7. Cellulose acetate, *Figure 7*, which shows a continuous drop of modulus, starting at −40°C with a correspondingly high damping peak resembles the copolymer curve of *Figure* 5. Data for *Figure* 8 on polyethylene were taken from Schmieder and Wolf (6). The same continuous drop-off of modulus is shown as for cellulose acetate in *Figure 7*, but a greater number of low temperature peaks occur. This complex sort of thermal-analysis curve is not uncommon for partly crystalline polymers and polyolefins in particular. Explanations of these complexities are not yet clear. The thermal analysis here may be identifying the co-existence of different degrees of crystalline perfection or order.

Whether or not all sharp modulus transitions in the thermal analysis curves truly identify a phase transition is still open to argument. However, despite uncertainties in interpretation of the significance of comparing sharp versus gradual rates of decline of modulus with increasing temperature, the interesting empirical fact emerges that the modulus temperature behavior can be related to non-equilibrium values of ultimate elongation observed in high speed tensile tests. *Table I* offers such a comparison. In order to obtain ductile behavior rather than fracture at high strain rates seems to require that a plastic must show at least one major transition at temperatures below the ambient temperature of the tensile test; that is, with respect to structure, if a glassy (or crystalline) component is present, then it must coexist along with an elastomer.

Relaxation Modulus Behavior

Tobolsky (9, 10) describes five time-temperature regions of modulus relaxation behavior: (1) a glassy region where the rate of decline of modulus is very slow, (2) a transition region, where the decay is very rapid, (3) a "rubbery plateau" region where again the decline is slow, (4) a rubbery-flow region and (5) a liquid flow region showing very little elastic recovery. To ascertain which behavior was characteristic of impact resistant

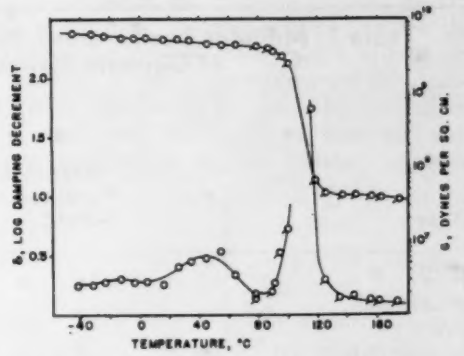

Figure 5. Shear Modulus (G') and Damping Decrement (δ) as a Function of Temperature for "Block Copolymer" of Styrene-Acrylonitrile-Butadiene—TERP (2)

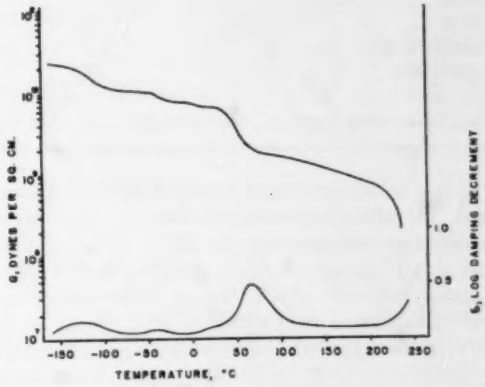

Figure 6. Shear Modulus (G') and Damping Decrement (δ) as a Function of Temperature for nylon-6

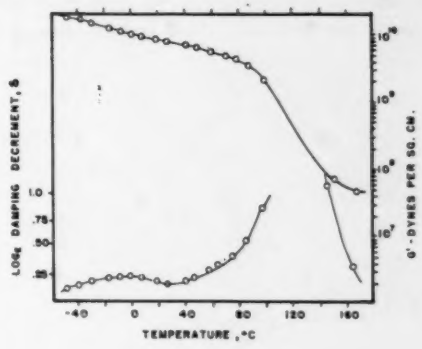

Figure 7. Shear Modulus (G') and Damping Decrement (δ) as a Function of Temperature for Cellulose Acetate—CA (2)

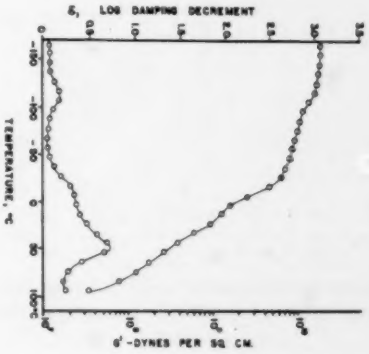

Figure 8. Shear Modulus (G') and Damping Decrement (δ) as a Function of Temperature for Low Density Type of Polyethylene

Table 1. Modulus Temperature. Behavior can be Related to Non-Equilibrium Values of Ultimate Elongation Observed in High Speed Tests

Plastic Type	Shear Modulus, G, in 10^9 dynes/cm^2 at —50°C	25°C	% Decline in G Between —50° & 25°C	Elongation (%)* at Break in 23°C, 0.333 in/sec. Tensile Test	Elongation (%) for Stress-Relaxation Tests of Figures 10-18. Second Figure is Elongation After Yielding	
Poly(styrene)	14	12	11	1.5	0.9;	—
Poly(vinylchloride)	15	12	20	7.0	0.9;	—
Polyblends:						
SBR + poly(styrene)-(A)	7.5	5.3	28	7.9	—	—
SBR + poly(styrene)-(B)	9.0	7.1	21	8.8	0.9;	2.7
SBR + Copolymer styrene/acrylonitrile	7.5	5.5	27	11	0.9;	8.0
"Block Copolymer" of styrene, acrylonitrile, butadiene (Inj. Molded)	12	6.5	48	15	0.9;	2.8
Crystalline:						
Nylon 6	10	5	50	19	0.9;	8.0
Cellulose Acetate	18	7.8	57	22	0.9;	9.0
Poly(ethylene)	9	1	89	100	1.1;	22.0

* Extensive tensile data for these polymers have been reported in SPE Journal, Vol. 16, Number 1, January 1960, pp. 76-83.

plastics in the temperature interval around room temperature, the stress-relaxation behaviors were examined at the constant temperature of 23°C.

Because all impact resistant thermoplastics showed a yield stress beyond which tensile behavior was much different from that prevailing before yield,[1] it seemed probable that significant differences in relaxation behavior should prevail depending upon whether or not the plastic had been strained beyond the yield value.

Tensile stress relaxation was determined with an Instron Tester, whose load cell was connected to a Sanborn Recorder. The samples were stretched at a rate of 450 per cent per minute, then halted automatically at a predetermined strain (*Table 1*). To determine relaxation after yield, samples were stretched beyond the yield point shown in tensile tests. The percentage decline of original stress was plotted against the logarithm of time. Because of considerable variation from sample to sample, it seems advisable to plot individual samples separately in *Figures 10-17*—hence points covered by different symbols span a band which contains the average curves for each condition of testing.

The brittle plastics, polystyrene, *Figure 9*, and rigid vinyl chloride, *Figure 10*, showed very little decay of stress over a two hour period. Most ductile plastics showed somewhat more decay of stress. The "medium-

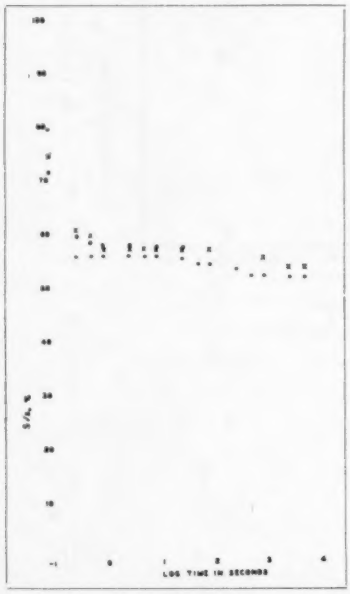

Figure 9. Stress Relaxation Ratio of Stress at time t to Initial Stress, s_o times 100 vs log time in seconds for Poly(styrene)—PS

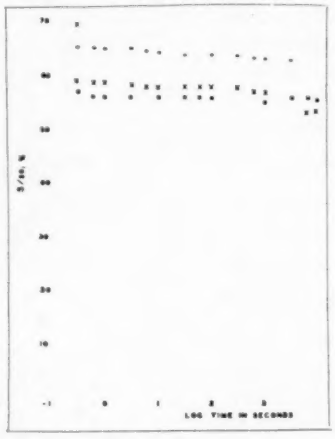

Figure 10. Stress Relaxation Ratio of Stress at time t to Initial Stress, s_o times 100 vs log time in seconds for Rigid Poly-(vinylchloride)—RVC

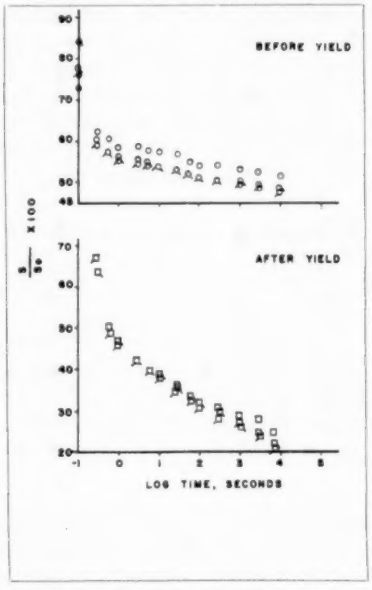

Figure 11. Stress Relaxation Ratio of Stress at time t to Initial Stress, s_o times 100 vs log time in seconds for Poly(styrene)—SBR polyblend—RSB

impact" poly(styrene), *Figure 11* and "block copolymer", *Figure 12* showing the least, followed by the blend of nitrile rubber-styrene copolymer, *Figure 13*, and the crystalline plastics, Nylon-6, *Figure 14*, cellulose acetate, *Figure 15*, and low density polyethylene, *Figure 16*. The curve for a typical SBR-Elastomer is shown for comparison in *Figure 17*. The bar graph of *Figure 18* compares the slopes of the curves of *Figures 10-17* when measured at constant strains below and above the apparent yield value. In all cases except polyethylene, a marked increase in slope was observed at strains exceeding yield. The exception polyethylene behaves as though it were past the transition and well into the rubbery plateau region of the Tobolsky classification

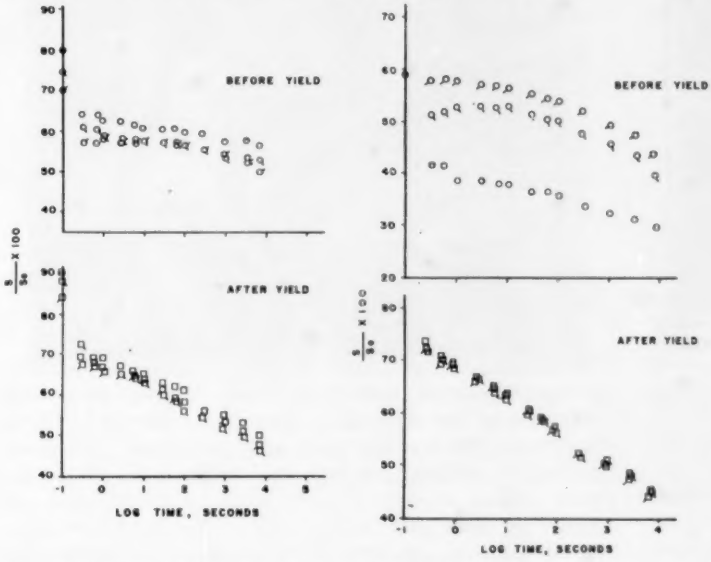

Figure 12. Stress Relaxation Ratio of Stress at time t to Initial Stress, s_o times 100 vs log time in seconds for Ternary "Block Copolymer"—TERP

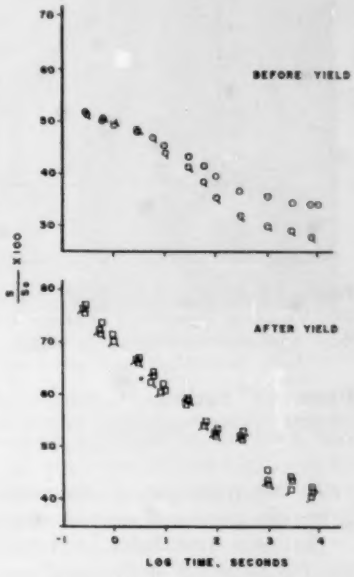

Figure 14. Stress Relaxation Ratio of Stress at time t to Initial Stress, s_o times 100 vs log time in seconds for nylon-6

Figure 13. Stress Relaxation Ratio of Stress at time t to Initial Stress, s_o times 100 vs log time in seconds for Styrene-Acrylonitrile Copolymer—NBR polyblend—CRS (2)

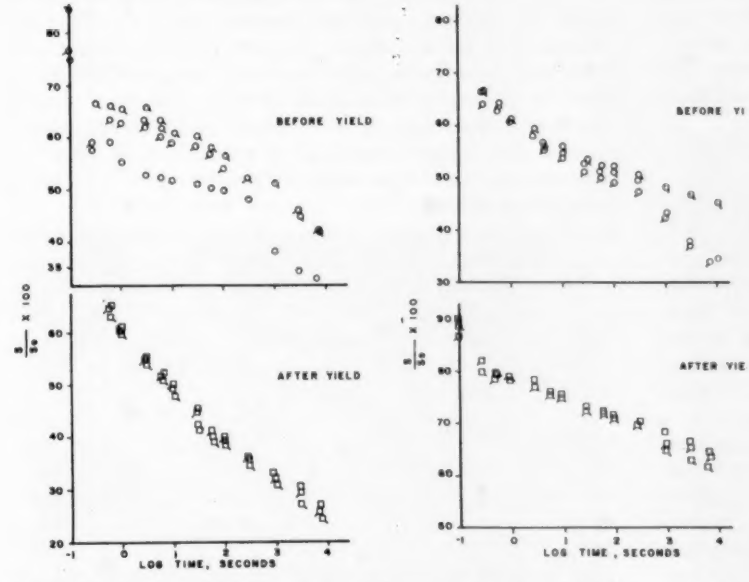

Figure 15. Stress Relaxation Ratio of Stress at time t to Initial Stress, s_o times 100 vs log time in seconds for Cellulose Acetate—CA

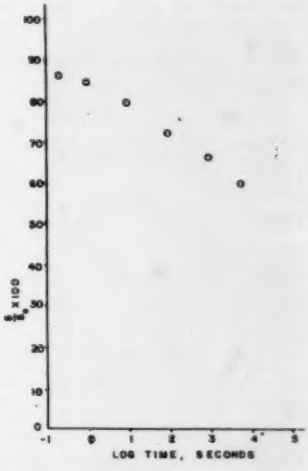

Figure 17. Stress Relaxation Ratio of Stress at time t to Initial Stress, s_o times 100 vs log time in seconds for Butadiene-Styrene Copolymer Rubber—RSB

Figure 16. Stress Relaxation Ratio of Stress at time t to Initial Stress, s_o times 100 vs log time in seconds for Low Density Type Polyethylenes

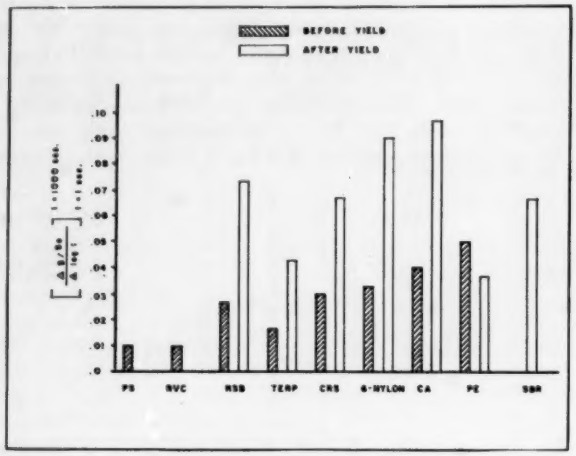

Figure 18. Slopes of Stress Relaxation Curves Between 1 and 1000 seconds compared at strain levels less than and greater than apparent yield stress in 450% per minute tensile test

Figure 19. Electron Micrograph of a Fracture Section of Poly(methyl methacrylate). MEME (2)

(10). When compared after yield much of the individual difference between samples disappeared.

The relaxation behavior of impact resistant plastics, like the behavior of dynamic modulus with temperature, suggest that at ambient temperatures the polymers behave as if they were somewhere in between the glassy and rubbery plateau regions of Tobolsky's classification (10). After yielding, the relaxation behavior becomes even more characteristic of the transition region. It seems as if high-speed straining beyond yield destroys the continuum of an apparent glassy structure and converts the plastic to some structure which resembles more a reinforced rubber in stress-compliance behavior. For sheet plastics in impact tests, these permanent changes are confined to the region of the impact blow (2).

Electron Microscope Morphology of Fracture Sections

Sometimes brittle amorphous polymers can be made impact resistant by milling them together with a compatible rubbery polymer at some elevated temperature usually above the glassy transition of both components. Upon cooling, a microscopically observable heterogeneity becomes apparent even at low magnifications of 400 x. Hence better impact resistant plastics are made up of two or more phases arranged in something like a grain structure in metals. Whether all rigid thermoplastics which are impact resistant are heterogeneous, poses an interesting question. In a most general sense, heterogeneity can be defined as coexistence of adjacent microscopic domains having dissimilar mechanical behavior. These may be distinct phases, or possibly not. Microscopy should help in clarifying this question if our interpretation of the micrographs is correct.

Fracture sections of the polymers here studied were examined by electron microscopy. The basic assumption was that differences in mechanical behavior in separate domains on a microscopic level would lead to structured fracture patterns and that these differences become sharper and less-dependent upon strain rate at low temperatures. The fracture tests were conducted as follows:

Slightly notched injection molded samples of plastics were chilled to −60°C with solid carbon dioxide and then fractured with a sharp blow. Replicas were prepared using the gelatin-silica-chromium technique described by Bobalek, Lacson, and Dawson (1). Transmission micrographs of the silica replicas were taken with an RCA-EMV, electron microscope usually at magnifications of 10,000 to 40,000 x. Some typical results are shown in *Figures 19 to 24.*

Figure 19 shows poly(methylmethacrylate), a brittle water-white plastic, whose tensile rupture energy at rates of 450 per cent per minute was only 24 inch-pounds per cubic-inch. *Figure 20* shows a bright poly(styrene) of tensile rupture energy less than 33 inch-pounds per cubic-inch. Both of these polymers show a fracture surface that is featureless. These homopolymers lack a domain structure which resembles anything like what exists in the amorphous polyblends or in partly crystalline polymers.

The blend of nitrile-rubber with styrene-acrylonitrile copolymer which has a tensile rupture energy of 630 inch-pounds per cubic-inch showed a very rough surface pattern, *Figure 21.* The ternary copolymer, *Figure 22,* with a rupture energy exceeding 518 inch-pounds per cubic inch had a rough surface quite similar to that of the mechanically mixed polyblends.

As might be expected, the fracture surface of opaque and partly crystalline nylon-6, *Figure* 23, showed considerable structure. It is very interesting that a similar structure of much finer dimensions is shown also by the transparent cellulose acetate, *Figure 24.* This seems to be about the lower limit of effective domain size. While fracture patterns can be observed in many polymers like poly(styrene) or poly(methylmethacrylate) at very high magnifications exceeding 60,000 x, coarser patterns are absent in the range of about 400-40,000 x, suggesting different details of the fracture mechanism.

There is no magic in heterogeneity alone. Many blends can be made which show structured fracture without

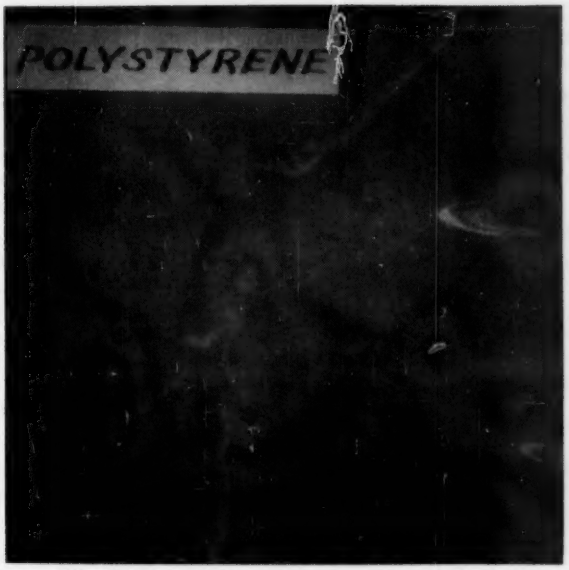

Figure 20. Electron Micrograph of a Fracture Section of Poly(styrene)—PS

being tough plastics. However, all rigid plastics which also behave somewhat like elastomers during and after loading seem to show a fracture pattern suggesting domain heterogeneity of topographical dimensions usually coarser than that shown in cellulose acetate.

Discussion

The differences between impact resistant and brittle thermoplastics are shown most clearly in the rate dependence of tensile properties and in the temperature dependence of low strain dynamic behavior. Some common features of behavior and structure encourage attempts to define the tough plastics as a separate family. The important distinctions are summarized in *Table 2*.

The differences here shown between the behavior of impact resistant and brittle plastics can be achieved either by milling rubber with a glassy plastic, by special techniques of copolymerization, or by altering crystallization kinetics through control of molecular architecture and composition so as to attain the proper degree

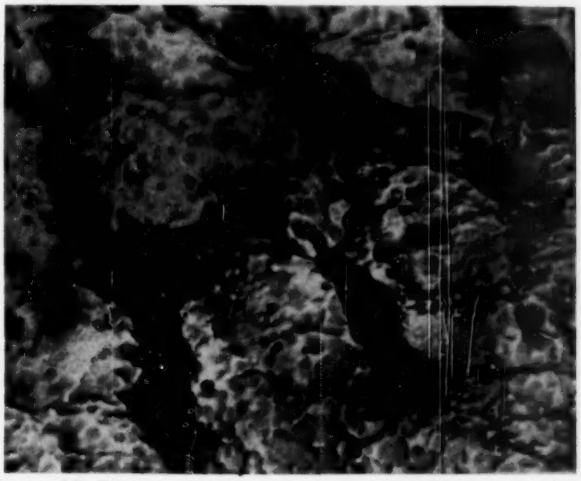

Figure 22. Electron Micrograph of a Fracture Section of "Block Copolymer" of Styrene-Acrylonitrile-Butadiene—TERP

Figure 21. Electron Micrograph of Styrene-Acrylonitrile Copolymer with Acrylonitrile-Butadiene Copolymer Rubber—CRS

of crystallinity or spherulite aggregation. In each case, an intimate mixture (but not solution) of high and low modulus component seems to be necessary so that a thermoplastic at room temperature can be made ductile under impact loading without sacrificing rigidity and strength.

Whether all rigid thermoplastics which show the "cold-draw" phenomenon at impact loading are heterogeneous is doubtful. Smith (12, 13) has observed cold-drawing in polyisobutylene and in RSB rubber at −67.8°C (just about its T_g of −63°C). There is no reason to presume that domain heterogeneity must occur in passing through the transition region. However, for the present, we can assume that domain heterogeneity of optimum size, distribution, and type, produced in one way or another, provides at least one approach to

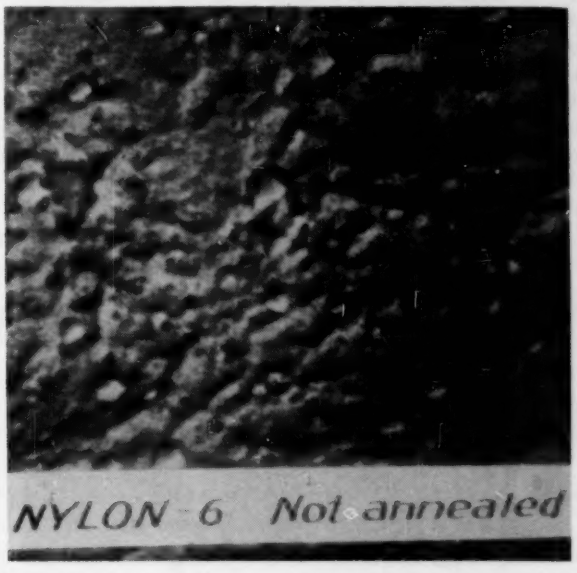

Figure 23. Electron Micrograph of a Fracture Section of Nylon-6

Table 2. Differences Between Impact Resistant and Brittle Thermoplastics

Observation	Not Impact Resistant	Impact Resistant
Stress-strain curve at speeds exceeding 450% per minute.	Brittle fracture short of a distinct yield value.	Shows critical yield stress, stress decline after yield followed by a region of plastic flow; possibly work-hardening region at high extensions.
Variation of dynamic shear modulus as a function of temperature.	Shear modulus almost as high at 25°C as at —50°C.	Marked rise in modulus with falling temperature. This takes place either gradually or with "terraces". Whichever is the case, ultimate elongation at 450%/min. is roughly proportional to total amount of rise of modulus curve between ambient and very low temperatures.
Relaxation modulus-time curve.	Very slight drop in modulus up to two hours for all degrees of strain short of break.	Significant drop in modulus with time before yielding. At strains above yield, relaxation rate much greater.
Damping properties as function of temperature in dynamic tests.	Low and flat below main glass transition temperature.	High damping either with several sharp peaks or one or two broad wide peaks.
Microstructure of fracture sections at magnifications of 400 to 50,000 x	Featureless.	Structured fracture patterns.

creating a plastic which at ambient temperatures shows the same desirable relaxation modulus behavior as occurs only at inconvenient temperatures for most polymers which fit the amorphous network rheological models. This approach is apparently more versatile than attempts to shift the glass transition range to a useful position in the thermal scale by synthesis of homogeneous copolymers of the amorphous type.

The empirical observations already accumulated suggest that much has been done rather easily by trial and error in simulating transition region behavior at room temperature through various means of controlling a quasi or real polyphase condition of optimum morphology. A more complete definition of the rheological system here needs to account for the interaction of adhesion forces between domains with the bulk elastic behavior of polymers in each domain. Such information would provide a basis for construction and optimization of rheological models which may be more easy to attain in practice than defect-free, homogenous net-work polymers which also should be very impact resistance even in the glassy region.

Figure 24. Electron Micrograph of a Fracture Section of Cellulose Acetate—CA

Literature References

1. Bobalek, E. G., Lacson, J., and Dawson, W. R., *J. Appl. Polymer Science 3*, 113 (1960).
2. Evans, R. M., Nara, H. R., and Bobalek, E. G. *SPE Journal, 16*, 76-83 (1960).
3. Nielsen, L., *Review Sci. Inst., 122*, 9, 690 (1951).
4. Buchdahl, R., and Nielsen, R. *SPE Journal* (May 1953).
5. Jaenckel, E., *Kolloid Z., 136*, 142.
6. Schmieder, K., and Wolf, K., *Kolloid Z, 134*, 2/3. 149.
7. Kuhn, W., Kunzle, O., and Preissman, A., *Rubber Chem. and Tech. 27*, 36, 154 (1954); 28, 694 (1955).
8. Sauer, J. A., and Woodward, A. E. Rev., *Mod. Phys. 32*, No. 1, 88-107 (Jan. 1960).
9. Tobolsky, A. V., and McLoughlin, J. R., *J. Polymer Sci. 8*, 543 (1952).
10. Tobolsky, A. V., "Properties and Structure of Polymers". John Wiley & Sons Inc., N. Y. 1960.
11. Payne, A. R., and Scott, J. R., "Engineering Design with Rubber". Interscience Publ. Inc., N. Y. 1960.
12. Smith, T. L., *J. Polymer Sci.* XXXII, 99-113 (1958).
13. Smith, T. L., *J. Polymer Sci.* XX, 89, (1956).
14. Smith, T. L., *SPE Journal 16*, 1211 (1960).

NOTE: This paper abstracts and updates a part of the experimental work reported by Robert M. Evans in a Ph.D. Thesis on "Microstructure and Mechanical Behavior of Impact Resistant Thermoplastic," Case Institute of Technology, 1958. The authors acknowledge the assistance of E. R. Moore and J. Lacson with the microscopic studies and A. Forsythe and W. R. Dawson with the tensile and dynamic testing.

This article was adapted from a paper presented to the American Chemical Society at its 138th Meeting, September 1960, N. Y., N. Y.

A *preview* of several articles for the third quarterly issue (July), SPE TRANSACTIONS

Thermodynamic Diagrams for Polyethylene Resins

by J. M. Lupton

Diagrams showing the effects of pressure, volume, and temperature on thermodynamic properties such as enthalpy, internal energy, and entropy are well known for simple substances and serve many purposes in science and engineering. Such diagrams for thermoplastic resins have been less frequently used, reflecting many complications in acquiring and interpreting the necessary data. However, recent studies show that a series of assumptions can be used to develop useful new diagrams of wide scope for polyethylene resins.

The Strength of Glassy Polymers

by J. P. Berry

The Griffith theory for brittle fracture predicts that the tensile strength should be inversely proportional to the square root of the size of a defect or flaw in the sample tested. The validity of this relation has been investigated for the glassy polymers, poly (methyl methacrylate) and polystyrene. The results indicate that the strength of the polymers depends on two factors: (1) the surface energy, and (2) the inherent flaw size. The surface energy is primarily that dissipated in a viscous flow process and the inherent flaw size is related to the tendency of the polymer to craze under stress.

The Effect of Extrusion Variables on the Fundamental Properties of Tubular Polyethylene Film

by N. D. Huck and P. L. Clegg

The mechanism of formation of tubular polythene film is a complicated process, and extensive studies have shown that the properties of the film made are influenced profoundly and in a complex way both by the processing conditions used and by certain design features of the equipment. Studies of the effect of the extrusion variables on the more important film properties, both optical and mechanical, are reviewed in this paper. The results are discussed in terms of the fundamental nature of polythene film, its surface, its crystalline structure and its orientation. It is shown that the properties are determined almost completely by the melt history from just before the die to just after the freeze line.

Flow Patterns in a Non-Newtonian Fluid in a Single-Screw Extruder

by W. D. Mohr, J. B. Clapp, and F. C. Starr

Flow patterns in the channel of a screw extruder have been investigated in a study utilizing a model extruder with stationary screw and a rotating, transparent barrel. Photographs of flow streamlines at conditions over the full range of output restrictions are presented for a non-Newtonian fluid. A technique employing photographs of particle tracers was used with the same apparatus to permit quantitative measurement of velocity profiles with both a Newtonian and a non-Newtonian fluid.

SPE
TRANSACTIONS